UNIVERSITY OF CALIFORNIA

Los Angeles

On Enabling Concurrent Communications in Wireless Networks

A dissertation submitted in partial satisfaction of the
requirements for the degree Doctor of Philosophy
in Electrical and Computer Engineering

by

Hemant Saggar

2020

© Copyright by

Hemant Saggar

2020

ABSTRACT OF THE DISSERTATION

On Enabling Concurrent Communications in Wireless Networks

by

Hemant Saggar
Doctor of Philosophy in Electrical and Computer Engineering
University of California, Los Angeles, 2020
Professor Gregory J Pottie, Co-Chair
Professor Babak Daneshrad, Co-Chair

Today innumerable devices use the wireless spectrum for communication, including cell-phones, WiFi devices, military radios, public safety radios, satellite phones etc. This crowding is limiting the experience of each device either through interference or by waiting for their turn to communicate. So, how do we allow a limited spectral resource to reliably scale to many more devices? This is possible through concurrent communication where multiple links share the spectrum and communicate simultaneously using multi-antenna techniques. One promising technique is Interference Alignment (IA), that has been shown to be Degrees-of-Freedom optimal under some conditions. Still, IA requires accurate channel knowledge to be effective and its ability to achieve high throughput under time varying wireless conditions is yet unproven. We make progress towards understanding these limitations and provide viable solutions.

We study an IA system under different models of the time varying channel and derive expressions for the achieved rate over time and the system throughput. Using these, we can arrive at the optimal duration of the data phase that maximizes throughput. We propose

two strategies that help to counter the effects of a time varying channel. First, data aided receiver beam-tracking along with link adaptation provides a sizable improvement in the received signal to interference and noise ratio. Second, updating the transmit beams during data transmission using short feedback pilots improves alignment at the receivers. In faster varying channels, we get a more stable achieved rate whereas in slower varying channels, we see additional throughput gains. The conclusion from this work is that an IA system must be trained more frequently than the channel coherence time to ensure high throughput and beam adaptation during the data phase gives significant robustness to the system.

Lastly, we present an IA based medium access control (MAC) protocol that outperforms traditional protocols. Our concurrent carrier sense multiple access (CSMA) protocol based on beam-nulling is compatible with CSMA and increases the sum throughput by 2 to 3x. We also show that IA outperforms optimal time division multiple access under time varying conditions. Hence a well-designed IA system can enable reliable concurrent communications in a wireless network.

The dissertation of Hemant Saggar is approved.

Christina Panagio Fragouli

Danijela Cabric

Babak Daneshrad, Committee Co-Chair

Gregory J Pottie, Committee Co-Chair

University of California, Los Angeles

2020

To teachers and parents, who have enthusiastically

given so much of their time to educate me.

Thank you.

Contents

List of Figures

List of Tables

ACKNOWLEDGEMENTS

I thank God for taking me through these wonderful six years at UCLA. Though, it was a long journey, I am really grateful that I have made it through without giving up hope and mostly sanely. This journey was definitely a learning experience and character building. I learned the value of discipline and hard work, and started becoming responsible of fighting with my problems bravely without giving up. I have even gained immense respect for the teacher's position and from their vantage point, I have seen the importance of being forgiving, earnest, and helpful. I have experienced great joy when an idea was validated in meetings and also weeks where I had no clue where I was heading. Through all this time, the serene campus of UCLA has been my silent well wisher and I thank UCLA for having a happy vibe.

Most of all, I want to thank my advisor Prof. Gregory Pottie for taking me under his able guidance and teaching me through his vast experience. He has answered countless questions and held long discussions with me whenever I needed. I am grateful that I have such a supportive and jolly advisor who helps me see the world's perspective beyond my narrow shell. I also want to sincerely thank Prof. Daneshrad for being my co-advisor and for introducing me to this exciting research area and supporting me while I did my work. He has always made time for me inside and outside UCLA and his mentor-ship has been inspiring.

I deeply thank Prof. Cabric and Prof. Fragouli for taking out valuable time from their busy schedules to take part in my qualifying and defense exams. I have listened intently to your suggestions and my thinking process has improved because of them.

Ph.D. student life is not complete without having friends to share your stories with. I have had some of the best times with my first year friends and roommates - Shashank, Pranjal, and Mayank. I also thank Ayush and Gaurav for being wonderful roommates and friends in the later years.

I want to especially thank the wonderful staff in our department who are the best human beings ever and have made doing Ph.D. here a joy and breeze. Thanks to Madam (Deeona)

Columbia, Ryo, Julio, Kyle, Tricia, Jackie, Jose, and Charlene for your warm gestures.

Working in the lab has been enjoyable all these years due to the company of friends and labmates like Heng Zhao, Ehsan Keramat, Kia Karbasi, and Nick Kauffroth who are great researchers and wonderful folks themselves.

In 2018, I had the great fortune of meeting and marrying Priyanka, and she has brought a wind of positive change in my life. She is like my father, strong willed and unflinching in care and affection. Even though she is a Ph.D. herself, she is devoid of superficiality and loves me as a whole. I am always indebted to her for her sacrifice and strength and I revere her as a true friend.

My sister & brother in law, Dr. Swati & Dr. Ashwani both have been very supportive of me since I came to the US. I owe much of my mental peace to them and thank them deeply. Finally, both my parents are proud of me and also relieved that I have finally finished what I stubbornly started in 2014! They have supported me steadfastly through these years with constant blessings and belief. This work is dedicated to their extraordinary skills as parents and teachers. I will keep doing wonderful things in life by their blessings.

I want to thank the Office of Naval Research, USA for supporting my thesis work as part of the project A MAC-PHY Architecture and Smart Radio Prototype to Maximize Network Spectral Efficiency, award number N00014-14-1-0104:P00002. I also thank the Guru Krupa Foundation for supporting me with the Guru Krupa fellowship during Spring 2018.

Chapter 3 is a combination of two papers [20] and [23], and Chapter 5 includes work published in [34], all three papers are © IEEE and reprinted with permission from the authors.

VITA

2006 – 2011	B.Tech. in Electronics & Communication Engineering
	M.Tech. in Wireless Communication
	Indian Institute of Technology Roorkee
2011 – 2013	Edison Engineer
	General Electric, Bengaluru
2013 – 2013	Project Scientist
	Department of CSE, Indian Institute of Technology Delhi
2013 – 2014	Doctoral Student
	Indian Institute of Technology Delhi
2014 – 2020	Graduate Student Researcher, Teaching Assistant/Associate/Fellow
	University of California, Los Angeles
Summer 2016	Intern
	Qualcomm, San Diego

PUBLICATIONS

1. Hemant Saggar, Babak Daneshrad, and Gregory J. Pottie, "The Distribution of SINR and the achieved Throughput in Interference Alignment under a Gauss Markov Channel, in 88th IEEE VTC, Chicago, Aug 2018.

2. Hemant Saggar, Greg Pottie, and Babak Daneshrad, "On Maximizing the Average Capacity with Interference Alignment in a Time Varying Channel, in Information Theory and Applications Workshop, San Diego, Feb 2016.

3. Hemant Saggar, Yi Jiang, Babak Daneshrad, and Greg Pottie, "A Concurrent CSMA MAC protocol for Mobile Ad Hoc Networks using beamnulling, in IEEE MILCOM, Tampa, Oct 2015.

4. Hemant Saggar, and D.K. Mehra, "Performance of Optimum Detector for Cyclic Prefixed OFDM with Induced Cyclostationarity for Spectrum Sensing in Cognitive Radio, in 7th IEEE ICIIS, Chennai, Oct 2012.

5. Hemant Saggar, and D.K. Mehra, "Cyclostationary Spectrum Sensing in Cognitive Radios Using FRESH Filters, in 1st National Conf. of ICEIT, New Delhi, Apr 2011.

Chapter 1

Introduction

1.1 Background on Wireless Networks

A wireless network is one where two or more users are communicating wirelessly. A communicating link always requires a transmitter and a receiver and in a wireless network, multiple such links may be active in the vicinity of each other. Ad-hoc wireless networks are infrastructure-less and non-hierarchical communication networks where any set of nodes can communicate with another set of nodes and there is no a priori fixed node that determines the parameters of communication. Cellular networks on the other hand, have a fixed base station moderates a communication between two nodes. When the nodes in an ad-hoc network are mobile, it is called a mobile ad-hoc network (MANET) such that neighboring nodes as well as the physical medium of communication keeps changing with time.

Applications of cellular networks include voice, video, and data for personal communication, industrial communication, and other commercial uses. Applications of MANETs are many such as communication networks for the military in tactical environments, reliable airborne and ground mesh networks to assist firefighting operations in the absence of cellular networks, augmenting satellite connected networks in emergency situations, video streaming from autonomous agents and drones. Nonetheless, both networks have to manage the users

such that their communications don't interfere and disrupt other users's communications. In MANETs the links are between mobile nodes, while in cellular networks, these links are between a cellphone and a base station. Further, the networks are becoming more dense as more devices are coming online, cell sizes are shrinking, and the quality of service (QoS) requirements of each device is becoming higher. Truly, wireless networks are facing a crunch!

1.2 Increasing interference and Spectrum Scarcity

The reality today is that the density of communicating devices is increasing dramatically while additional bandwidth is hard to come by, especially in the low frequency (sub 6 GHz) bands where most communication today takes place, because it is being heavily used by different licensed and unlicensed users such as cellular companies, radio navigation, satellite communication, broadcasting, WiFi etc. Random access protocols like carrier sense multiple access (CSMA) allow multiple user pairs to contend and share the spectrum. But under a limited bandwidth, the peak throughput of a network using CSMA remains fixed, meaning that per link throughput is inversely proportional to the number of links in the network. As the network densifies, each user's QoS degrades leading to a worsening experience for every user. To clarify, this is not a limitation of CSMA, but an inherent outcome of the basic paradigm in wireless communication that successful communication depends on *avoiding interference* and ensuring that each distinct signal is allocated its own resource block (time, frequency, or code) without sharing. Naturally the problem of diminishing throughput per user persists even with other multiple access schemes namely time division multiple access (TDMA) and frequency division multiple access (FDMA), which are centralized resource allocation schemes.

Overcoming this spectrum scarcity requires us to rethink how multiple communication links are sustained in a network. The usual way to avoid interference between simultaneous transmissions has been to separate them into orthogonal frequency, time, or code slots. But

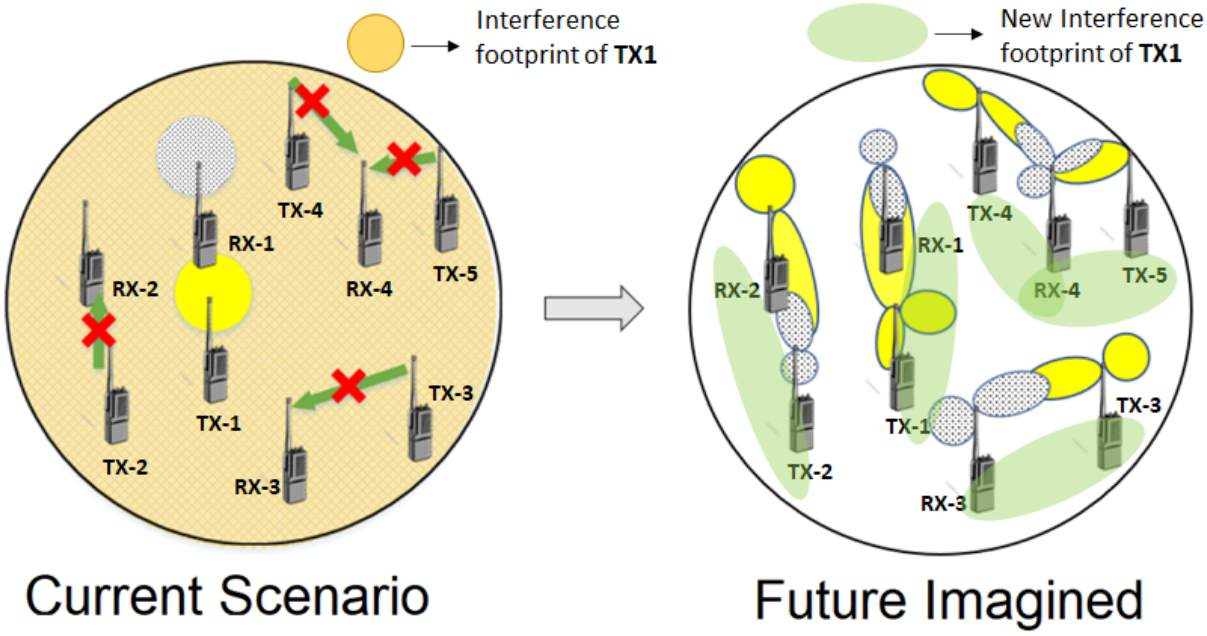

Figure 1.1: A comparison between the state of current Mobile Ad-Hoc Networks and the envisaged future of concurrent communication.

this strategy is unsustainable in the face of growing demand for communication services and we must utilize the available spectrum as efficiently as possible, as we explore higher frequencies to get more bandwidth. By using multiple antennas, it is known that multiple information streams can co-exist without interference. We wish to evaluate the limits of multi-antenna techniques in interference management in wireless networks.

The goal of this thesis is to provide ways to transition from avoiding interference to accepting and designing the interference in wireless networks in real world settings. Such techniques will be applicable to both MANETs and cellular network as both face similar multi-user interference problems. We envision a future where multiple radios co-exist using intelligent multi-antenna techniques at both transmitters and receivers such that all links can attain a high throughput. This future is shown in fig. 1.1. We call this future *concurrent communication*, where multiple links are operating simultaneously in the same frequency and time resource, with minimum interference to each other. To realize this future we must utilize the power of multiple antennas to the fullest.

1.3 Enabling Concurrent Communication

In the past two decades, multiple antennas have become a norm on all radio devices, be it cellphones, laptops, cellular base stations, WiFi access points, military radios and software-defined radios (radio kits including baseband and Radio Frequency components whose parameters like frequency, waveform, processing can be easily configured through software). From omni-directional transmission where everyone in the vicinity is equally affected by the signal, it is possible to now have directional beams that focus energy in a desired direction or avoid an undesired direction. This is called *beamforming* and *beamnulling* respectively. Multiple antennas also give us the possibility of sending and receiving more than one stream of information, called a *spatial stream*, at the same time from a radio. This helps increase the data throughput over a link because we now have two independent streams of information being sent over the air in the same bandwidth. Alternatively, one spatial stream can benefit from increased reliability in noise and/or random drops in signal energy called fading. Both these and all other multi-antenna techniques fall under the class of Multiple Input Multiple Output (MIMO) techniques.

Applying MIMO techniques to multi-user communication has opened up new avenues to increase the system throughput and reliability. Multiple user pairs can now potentially talk in the same time and frequency slot, dramatically increasing spectral efficiency. Some applications are wireless sensor networks, military communication between platoons, and inter-cell coordination in cellular networks. While there is no one MIMO technique that is known to maximize sum capacity in a multi-user interference network, one recently discovered technique that is close to optimal at high signal to noise ratio (SNR) is called Interference Alignment (IA).

Interference Alignment works by designing the MIMO beams at the transmitter and receiver so that interference aligns into a small enough subspace, leaving sufficient dimensions for the desired signal. With correct channel knowledge, IA can allow the maximum number of links to be simultaneously active, more than any other known technique. While this makes

IA a promising candidate for concurrent communication, it is still untested how it holds up to practical challenges like inaccurate channel estimates, moving users, and more users in the network. Answering some of these questions will help us design the implementation of Interference Alignment and similar strategies to be both robust to common problems and efficient. It will also provide insight into the behavior and challenges of a system of interfering users over time, which will be applicable to not just IA, but to any other MIMO strategy that deals with interference that is time varying.

1.4 Aims of the thesis

The aim of this thesis is to investigate the different algorithms used to achieve Interference Alignment under multiple practical real-world challenges such as time variation of the channel and estimation inaccuracies. The broad aims of this thesis are as follows.

- First, we aim to analytically model the effect of time variation in the channel on the throughput of a multi-user interference aligned system and gain insight into what factors determine its sensitivity or robustness.
- Second, we aim to optimize the interference alignment system parameters and propose techniques to improve system performance under a time varying channel. The goal is to make alignment robust and achieve a high sum throughput.
- Third, we aim to show that multi-antenna interference management techniques can do better at multi-user concurrent communication than existing approaches like TDMA and CSMA, and they can also co-exist with them.

1.5 Organization of the thesis

Chapter 2 gives a background on Interference Alignment, its history, important works, and algorithms to achieve alignment. It also discusses different practical challenges that such a

system must face in order to work well in practice. Chapter 3 gives analysis of the performance of an IA system under different time varying channel models and also presents results on optimization of protocol parameters to maximize throughput. Chapter 4 discusses practical techniques that can be used to further improve system performance under a time varying channel. It discusses the benefits of receiver beam-tracking and short re-training in the middle to let the transmitter and receiver update their beams to ensure good alignment. Chapter 5 presents a beamnulling based medium access control (MAC) protocol that allows concurrent communication and is backward compatible with CSMA. It also presents a throughput comparison between an IA and a TDMA system in a many user scenario. Finally, conclusions from this work are presented and references are given.

Chapter 2

Concurrent Communication Techniques for Mobile Ad-Hoc Networks

2.1 Background on Interference Alignment

MIMO techniques can allow more than one link to be active in the same time and frequency slot, by using beamforming and beamnulling. It is relatively simple to design the beams when only two links are transmitting. The receiver tries to beamnull the interfering transmitter, while the transmitter tries to beamform towards its desired receiver. But as soon as we move to 3 or more MIMO links, we are at a loss for a simple solution to allow interference free operation of links. A single concurrent communication technique that maximizes the sum capacity in a general interference network is still unknown. But information theory has recently discovered a technique that comes close to being optimal in some sense, and it offers us a real possibility of designing concurrent communication networks with many active links and large network spectral efficiency. This is the technique of Interference Alignment (IA).

IA is a technique of concurrent communication, where multiple transmitters transmit in

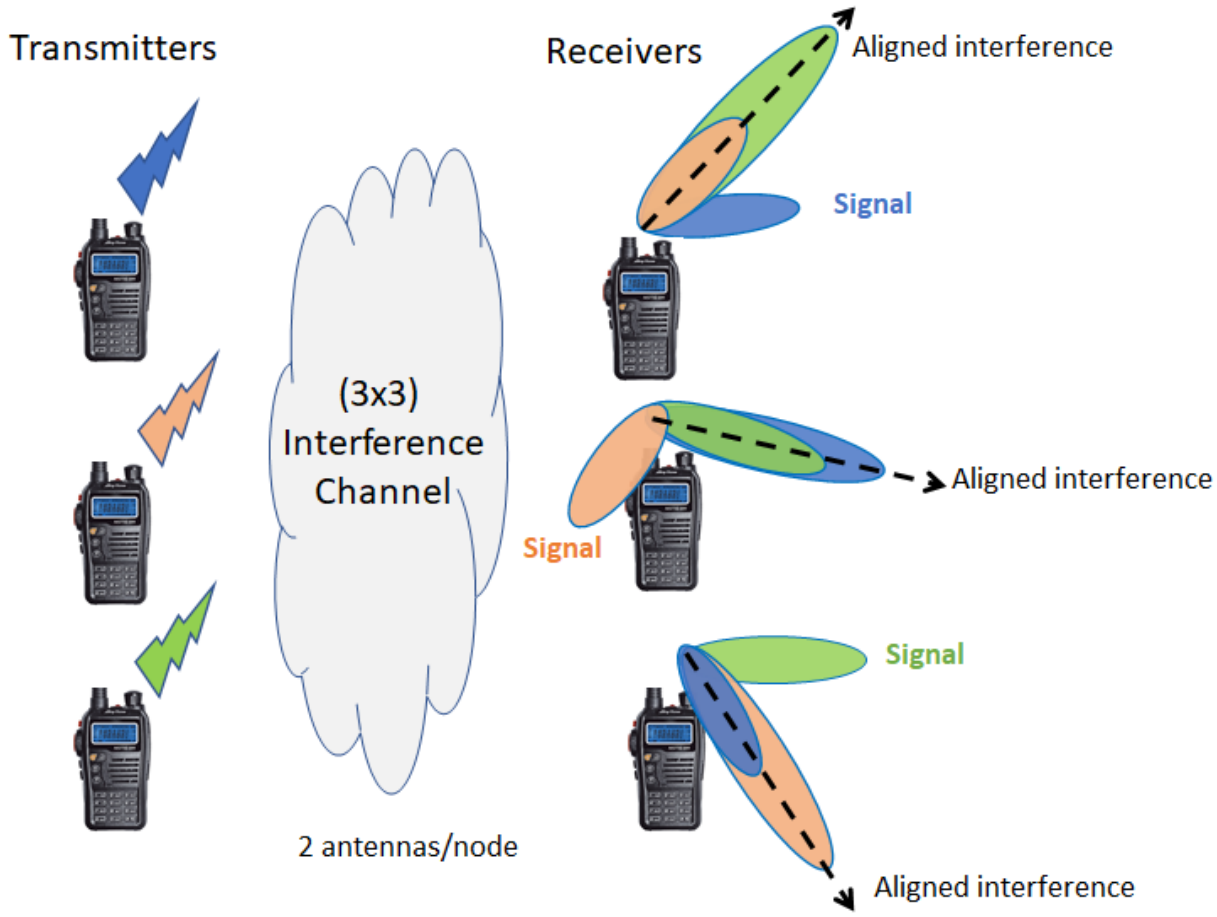

Figure 2.1: A system with 3 users and 2 antennas per user depicting how Interference Alignment is achieved.

such a way that the interference at any receiver aligns and spans a space with less dimensions than the number of interferers, leaving enough dimensions for the signal to be received interference free. A graphical depiction of IA is shown in fig. 2.1. It is obvious from the figure that Interference Alignment can achieve 3 interference free streams which is more than what simply receiver zero-forcing can achieve. Each interference free stream is called a degree-of-freedom (dof). IA was discovered by Cadambe and Jafar in [1] as a technique that allows a user to use half its signalling dimensions interference free irrespective of the number of interfering users. To give an analogy, imagine that the spectrum is a cake and it is being shared by K users, then instead of each user getting $1/K$ of the cake, **every** user gets $1/2$ the cake, irrespective of how large K is. This is astonishing at first sight but it has surprising mathematics behind it[2]. In fact, IA has been shown to achieve the optimal (maximum) sum dof of the system in many kinds of interference channels [1] [3]. Thus IA is a promising technique to enable concurrent communications in wireless networks. In fact IA has inspired many other joint transmitter (TX)- receiver (RX) beamforming techniques that can provide higher sum capacity than IA at low to moderate SNRs. In this thesis, we will include them all under the umbrella of Interference Alignment since all these techniques are sum capacity maximizing approaches and achieve the same dof.

In general, alignment may be performed over time, frequency, antennas, or even signal levels. For many systems, achieving Interference Alignment may necessarily require coding over many time slots while for others it can be achieved simply in a single slot using multiple antennas [4]. Restricting the achievability to a single time slot, definitely limits the number of systems where IA achieves optimality. But aligning over time requires exponentially many independent realizations, which quickly goes beyond the finite decoding delay requirement of most applications even with few (3 or more) users. Hence in this thesis we focus on alignment achievable using multiple antennas and over a single coherence interval only, which still offers a sizable gain in dof.

In this thesis, we will say K users to mean K pairs of radios, each pair having one trans-

mitter wanting to talk to one receiver. Hence unless stated otherwise, K user interference channel means K TX and K RX nodes as per convention. Using IA over multiple antennas it has been shown that ([4] Thm. 6) that a K user system, $K \geq 3$, with M antennas at each transmitter and receiver, can achieve a symmetric dof d per user, if and only if

$$(K+1)d \leq 2M \tag{2.1}$$

A corollary of the above result is that the symmetric (or common) dof per user is limited to $d \leq \lfloor \frac{2M}{K+1} \rfloor$. For example a $K = 2$ user interference channel with $M = 22$ antennas per node can achieve $d = 1$ dof per user. We know that receiver zero forcing can achieve this by canceling out the interfering user stream. But by the above corollary, a $K = 3$ user system with $M = 2$ antennas per node can also achieve 1 dof per user which is not achievable by simple zero forcing. Achieving the strictly larger sum dof of 3 than 2 relies on performing Interference Alignment between the TX and RX nodes.

2.1.1 Interference Alignment Techniques

Two flavors of Interference Alignment techniques have been discussed in the literature corresponding to two ways of obtaining the desired antenna beams to achieve alignment. First is feedback based or centralized IA. The second is over-the-air iterative or distributed IA. Both techniques can lead to alignment but they impose different overheads and have their own strengths and weaknesses. A comparison is presented below.

Centralized vs Distributed IA

In centralized IA, one must collect all forward and reverse channel estimates at a centralized node. This requires that both TX and RX must perform MIMO channel estimation and the receivers must send the forward channel estimates as feedback to the transmitters. These processes take up precious air-time. Different optimized ways of sending channel state feed-

back have been explored including limited feedback and analog feedback [5][6]. Centralized IA does not need the channel to be reciprocal and this makes it simpler and many times the goto choice for achieving IA.

In distributed IA, over-the-air iterative optimization is done to arrive at the optimum antenna beams. Channel reciprocity is very necessary here and must be established through tight calibration. Although this method skips MIMO channel estimation, it may take many iterations to converge which again increases overhead. On the other hand, this method is robust to changes in the channel, interference, errors in channel estimation, and node failure as those can get reflected in the iterative process.

Multiple algorithms have been proposed in the literature that either achieve Interference Alignment in a system or are inspired by it with the objective of maximizing the sum capacity of the network. We explain some of the major ones below.

Concurrent Communication Algorithms

Closed form Alignment Solution for $K = 3$ The closed form solution for IA was derived only for $K = 3$ users and $M = 2$ antennas per node by Cadambe and Jafar [1]. The conditions on alignment are stated as,

$$\begin{aligned} H_{13}p_3 &= H_{12}p_2, \quad \text{At rx 1} \\ H_{21}p_1 &= H_{23}p_3, \quad \text{At rx 2} \\ H_{32}p_2 &= H_{31}p_1, \quad \text{At rx 3} \end{aligned} \tag{2.2}$$

where H_{ij} is the channel between receiver i and transmitter j and p_j is the transmit beam of j-th transmitter. Eqs. (2.2) lead to

$$H_{21}H_{31}^{-1}H_{32}p_2 = H_{23}H_{13}^{-1}H_{12}p_2,$$
$$\implies p_2 = H_{32}^{-1}H_{31}H_{21}^{-1}H_{23}H_{13}^{-1}H_{12}p_2. \tag{2.3}$$

Thus p_2 is an eigenvector of a big matrix. Choosing p_2, both p_1 and p_3 can be fixed. The receive beam w_1 is chosen to be orthogonal to the sole interference direction $H_{13}p_3$. Similarily w_2 and w_3 are chosen to be orthogonal to the received interference vectors.

Minimum Interference Leakage Alignment In this technique, the transmit and receive beams are chosen to minimize received interference. The iterations proceed as [7]

$$w_j = \min \text{ eigvec}(Q_j) \quad \text{at rx j},$$
$$p_i = \min \text{ eigvec}(Q_i^{\text{rev}}) \quad \text{at tx i}, \tag{2.4}$$

where again w_j is the receive beam for the j-th receiver and p_i is the transmit beam for the i-th transmitter. Q_j is the covariance matrix of received *interference* at the j-th receiver, either measured or constructed from channel estimates. Q_j^{rev} is the covariance matrix of received interference in the reverse channel (i.e. RX to TX). Iteratively doing these steps leads to the alignment solution, if it exists (e.g. if eq. (2.1) is satisfied).

Maximum SINR Alignment In this technique, instead of minimizing interference received, beams are chosen to maximize signal to interference and noise ratio (SINR) at each

step. The steps are as follows [7],

$$
\begin{aligned}
w_j &= (Q_j + \sigma_n^2 I)^{-1} H_{jj} p_j \quad \text{at rx j,} \\
w_j &= \frac{w_j}{||w_j||} \quad \text{at rx j,} \\
p_i &= (Q_i^{\text{rev}} + \sigma_n^2 I)^{-1} H_{ii}^{\text{H}} w_i \quad \text{at tx i,} \\
p_i &= \frac{p_i}{||p_i||} \quad \text{at tx i,}
\end{aligned}
$$

where H_{jj} is the channel from j-th receiver to j-th transmitter, σ_n^2 is the noise variance, and I the identity matrix of appropriate size.

Other approaches Other approaches have also been suggested. Interference Alignment has been formulated as a rank constrained rank minimization by Papailiopoulos and Dimakis [8] with better results than traditional IA. Another alternating minimization algorithm was proposed by Peters and Heath in [9]. Santamaria et al. proposed a maximum sum rate IA algorithm in [10]. Sridharan and Yu proposed a rank minimization based approach on the interference matrix in [11].

2.1.2 Challenges in Obtaining Alignment

All the above IA algorithms depend critically on having accurate, timely channel estimates. Interference Alignment, and generally, any interference cancellation technique, is very sensitive to the following inaccuracies, which may lead to increased symbol errors.

Accurate Channel Estimation

Achieving optimal dof with IA depends critically on having accurate channel estimates and this achievability is lost as soon as the estimates are imperfect [12][13]. Channel estimation for each link can be done either sequentially or concurrently. Concurrent estimation requires use of orthogonal codes like Zadoff-Chu (ZC) sequences that are circularly shifted

[14]. Concurrent channel estimation places harder requirements on hardware and may fail to live up to its promise due to non-idealities such as carrier frequency offset (CFO), timing offset, automatic gain control (AGC) firing errors, non-integer sample delays causing loss of orthogonality, RF front end saturation or non-linear mixing of signals. Sequential channel estimation takes more time but is only noise limited and hence gives better channel estimates with the same length pilots. One must decide based on one's hardware, required accuracy, and acceptable training overhead, which scheme is more suitable. Hardware implementations of IA have been done that have dealt with channel estimation and offset problems such as [15], [16].

Carrier Frequency Offset and Timing Estimation

CFO must be estimated well otherwise it can corrupt channel estimates. Jiang et al [14] has suggested using a pair of ZC sequences to estimate CFO and timing offset jointly. Timing synchronization can be achieved either using a GPS oscillator or a beacon node. For our work, we assume a beacon node is available that can be heard by every node and which signals them when to start transmission and reception. Experimental setup in the Wireless Integrated Systems Research Lab (WISR) at UCLA has succesfully demonstrated operation of a 3 user interference system with a beacon node in the lab and small areas like a parking lot.

AGC Issues

The AGC must remain locked while capturing the signal during channel estimation and also during signal transmission or reception. Inadvertant firing of the AGC can cause sudden changes in the signal amplitude that would add error to the estimate of channel or data symbol.

Time Variation of the Channel

A packet cannot be arbitrarily long because the channel changes over time. If the channel changes after the alignment beams have been computed, the beams will be inaccurate and unable to cancel all the interference during the data transmission. This would lead to decreased SINR and increased probability of error. Time variation in a channel is an outcome of either user motion or motion of the scatterers and hence cannot be avoided through improved hardware calibration or trying to ensure orthogonality through staggering transmissions in time. A well designed system must take into account this channel variation and resultant mis-alignment over the data phase and design the beam training protocol to maximize the data throughput while ensuring good estimates of the channel are still obtained. This problem is dealt with in detail in the next two chapters. Channel variation also affects computer in the loop hardware prototype demonstrations where software such as MATLAB is used to compute beams and the hardware's job is to pass on the acquired data to the software. Since data transfer and computation on a PC can take a significant fraction of a channel coherence time, such prototypes usually have short data phases as the beams computed may become inaccurate quite soon.

Reciprocity Calibration

Distributed algorithms for IA require the channel to be reciprocal. Establishing reciprocity requires calibrating the radio front ends such that the TX-RX forward chain and the RX-TX reverse chain have the same gain and phases. This is usually not the case due to independent phase locks of the transmit and receive chains on a radio. Thus calibration and compensation needs to be done. Calibration can be done using a reference antenna to estimate diagonal phase compensation matrices. Mutual coupling may cause problems in getting accurate reciprocity and must be accounted for if we need highly accurate estimates such as for interference alignment as demonstrated recently in [17].

2.2 Summary

This chapter presents the background on the technique of Interference Alignment as an umbrella of joint TX-RX beamforming techniques that can achieve higher degrees of freedom than simple receiver zero forcing in some networks. IA provides a way to enable concurrent communications in a wireless network but it also faces significant challenges due to its heavy dependence on accurate channel estimates.

Chapter 3

Interference Alignment in a Time Varying Channel

A wireless channel is dynamic and can change if the transmitter, receiver or the intermediary components like scattering objects change position or configuration. The rate of change of the channel is then dependent on the speed of motion of its constituents which also incidentally defines the Doppler spread (shift) of a communication channel. It is no wonder then that these two quantities are related. As we know, the absolute Doppler spread for a signal of center frequency f_c, with a transmitter/receiver moving at speed v is given we $f_d = vf_c/c$. The *coherence time* T_c of the channel, which is the time for which the channel remains almost unchanged, can be defined as

$$T_c = \frac{0.1}{f_d}, \tag{3.1}$$

where the constant 0.1 is sometimes chosen as 0.25 or 0.4 depending on how much variation in the channel can be taken in a coherence period.

Time variation in the channel has a significant effect on Interference Alignment because IA relies heavily on beam-alignment and interference cancellation. As the channel changes, beams from interfering sources that were aligned before become misaligned and as a result some interference leaks into the signal subspace. Thus the receiver starts to see higher

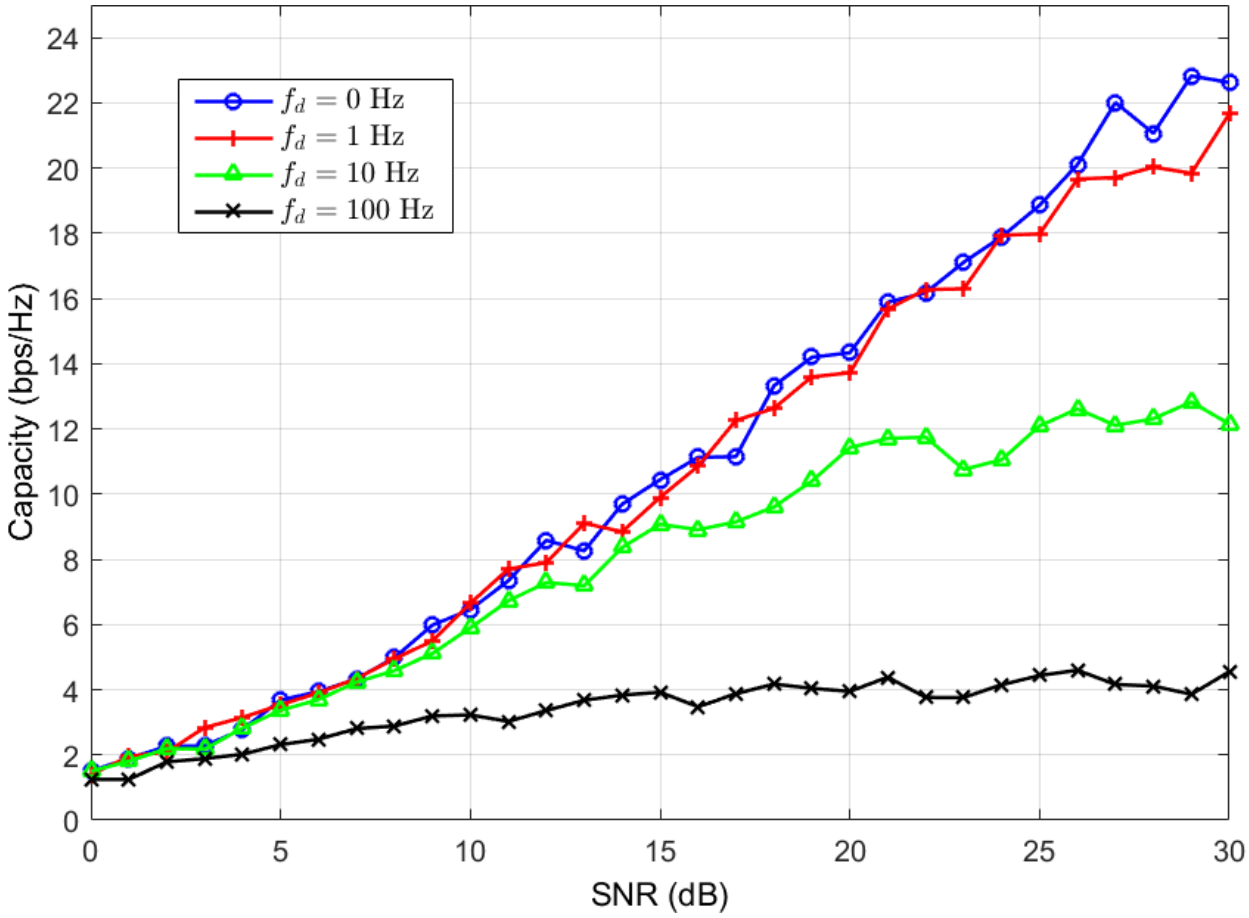

Figure 3.1: Sum capacity scaling of a system with 3 user-pairs and 2 antennas per user for increasing Doppler spreads.

interference and low SINR. The more tha channel changes, the lower the receiver SINR and it drops quite fast. Fig. 3.1 shows a graph of how capacity vs SNR plot becomes flatter as Doppler increases denoting the lost degrees of freedom.

3.1 Models of the Time Varying Channel

Different models have been proposed to model the variation of the wireless channel over time. A channel model helps us quantify the performance of a signaling strategy over time and hence is useful, even though it may be simplistic with respect to all the time variation effects.

One popular model used since many years is the block fading model, where the channel

is assumed to remain constant for a block of symbols, following which it changes to a new independent value. This helps us take expectations over many coherence intervals and talk about average capacity. A variation of the block fading model with independent realizations per block is the block fading model with correlated realizations. Here successive blocks have correlated fading channels.

The correlation profile of the channel across time can be modeled by considering 2D or 3D scattering, either uniformly or in a certain angle profile. The simplest and most used correlation profile, which assumes uniform scattering, is Jake's channel model. Jake's model specifies the correlation of the channel at time τ in a Doppler spread of f_d Hz is [31]

$$r_h(\tau) = J_0(2\pi f_d \tau), \tag{3.2}$$

where $J_0(.)$ is the Bessel function of zeroth order. The block fading model may be designed such that correlation between successive block channels is $r_h(T_B)$ where T_B is the chosen block size. This allows an approximation of the continuous time varying channel.

While this model works well in many cases like point to point communications, it fails badly in modeling the performance of interference cancellation systems such as IA. This is because sharp nulls are highly sensitive to change in the channel and small variations lead to large drops in the SINR, a phenomenon that is not visible in the block fading model. Thus, we need a continuously time varying channel model if we are to precisely model the performance of interference nulling systems like IA and ensure their robustness and practicality in the real world.

3.2 Continuous Time Varying Channel Models

Multiple models for the continuously time varying channel have been proposed such as the Basis Exponential Model (BEM) [18] and Autoregressive Model. While the BEM can be made quite accurate through proper choice of basis, such as Fourier basis or Slepian-

Wolf functions [19], it also increases complexity of the modeling process and produces less insightful conclusions. A simpler model may lead to closed form expressions that provide a valuable insight into the dynamic response to the channel.

Autoregressive (AR) models are much simpler models that predict the channel's present state as a linear combination of its past states. AR models can be chosen of any order, i.e. the number of past values that the present channel depends upon, but it has been seen that even with an order 1, an AR model closely matches the ideal Jakes' correlation initially when the channel is still highly correlated. This match is sufficient for us because interference cancellation systems are highly sensitive to channel change and are rendered ineffective by a small change in the channel. Hence the system must re-train with up to date channel information to null the interference. We will introduce the Autoregressive model of order 1 or the AR(1) model below and use it to derive the performance of an Interference Alignment system. As we will see, the AR(1) model provides useful insights about how long the data packet should be between re-trainings and it retains its accuracy as well.

3.2.1 Autoregressive Model of the Channel

A wireless MIMO channel with N transmit and M receive antennas is denoted by a $M \times N$ matrix H. Let t denote the discrete time when the channel is sampled. The channel matrix varies with time as follows:

$$H(t) = \beta H(t-1) + \sqrt{1-\beta^2}E(t), \tag{3.3}$$

where $\beta < 1$ but close to 1 is a fixed correlation constant that decides how fast the channel varies per sample. $E(t)$ is a matrix that constitutes the innovation or error terms added to the channel. All entries of $E(t)$ are indepedent and identically distributed (i.i.d.) as zero mean complex Gaussian (ZMCG) elements with a unit variance.

3.3 Combating Time Variation in the Channel

As discussed before, a time varying channel specially impacts interference cancellation systems like IA as their nulls are very sensitive to changes in the channel. There are multiple options on how a TX & RX beamforming system can adapt to changes in the channel.

1. **Receiver Tracking:** In this technique, no feedback is sent to the TX but the receiver constantly updates its beams to optimize its desired criterion. The transmitter has its beams frozen because it cannot get up-to-date information about the channel in the absence of feedback. The receiver may either use *data-aided tracking* i.e. use the decoded symbol to adapt the receive beam using adaptive algorithms like least mean squares (LMS), recursive least square (RLS), Kalman filter etc. This strategy adds no to minimum additional signaling overhead.

2. **RX-TX Update in the Middle:** In this scheme, a few pilot symbols are sent during data transmission from RX to TX allowing the TXs to re-position their beams. Following this, pilot symbols are sent from TX to RX to help re-calibrate the RX beams. This process may be repeated a few times back and forth to achieve good beam positioning. Importantly, no new channel estimates are shared among the nodes. This strategy is essentially the same as doing a few ping-pongs of the distributed IA protocol. It adds a medium signaling overhead.

3. **Full Beam Re-Training:** Old beams are discarded at both TX and RX and new beams are computed after every data packet. The designer can play with the frequency of this re-estimation to suit the channel conditions. Pilot symbols are exchanged bidirectionally and are used to compute a new channel or beam estimate. The beam estimate may be refined multiple times in distributed IA while in centralized IA, all the channel estimates are shared with a central node. This strategy incurs the highest overhead compared with both previous strategies.

We want to find out how much each strategy helps a system to operate well in a time varying environment. The no feedback receiver tracking strategy gives improved SINR at no or low cost and hence should be used along with strategy 3. But it is difficult to analytically quantify the performance improvement with strategy 1 because it uses stochastic algorithms and symbol decisions. Similarly strategy 2 is promising as it allows one to perturb the current beam to reflect the changed channel by adding a small overhead. But its iterative nature creates difficulty in characterizing its performance analytically. Strategy 3 where we do full beam re-estimation after every data phase and can only alter the packet length is amenable to analytical exploration.

We will demonstrate the effectiveness of all three strategies for IA in simulation but, in the next section, we present an analysis of strategy 3 i.e. optimizing the length of the data phase while doing full beam re-estimation.

3.4 Choosing Optimal Data Packet Duration Per Fading Realization [1]

As alignment of interference requires tight coupling to estimates of the channel, time variations in the channel lead to loss of capacity. Thus, the length of the data and training phase should be appropriately chosen so as to maximize the average capacity. In this section we present a way to model the sum capacity achieved by interference alignment in a time varying wireless channel and show that in slowly changing channels, it is possible to maximise the average capacity using just the knowledge of the maximum Doppler frequency of the interferers.

For a given training duration, we select a new data phase duration per channel fading instance and show that our predicted average capacity strongly tracks the true average capacity using the optimized data phase duration. In high Doppler scenarios, we do not

[1] This section is reproduced from [20] ©2016 IEEE.

see a benefit from our scheme because the channel capacity has high variance and a first order description is no longer sufficient. We further propose that the receiver can adapt its beamweights using a least-squares technique and approach the instantaneous sum capacity of interference alignment.

3.4.1 Capacity of the Time Varying Channel

Let H_{kl} denote the channel from the transmitter of the $l-$th user to the receiver of $k-$th user. Assume that the direct channel at time 0, $H_{kk}(0)$, and the interference channels at time 0, $H_{kl}(0)$ are estimated perfectly at the $k-$th receiver, through a channel training algorithm that finishes at time t=T_r. For the sake of simplicity, we assume that the channel does not change in this period, hence $H_{kl}(0) = H_{kl}(T_r)$, though this assumption is easy to shed. We normalize the noise power to unity. Let $C(t)$ denote the sum capacity of the IA system at time t.

$$C(t) = \sum_{k=1}^{L} \log \left(\frac{\sum_{l=1}^{L} |w_k^* H_{kl} p_l|^2 + ||w_k||^2}{\sum_{l=1, l\neq k}^{L} |w_k^* H_{kl} p_l|^2 + ||w_k||^2} \right), \tag{3.4}$$

where p_k and w_k are the transmit and receive beamvectors respectively. For now, let us neglect the contribution of noise in this equation in both the numerator and denominator. Later, we will revisit this equation to include the effect of noise. With this understanding, we will call the new expression the interference limited capacity $C_{IL}(t)$.

$$C_{IL}(t) = \sum_{k=1}^{L} \log \left(\frac{\sum_{l=1}^{L} |w_k^* H_{kl} p_l|^2}{\sum_{l=1, l\neq k}^{L} |w_k^* H_{kl} p_l|^2} \right). \tag{3.5}$$

Even though $C_{IL}(0)$ is a known quantity, $C_{IL}(t)$ is a random variable (due to the unpredictability of the channel at time t). Our aim is to find information about the pdf of $C_{IL}(t)$ (such as its moments) to be able to predict the expected capacity at time t. This can enable us to make better decisions on questions such as when to retrain. We note here that to achieve the sum capacity in eq. 3.4, we need feedback from the receiver about instantaneous SINR so that the transmitter can adjust its modulation and coding accordingly. For

simplicity, we assume that a low rate feedback is periodically available to the transmitter for this purpose. Let p_l be the beamforming vector used at the $l-$th transmitter and w_k be the receive beamformer used at the $k-$th receiver. Define the beamformed channel at time t as $x_{kl}(t) = H_{kl}(t)p_l$, $\forall k, l$. We assume that $x_{kl}(t)$ and $x_{kl}(0)$ are jointly Gaussian and that the elements h_{ij} of a channel matrix are independent and identically distributed (i.i.d.) complex Gaussian random variables and are correlated in time as $\mathrm{E}[h_{ij}(t)h_{ij}^*(0)] = \rho(t)$. For example, according to the Jake's model of channel correlation, $\rho(t) = J_0(2\pi f_d t)$, where $J_0()$ is the zero-order Bessel function of the first kind and $f_d = vf_0/c$ is the maximum Doppler frequency, where v is the vehicle speed, f_0 is the carrier frequency and c is the speed of light.

Lemma 1. *The pdf of $x_{kl}(t)$ conditioned on $x_{kl}(0)$ is given by $f_{x_{kl}(t)|x_{kl}(0)} = \mathcal{CN}(\rho_t x_{kl}(0), ||p_l||^2(1-\rho_t^2)I_M)$.*

Proof. See Appendix A. □

It is logical to condition on $x_{kl}(0)$ because we have estimated $x_{kl}(0)$ during channel estimation. Thus, the conditional pdf of $w_k^* x_{kl}(t)$ is given by $w_k^* x_{kl}(t)|\{x_{kl}(0)\}_{l=1}^L \sim \mathcal{CN}(m_{kl}(t), \sigma_{kl}^2(t))$ where $m_{kl}(t) = \rho_t w_k^* x_{kl}(0)$ and $\sigma_{kl}^2(t) = ||p_l||^2||w_k||^2(1-\rho_t^2)$. As we will show later, $||p_k||^2 = 1$ and $||w_k||^2 = 1$, $\forall k$ due to the way the beamforming vectors are chosen by the interference alignment algorithm. Hence $\sigma_{kl}^2(t) = \sigma^2(t) = (1-\rho_t^2)$. Thus, the conditional density of the numerator of the $k-$th log term in eq. (3.5), given $\{x_{kl}(0)\}_{l=1}^L$, is non central chi-square with $2L$ degrees of freedom, with non centrality parameter $\lambda_{k,num} = \sum_{l=1}^L (m_{kl}(t))^2$ and variance of each Gaussian equal to $\sigma_r^2(t) = \sigma^2(t)/2$ [21].

We can view a non central chi square distribution with parameters λ and σ_r^2, as a Poisson mixture of central chi square random variables with parameter σ_r^2 [22], i.e.

$$f_{\chi'^2_{2L}}(z) = \sum_{j=0}^{\infty} e^{-\frac{\lambda}{2}} \frac{(\lambda/2)^j}{j!} f_{\chi^2_{2L+2j}}(z) \tag{3.6}$$

If Y is the log of the above non central chi-square random variable, then its pdf is given by $f_Y(y) = e^y f_{\chi'^2_{2L}}(e^y)$. As a result, we can write the moments of the log non central chi-square

distribution in terms of moments of the log central chi-square distribution, viz.

$$\mathrm{E}[Y^r] = \sum_{j=0}^{\infty} e^{-\frac{\lambda}{2}} \frac{(\lambda/2)^j}{j!} \int_{z=0}^{\infty} e^z f_{\chi^2_{2L+2j}}(e^z)\, z^r\, dz \tag{3.7}$$

Moments of the log central chi square distribution can be easily found as described in [22] which we summarize here for completeness. If $p \sim \chi^2_\nu$ with parameter σ^2 and $q = \log p$, then the cumulant generating function of q is

$$K(t) = \log \mathrm{E}[e^{qt}] = \log \mathrm{E}[p^t]. \tag{3.8}$$

The moments of p are easily found from its pdf, yielding the expression

$$K(t) = t \log 2\sigma^2 + \log \Gamma(\frac{\nu}{2} + t) - \log \Gamma(\frac{\nu}{2}). \tag{3.9}$$

Hence, the $j-$th cumulant is given by $\kappa_j = \log 2\sigma^2 + \psi(\nu/2)$ for $j = 1$ and $\kappa_j = \psi^{(j-1)}(\nu/2)$ for $j > 1$, where $\psi(.)$ is the digamma function and $\psi^j(.)$ is the polygamma function. The raw moments $\mu_n = \mathrm{E}[q^n]$ can then be computed via the formula

$$\mu_n = \kappa_n + \sum_{m=1}^{n-1} \binom{n-1}{m-1} \kappa_m \mu_{n-m} \tag{3.10}$$

Importantly, the first moment is $\mu_1 = \log 2\sigma^2 + \psi(\nu/2)$.

Using the eq. (3.4) through (3.10), we can calculate the conditional expected capacity at time t, conditioned on the initial channel information, i.e.

$$\begin{aligned} \mathrm{E}\left[C_{IL}(t) | \{x_{kl}(0)\}_{l=0}^{L}\right] = &\sum_{k=1}^{L} \mathrm{E}\left[\log \sum_{l=1}^{L} |w_k^* H_{kl} p_l|^2\right] \\ &- \sum_{k=1}^{L} \mathrm{E}\left[\log \sum_{l=1, l\neq k}^{L} |w_k^* H_{kl} p_l|^2\right] \end{aligned} \tag{3.11}$$

The intuition behind finding conditional expectation is to be able to predict the capacity

curve for every channel realization and not just average statistics. We will later present results of the performance of this capacity metric, averaged over the channel, which will justify its use. Calculation of the expectations in eq. (3.11) is feasible because the arguments of log are non central chi-square distributed random variables, for which we have already described a method for computing its moments.

Noise Limited versus Interference Limited System

To obtain eq. (3.5) from eq. (3.4), we neglected the contribution of noise power to the capacity, assuming that the system is inherently interference limited. This allowed us, for instance, to easily compute the expectations in eq. (3.11). Neglecting the noise term is justified for the numerator of the log term in eq. (3.4) because we assume the SINR is high, but for the denominator, we require the interference power to be more than the noise power. The latter assumption is frequently not true at $t << T_c$, where T_c is the coherence time, because IA essentially converts an interference limited system into a noise limited system. At small t, the power leakage from interference into the signal subspace may be very low. This leakage increases with time due to the changes in the channel and becomes significant enough to justify neglecting the noise term, when t is on the order of T_c. Without neglecting the noise term, the numerator and denominator of eq. (3.4) are no more non central chi-square, which leads to further complications in modeling the capacity. To avoid this, we simply assume that the system is noise limited when noise power is more than the interference power and replace the interference term in the denominator of (3.4) by a constant value equal to its mean and call the resulting expression the noise limited capacity.

$$C_{NL}(t) = \sum_{k=1}^{L} \log\left(\frac{\sum_{l=1}^{L} |w_k^* H_{kl}(t) p_l|^2}{\lambda_{k,den} + ||w_k^2||}\right), \tag{3.12}$$

where $\lambda_{k,den} = \mathrm{E}\left[\sum_{l=1,l\neq k}^{L} |w_k^* H_{kl}(t) p_l|^2 | \{x_{kl}(0)\}_{l=0}^{L}\right]$. Defining the interference leakage at the $k-$th receiver as $\mathcal{I}_k = \sum_{l=1,l\neq k}^{L} |w_k^* H_{kl}(t) p_l|^2$, we can write our proposed capacity model

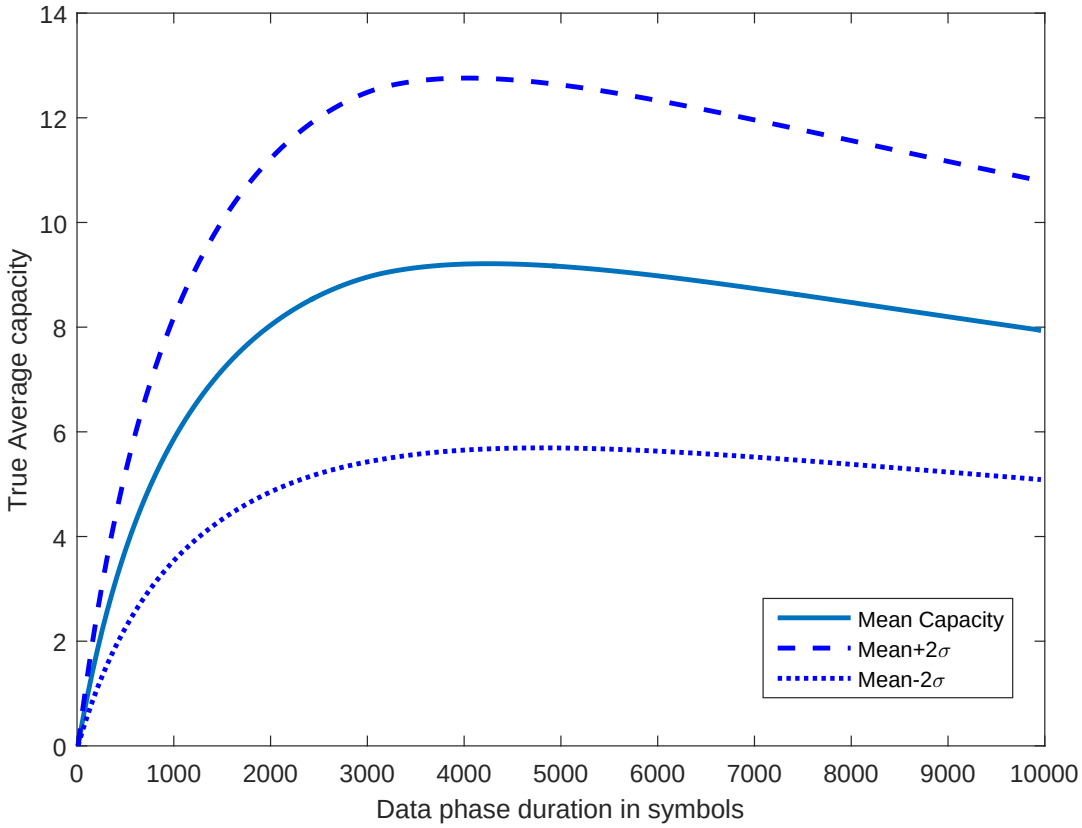

Figure 3.2: Plot of $C_{H,av}(T_d; T_r)$ against T_d with fixed $T_r = 1270$ symbols and $f_d = 10$ Hz, showing the concave nature of the curve.

concisely as,

$$C(t) = \sum_{k=1}^{L} \mathbb{1}(\mathcal{I}_k < 1) C_{NL}(t) + \mathbb{1}(\mathcal{I}_k \geq 1) C_{IL}(t), \tag{3.13}$$

where $\mathbb{1}(.)$ is the indicator function.

3.4.2 Optimising the Data Phase Duration

The duration after which an IA system must retrain itself can be optimized to maximize the average sum capacity. The average capacity for a specific channel realization can be stated as

$$C_{H,av}(T_d; T_r) = \frac{\int_{T_r}^{T_d+Tr} C(t)}{T_d + T_r} \tag{3.14}$$

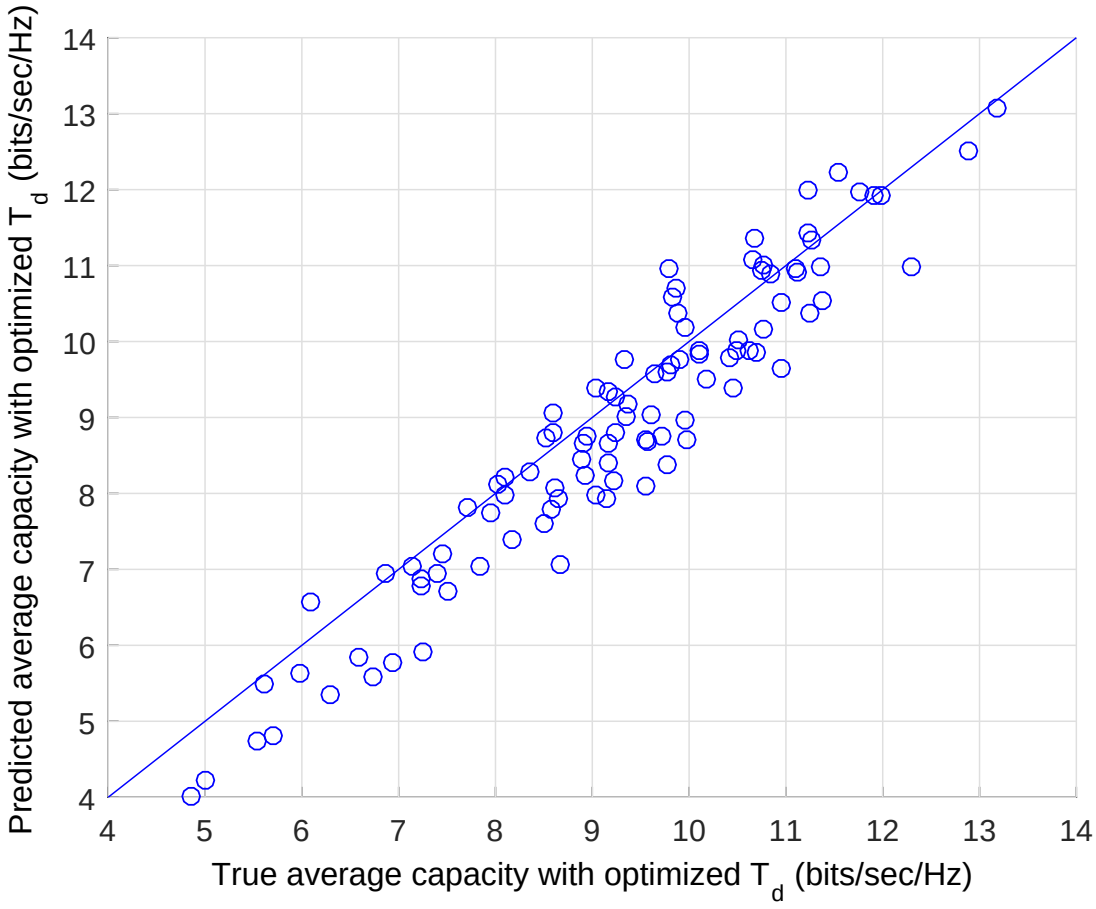

Figure 3.3: A plot of the true average capacity and predicted average capacity calculated using the optimized data phase length for $f_d = 10$ Hz.

where T_d is the length of the data phase and T_r is the length of the training phase. We can use our estimated conditional expected capacity from eq. (3.13) in eq. (3.14) and find the T_d that maximizes $C_{H,av}$. Here, we do this optimization numerically.

3.4.3 Simulations and Results

We simulate a $L = 3$ user scenario where each user consists of a transmitter and receiver separated by some distance d so that the receive SNR is 20dB. All the transmitters are equidistant from all the receivers. Each transmitter and receiver has $M = 2$ antennas. The users follow the distributed MAX-SINR Interference Alignment algorithm proposed in [7] to iteratively find the transmit and receive beamvectors. The IA algorithm also provides

an estimate of the beamformed channels $x_{kl}(0) = H_{kl}(0)p_l$ to the $k-$th receiver. Using eq. (3.13), we can find the conditional expected capacity at time t, given $\{x_{kl}(0)\}_{l=1}^{L}$. We choose the Jake's model for channel correlation with three values of Doppler frequency, $f_d = 1$ Hz, 10 Hz and 100 Hz. Channel estimation is performed using a Zadoff-Chu sequence of length 127. The IA algorithm is run for 5 iterations in a ping-pong fashion. The symbol time is $t_s = 10^{-6}$ sec/symbol, hence coherence time $T_c = \frac{0.1}{f_d}$ sec. For example, for $f_d = 10$ Hz, $T_c = 10^4\, t_s$ sec, which means 10^4 symbols can be transmitted in one coherence period.

Fig. 3.2 shows the ensemble mean of average capacity $C_{H,av}(T_d; T_r)$, and $\pm 2\sigma$ curves for $f_d = 10$ Hz, versus T_d, depicting the concave nature of the curve. We choose T_d equal to the abscissa that maximizes this curve. Fig. 3.3 shows that when using this optimized T_d, a strong linear relationship exists between our predicted average capacity and the true average capacity with the true optimized T_d. Thus, the prediction can be used to set the time between retraining epochs in order to maximize system throughput.

We have computed the expected capacity as a function of time assuming a fixed training period, and optimized the data interval according to the predicted capacity. We compare this to simply assuming that the coherence time is the correct data interval. Fig. 3.4 shows that for $f_d = 10$ Hz, the gain from optimization varies from -5% to $+20\%$ in throughput compared to using the coherence time. The negative results occur because of the error in predicting T_d due to channel variations. The relatively modest gains for the better predictions are a consequence of the flatness of the average capacity curve beyond its maxima as seen in fig. 3.2. A pessimistic interpretation of these results is that all the trouble involved in making a good capacity prediction yields little. A more optimistic view is that it is sufficient from an information theoretic point of view to use an easily measured quantity such as the Doppler to optimize the training duty cycle.

For $f_d = 1$ Hz similar but better results are obtained. Fig. 3.5 shows that the predicted and true average capacity are strongly correlated when using the optimized T_d. Fig. 3.6 shows that the gain from optimization varies in throughput from -6% to 60% with respect

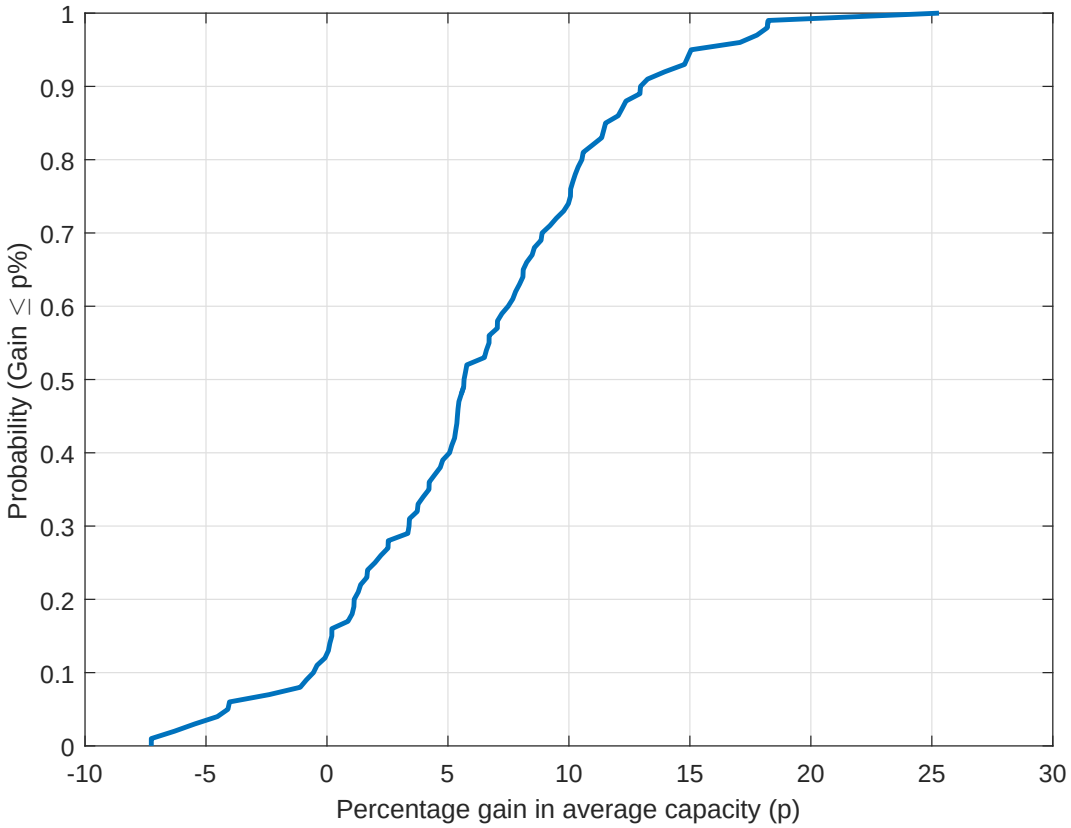

Figure 3.4: Cumulative distribution function of the percentage gain in average capacity by using optimized T_d against $T_d = T_{coherence}$ for $f_d = 10$ Hz.

to simply using the coherence time for the data interval. The gain is noticeably higher for this slower varying channel than at $f_d = 10$ Hz. However, for high Doppler, the chosen training interval is a large proportion of the coherence time which means the channel estimates are not good. Hence, we see no no net gain from predicting capacity in this fast varying channel. This suggests that a much more complex optimization is required in such conditions. We defer discussion of possible fixes and characterization of the capacity cost of high Doppler to future work.

We now propose a simple method to approaching the promised predicted capacity for slowly changing channels. In the data transmission epoch the receivers can track the SINR and also adaptively adjust receiver weights to maximize it using least squares techniques. Periodic short messages to the transmitter can inform it when the number of bits per symbol in the constellation needs to be reduced. In this way, the transmitter will always send the largest number of bits the channel can support. It is also possible by this means to adaptively change the balance between training and data transmission by triggering retraining when the measured SINR indicates the data rate will soon fall below some programmable but fixed fraction of the maximum.

Our simulations have so far considered only the case of a common Doppler, with both interference sources having similar strength. In practice it is rare to have two interferers with similar strength for any protracted period of time. It is much more likely that one interferer will dominate. This suggests that we should base retraining on the maximum of the Doppler for the desired link and strongest interferer. Nonetheless, since a high degree of suppression can be achieved for the dominant interferer, it is possible that the rate of change of the interference from the second strongest interferer cannot be entirely neglected. Given interference coupling across the network, this could result in many links being forced to have high training duty cycles. One solution is to consider Doppler as well as SINR in making dynamic channel assignments so that global estimated capacity can be maximized, accounting for the loss in achievable capacity due to high Doppler. This is a fruitful area for

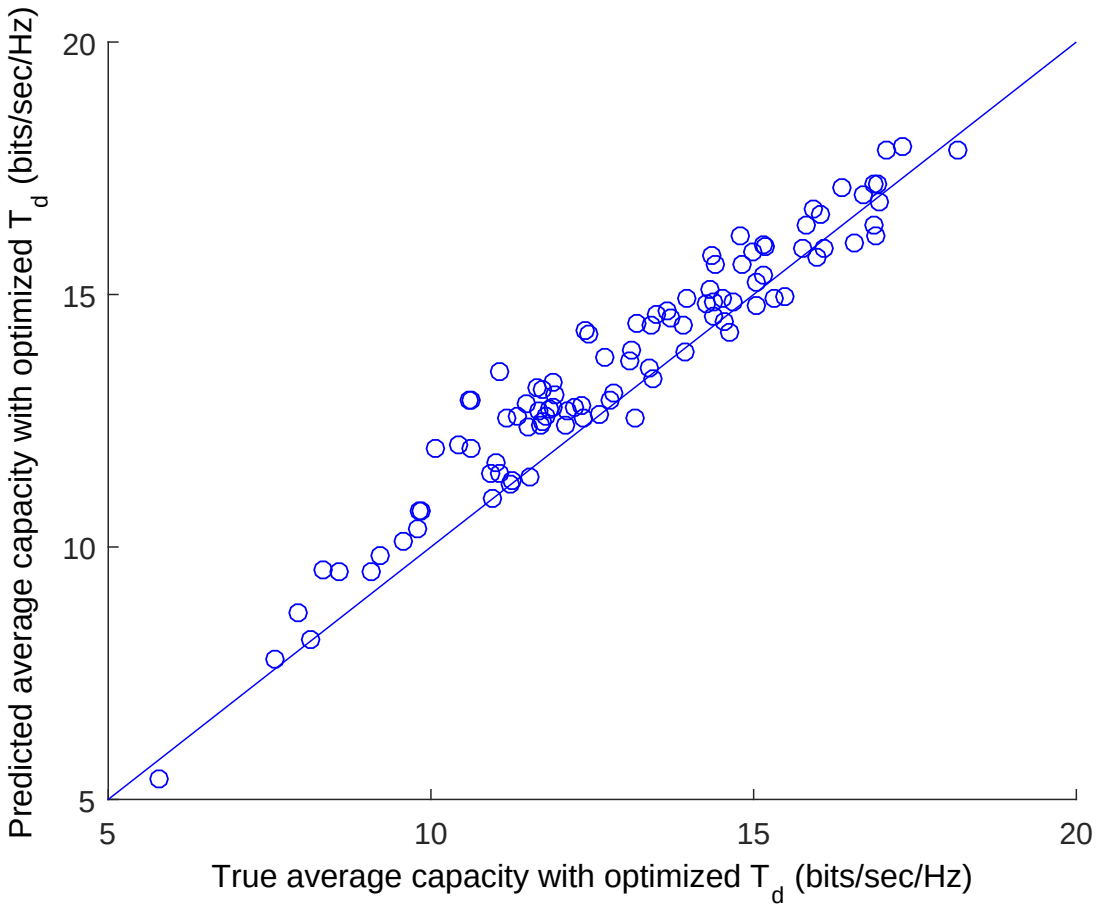

Figure 3.5: A plot of the true average capacity versus the predicted average capacity using the optimized data phase duration for $f_d = 1$ Hz.

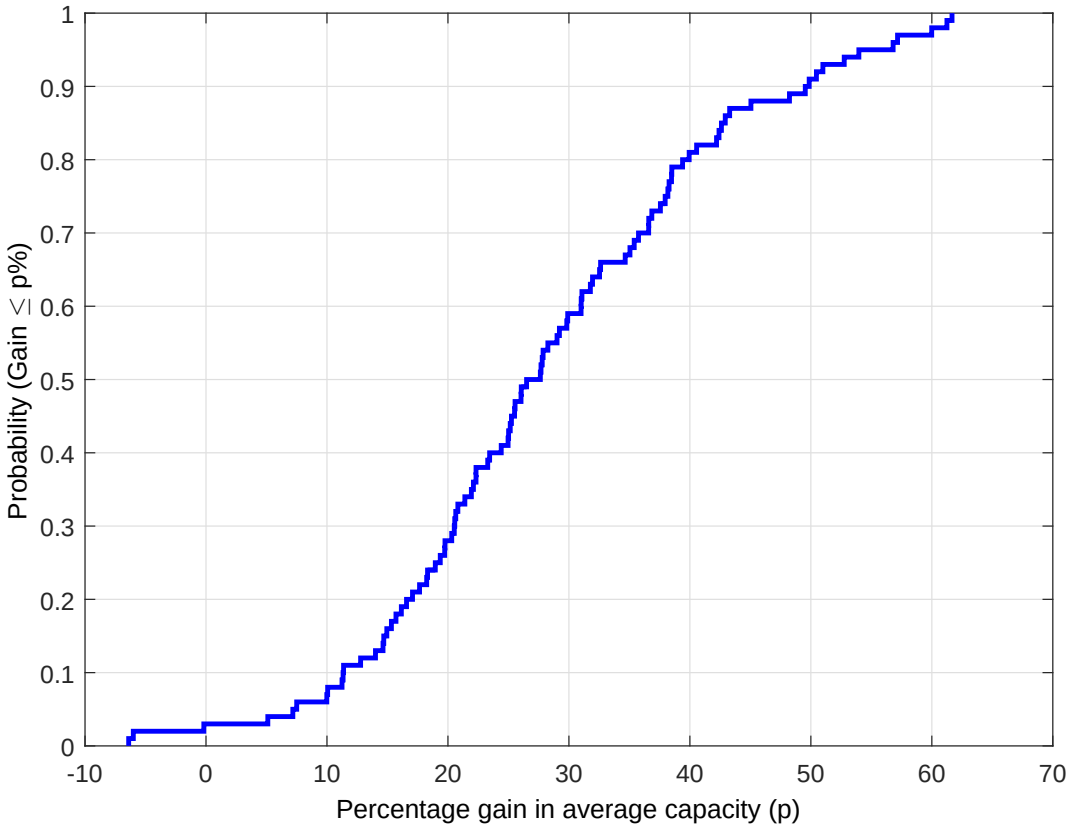

Figure 3.6: Cumulative distribution function of the percentage gain in average capacity by using optimized T_d against $T_d = T_{coherence}$ for $f_d = 1$ Hz.

future investigation.

3.5 IA Under a Gauss Markov Channel[2]

The objective of this section is to present analysis of the performance of an IA system under a Gauss-Markov or AR(1) channel and to optimally decide the data phase length that maximizes throughput *on average* (instead of per channel realization in the previous section). This data phase length can be used as a protocol parameter that is shared among all nodes. It depends only the large scale pathloss conditions and is independent of the small scale fading condition (assuming Rayleigh fading).

There can be multiple models of the fading channel under which the performance of IA can be studied. A block fading channel is simpler to analyze. Authors in [24] have analyzed the overhead of achieving alignment along with feedback under a block fading channel. A continuously fading channel model, on the other hand, is more tedious to analyze than a block fading model but also more insightful because as the channel changes over time, increasingly misaligned interference will affect the SINR, rate and error performance. Works [25] and [26] present simulation results of IA in this setting and tune the data phase duration or adapt the receiver or transmitter beams (which requires much more feedback) to maximize throughput. In [27] authors present theoretical results on the optimum data and pilot duration under a time varying channel with the assumptions of equal power links and a limiting high SNR.

But the question, how does a generic IA system perform under a continuously time varying channel is unanswered. We provide results that answer this question and provide critical insights about the performance of IA. We choose a continuously time varying channel model called the Gauss-Markov channel which has been used extensively previously [28], [29], [30], ([31], pg. 45).

The contribution of this section is to present a closed form expression for the complementary cumulative distribution function (CCDF) of the SINR over time of a link in a K

[2]This section is reproduced from [23] ©2018 IEEE.

link IA system in a Gauss-Markov channel[3]. We assume that the node designing the IA beam vectors knows the long-term path gains for each link. We use the SINR CCDF to compute the time varying expected rate achieved per link and then integrate it to get the link throughput. Thus we obtain an expression for the system throughput in terms of the data phase duration T_d and the training overhead T_r which enables optimizing the data phase duration to maximize network throughput in the current interference conditions. We also present a simplified expression for the SINR CCDF that is much easier to work with but still quite accurate.

Closest to our work is [27] where they present the average SINR and throughput expressions assuming that the misalignment over time simply increases the effective noise power whereas we model the additional interference as Gaussian random variables. Further, we can simplify our rate expression so we don't need the high SNR assumption for integration since like practical systems we assume fixed modulation and coding Schemes (MCS). Other works such as [29] obtain outer bounds on the decrease in expected rate over time using Jensen's inequality but not a expression for the expected rate over time.

The section is as organized as follows. First we present the system and explain the time varying channel model. Then we give the expressions for the SINR CCDF (both accurate and simplified) and the system throughput followed by simulation results to validate the theory. We also give results showing how the right balance between data and training can be achieved. A word on notations: Upper case letters like H denote matrices, lower case letters x denote vectors or scalars, $(.)^{\mathrm{H}}$ denotes conjugate transpose operation and $\mathcal{CN}(\mu, \sigma^2)$ denotes a complex Gaussian distribution with mean μ and variance σ^2.

3.5.1 System and Channel Model

We consider a set of $2K$ users or radios where K users(transmitters) wish to communicate with the other K users(receivers) in a one-to-one fashion. Each receiver can hear all the

[3]Complementary CDF = 1- CDF

transmitters and all use the same frequency band. Each node is equipped with M antennas. Transmitter j transmits an information symbol $x_j(t)$ at time t multiplied by a $M \times 1$ beam-vector p_j. Receiver i uses a $M \times 1$ receive beam-vector w_i. These beams are computed after a training (channel estimation) phase of length T_r and kept unchanged during the data phase of length T_d. The wireless channel between the transmitter j and receiver i is denoted by $G_{ij} = H_{ij}\sqrt{P_{ij}}$ and is a matrix of dimension $M \times M$. H_{ij} is the short term fading component of the $j \rightarrow i$ link and P_{ij} includes the transmit power of the j-th (transmit) user and the path gain. Additive white Gaussian noise (AWGN) of constant variance σ_n^2 is present independently at each receiver antenna. For a stationary channel, the received vector at user i can be written as

$$y_i(t) = H_{ii}\sqrt{P_{ii}}p_i x_i(t) + \sum_{\substack{k=1 \\ k \neq i}}^{k=K} H_{ij}\sqrt{P_{ij}}p_j x_j(t) + n_i(t). \tag{3.15}$$

3.5.2 Time Varying Channel Model

In the previous section we considered a block constant channel. Now we relax the channel to be continuously time varying. Our MIMO channel H_{ij} has i.i.d. Rayleigh fading entries with unit power. The MIMO channel itself is varying every symbol in a Gauss-Markov model as follows,

$$H_{ij}(t) = \beta_{ij}H_{ij}(t-1) + \sqrt{1-\beta_{ij}^2}E_{ij}(t), \tag{3.16}$$

where $0 < \beta_{ij} < 1$ is a fixed correlation constant depending on the Doppler rate of link $j \rightarrow i$ and $E_{ij}(t)$ is a error matrix with i.i.d. Zero Mean Complex Gaussian (ZMCG) unit variance elements. Here t denotes the symbol number. The value of β_{ij} can be chosen to match a known channel correlation at some specific time. For instance, if the channel coherence time T_c is selected according to the Jakes model to give a correlation value of 0.9, then approximately $T_c = 0.1/f_d$ where $f_d = vf_c/c$ is the Doppler frequency. We choose β_{ij}

through the equation $\beta_{ij}^{T_c} = 0.9$. To see why β_{ij} is chosen this way, we recursively unroll (3.16) to get,

$$H_{ij}(t) = \beta_{ij}^{t} H_{ij}(0) + \sqrt{1 - \beta_{ij}^{2t}}\bar{E}_{ij}(t), \tag{3.17}$$

where again, $\bar{E}_{ij}(t)$ is a matrix with i.i.d. ZMCG unit variance entries. The channel correlation from this model at time t is β_{ij}^{t}.

3.5.3 Interference Alignment in Gauss-Markov Channel

The transmit and receive beams w_i and p_i are unit norm vectors chosen through the procedure of Interference Alignment [7]. The time variation of channel is as derived in (3.17). Then the SINR of link i at time t can be written as

$$\mathrm{SINR}_i(t) = \frac{|w_i^{\mathrm{H}} H_{ii}(t) p_i|^2 P_{ii}}{\sum_{\substack{j=1 \\ j \neq i}}^{j=K} |w_i^{\mathrm{H}} H_{ij}(t) p_j|^2 P_{ij} + \sigma_n^2}, \tag{3.18}$$

where we model the noise contribution as a constant σ_n^2 (and not as a Gaussian) to avoid a situation where the SINR distribution does not have defined moments. The beam vectors w_i and p_i are found based on channel estimates obtained in the training phase. We assume that our system always has $K \leq 2M - 1$ which allows perfect interference alignment to be achievable [4]. Let $\mathcal{H}_{ij} = H_{ij}\sqrt{P_{ij}}$. Channel estimates are obtained during the training phase using minimum mean-squared error (MMSE) and contain error with known variance $\sigma_{\mathcal{E}_{ij}}^2$. Hence $\hat{\mathcal{H}}_{ij} = \mathcal{H}_{ij} + \mathcal{E}_{ij}$ where $\mathcal{E}_{ij} \sim \mathcal{CN}(0, \sigma_{\mathcal{E}_{ij}}^2)$. IA designs the beams so that the observed interference $w_i^{\mathrm{H}} \hat{\mathcal{H}}_{ij}(0) p_j = 0$ (or a negligible value) for $j \neq i$ [7]. Hence for the true channel we have, $w_i^{\mathrm{H}} \mathcal{H}_{ij}(0) p_j = -w_i^{\mathrm{H}} \mathcal{E}_{ij} p_j = \phi_{ij}$ where $\phi_{ij} \sim \mathcal{CN}(0, \sigma_{\phi_{ij}}^2)$. It is easy to see

that $\sigma^2_{\phi_{ij}} = \sigma^2_{\mathcal{E}_{ij}}$. Using (3.17), the residual interference term in the $j \to i$ link at time t is

$$w_i^{\mathrm{H}} \mathcal{H}_{ij}(t) p_j = \beta_{ij}^t \phi_{ij} + \sqrt{(1-\beta_{ij}^{2t}) P_{ij}} \underbrace{w_i^{\mathrm{H}} \bar{E}_{ij}(t) p_j}_{\bar{e}_{ij}}. \tag{3.19}$$

Since w_i and p_j are unit norm vectors independent of $\bar{E}_{ij}$, $\bar{e}_{ij} \sim \mathcal{CN}(0,1)$. The signal part $s_i = w_i^{\mathrm{H}} H_{ii}(t) p_i$ in (3.29) is also distributed as $\mathcal{CN}(0,1)$. Using the true signal s_i instead of the receiver's estimated signal is a minor assumption because SINR is affected highly by misaligned interference while the signal variation has un-noticeable effect. Also w_i and p_i are chosen independent of H_{ii}. Thus from (3.29),

$$\mathrm{SINR}_i(t) = \frac{|s_i|^2 P_{ii}}{\sum_{\substack{j=1 \\ j \neq i}}^{K} |\underbrace{\beta_{ij}^t \phi_{ij} + \sqrt{(1-\beta_{ij}^{2t}) P_{ij}} \bar{e}_{ij}}_{\sim \mathcal{CN}(0, \frac{1}{\lambda_{ij}})}|^2 + \sigma_n^2} \tag{3.20}$$

where $\frac{1}{\lambda_{ij}} = \beta_{ij}^{2t} \sigma^2_{\phi_{ij}} + (1-\beta_{ij}^{2t}) P_{ij}$. Next we present two useful lemmas. Lemma 2, restated from the literature, gives the probability density function of the interference term in (3.20). Lemma 3 uses lemma 2 to give us the complementary CDF of $\mathrm{SINR}_i(t)$ and corollary 1 derives the expected SINR at time t. The proofs of lemmas are given in the appendices.

Lemma 2. *Let Y be a sum of L independent exponential random variables with parameters $\lambda_1, \lambda_2, \cdots, \lambda_L$. Then the probability density function (pdf) of Y is given by*

$$f_Y(y) = \left[\prod_{i=1}^{L} \lambda_i \right] \sum_{j=1}^{L} \frac{e^{-\lambda_j y}}{\prod_{\substack{k=1 \\ k \neq j}}^{L} (\lambda_k - \lambda_j)} u(y). \tag{3.21}$$

where $u(y)$ is the unit step function.

The proof of lemma 2 is given in [32].

Lemma 3. *Consider a random variable $S = \frac{X}{Y + \sigma_n^2}$ where X is a exponential random variable with parameter λ_0, Y is a sum of L independent exponential random variables with parameters $\lambda_1, \lambda_2, \cdots, \lambda_L$, X and Y are independent, and $\sigma_n^2 > 0$. Then the Complementary CDF*

of S is given by

$$1 - F_S(s) = \sum_{j=1}^{L} \frac{\left[\prod_{i=1}^{L} \lambda_i\right] e^{-\lambda_0 s \sigma_n^2}}{\prod_{\substack{k=1 \\ k \neq j}}^{L} (\lambda_k - \lambda_j)(\lambda_j + \lambda_0 s)} u(s). \tag{3.22}$$

The proof is given in Appendix B.

Corollary 1. *The Expected value of S is given by*

$$\mathrm{E}[S] = \left[\prod_{i=1}^{L} \lambda_i\right] \sum_{j=1}^{L} \frac{e^{\lambda_j \sigma_n^2} E_1(\lambda_j \sigma_n^2)}{\prod_{\substack{k=1 \\ k \neq j}}^{L} (\lambda_k - \lambda_j)\lambda_0} \tag{3.23}$$

The proof is given in Appendix B.

The CDF of $\mathrm{SINR}_r(t)$ of the r-th link is given by lemma 3 and the expected value of SINR is given by corollary 1 where the number of interferers $L = K - 1$, $\lambda_0 = 1/P_{rr}$ and λ_i is the contribution of the i-th interferer which counting from user 1 onwards would mean the i-th user if $i < r$ or i+1-th user if $i > r$. With this mapping, the i-th user contributes $\lambda_i = \frac{1}{P_{ri}(1-\beta_{ri}^{2t}) + \beta_{ri}^{2t}\sigma_{\phi_{ri}}^2}$ for $i = 1, 2, \cdots, r-1, r+1, \cdots, K$.

3.5.4 Expected Rate and Throughput

We focus on the achieved link rate and not link capacity for calculating throughput. The system supports one of $\mathcal{C}$ discrete modulation and coding schemes with SINR requirements of $\gamma_1 < \gamma_2 < \cdots < \gamma_{\mathcal{C}}$ and corresponding rates $r_1 < r_2 < \cdots < r_{\mathcal{C}}$ to support a fixed bit error rate threshold. If $\mathrm{SINR}(t) < \gamma_1$ then zero rate is supported. We assume the ability to constantly perform link adaptation with the help of a negligible amount of feedback. Let S_i denote $\mathrm{SINR}_i(t)$ for brevity. Then the expected achieved rate on link i at time t is simply the sum over the MCS of the probability of S_i lying in the right range, multiplied by the

corresponding MCS rate.

$$\bar{R}_i(t) = (F_{S_i}(\gamma_2) - F_{S_i}(\gamma_1))r_1 + \dots$$
$$\dots + (F_{S_i}(\gamma_{\mathcal{C}}) - F_{S_i}(\gamma_{\mathcal{C}-1}))r_{\mathcal{C}-1} + (1 - F_{S_i}(\gamma_{\mathcal{C}}))r_{\mathcal{C}}. \tag{3.24}$$

Here $F_{S_i(t)}(\gamma_c)$ can be evaluated precisely using lemma 3. Since the expected rate is time dependent, the sum throughput for a data phase of length T_d is approximated by integrating the rate over time

$$\mathrm{TH}(T_d) = \frac{1}{T_d + T_r} \sum_{i=1}^{K} \int_{t=1}^{T_d} \bar{R}_i(t). \tag{3.25}$$

To calculate the integral of the terms in (3.24) we make the following assumptions and approximations: A1) All links have equal Doppler rate β. A2) All links have equal initial CSI error variance $\sigma_{\mathcal{E}}^2$. A3) $\beta = 1 - 1/\alpha$ with $\alpha >> 1$ and hence $1 - \beta^{2t} = 2t/\alpha$. A1 is justified because links with very different Doppler will not align well and must be on separate channels. A3 will be justified through simulation in the next section. The equal CSI error variance $\sigma_{\mathcal{E}}^2$ assumption in A2 is justified when the interferers are above signal level and all users use the same length and type of pilots. More will be said on this in Remark 1.

With the above three assumptions, to perform the integration over time in (3.25) we put the values of λ_i into (3.22) and write the resulting CCDF of the SINR of link m at time t.

$$1 - F_{S_m(t)}(\gamma_c) =$$
$$\sum_{\substack{j=1 \\ j \neq m}}^{K} \frac{e^{-\lambda_0 \gamma_c \sigma_n^2} (P_{mj} - \sigma_{\phi_m}^2)^{K-3}}{\lambda_0 \gamma_c \prod_{\substack{k=1 \\ k \neq j,m}}^{K} (P_{mj} - P_{mk})} \underbrace{\frac{(\frac{2t}{\alpha} + \theta_0)^{K-2}}{(\frac{2t}{\alpha})^{K-2}(\frac{2t}{\alpha} + \theta_1)}}_{\text{time dependent term}}, \tag{3.26}$$

where $\theta_0 = \frac{\sigma_{\phi_m}^2}{P_{mj} - \sigma_{\phi_m}^2}$ and $\theta_1 = \frac{1 + \lambda_0 \gamma_c \sigma_{\phi_m}^2}{\lambda_0 \gamma_c (P_{mj} - \sigma_{\phi_m}^2)}$. Now we present a lemma that gives a general formula for integrating the time dependent term in (3.26).

Lemma 4. *The integral* $I_1(a,b) = \int_a^b \frac{(x+\theta_0)^{K-2}}{(x+\theta_1)x^{K-2}}\,dx$ *has a solution*

$$I_1(a,b) = \sum_{p=1}^{K-3}\left(1-\left(1-\frac{\theta_0}{\theta_1}\right)^p\right)\Big|\frac{x^{K-2-p}}{K-2-p}\Big|_l^u + \ldots \\ \left|\log(x-1) - \left(1-\frac{\theta_0}{\theta_1}\right)^{K-2}\log\left(x-1+\frac{\theta_0}{\theta_1}\right)\right|_l^u \tag{3.27}$$

where $l = \frac{b+\theta_0}{b}$ *and* $u = \frac{a+\theta_0}{a}$ *and* $|f(x)|_l^u = f(u) - f(l)$.

The proof is given in Appendix B. Using lemma 4 the integral of the time dependent term from $t = 1$ to T_d in (3.26) can be written as $\frac{\alpha}{2} I_1\left(\frac{2}{\alpha}, \frac{2T_d}{\alpha}\right)$. Now our analysis is complete and we are able to compute every term in (3.25) and (3.24) to calculate the throughput achieved for each T_d. The final step is to find $T_d^{\text{opt}} = \arg\max TH(T_d)$ and we will do this numerically because even though $TH(T_d)$ is a concave function (see simulation), setting the derivative to zero makes the expression unmanageable. We do not optimize over T_r due to two reasons a) initial CSI error $\sigma_{\mathcal{E}}^2$ depends on other factors besides T_r such as the cross correlation of the pilots used b) choice of T_r may be dictated by the other requirements such as initial frequency and phase offset correction.

Remark 1. $\sigma_{\mathcal{E}_{ij}}^2$ *depends on the power* P_{ij} *by MMSE estimation (e.g. for a scalar channel estimation at SNR* P_{ij}/σ_n^2, $\sigma_{\mathcal{E}_{ij}}^2 = \frac{P_{ij}\sigma_n^2}{P_{ij}+\sigma_n^2}$*). When some interferers have power below the noise floor, assumption A2 is invalid and we cannot use (3.26) or (3.27). Nonetheless, (3.24) and (3.22) still hold true so we do numerical integration in (3.25). However, for one hop systems, interference is expected to dominate noise.*

3.5.5 Simplified expression for CCDF of SINR

We can also find a simplified expression for the CCDF of SINR by considering the total interference, which is a sum of independent non-identically distributed (i.n.i.d.) exponential random variables, as a Gamma random variable [33]. This expression has far less terms and is much cleaner. It can be used in a similar manner to find a approximate expected rate

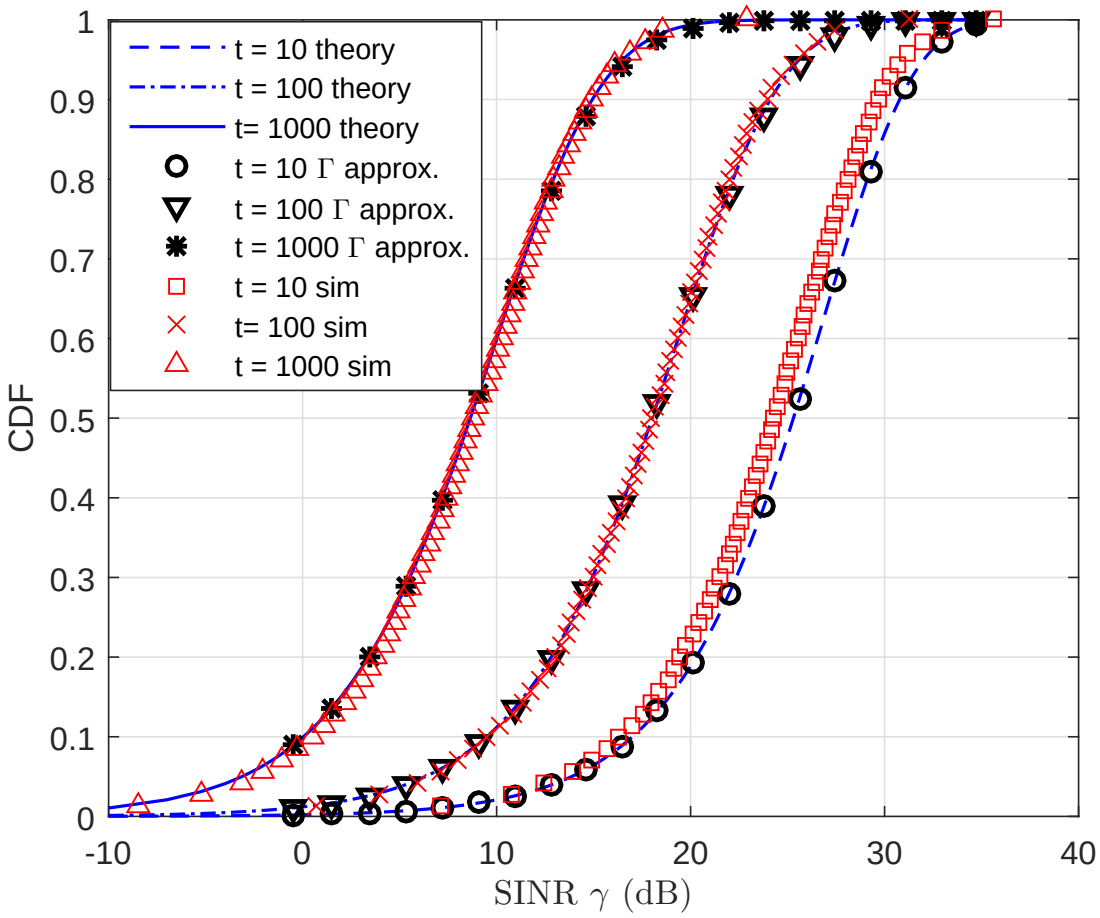

Figure 3.7: $K = 7$, $M = 4$, $\sigma_{\mathcal{E}}^2 = 0$, $\beta^{1875} = 0.9$. CDF of SINR of a link at $t = 10, 100,$ and 1000. The slight offset at $t = 10$ is because in simulation interference is not completely cancelled out in 50 iterations of IA.

$\bar{R}_i(t)$ and $TH(T_d)$. But we do not have a closed form integral of its terms with respect to t. We numerically evaluate the integral and show that the approximation is quite accurate.

Lemma 5. *A simplified expression for the CCDF of SINR of m-th link at time t is*

$$\Pr(\text{SINR}_m(t) > s) = \frac{e^{-\lambda_0 \sigma_n^2 s}}{(1 + \lambda_0 \theta s)^k} \tag{3.28}$$

where $k = \dfrac{\left(\sum_{\substack{i=1 \\ i \neq m}}^{K} 1/\lambda_i\right)^2}{\sum_{\substack{i=1 \\ i \neq m}}^{K} 1/\lambda_i^2}$, $\theta = \dfrac{\sum_{\substack{i=1 \\ i \neq m}}^{K} 1/\lambda_i^2}{\sum_{\substack{i=1 \\ i \neq m}}^{K} 1/\lambda_i}$, *and* $\lambda_i = \frac{1}{P_{mi}(1-\beta_{mi}^{2t}) + \beta_{mi}^{2t}\sigma_{\phi_{mi}}^2}$ *for* $i = \{1, \ldots, K\} \setminus m$.

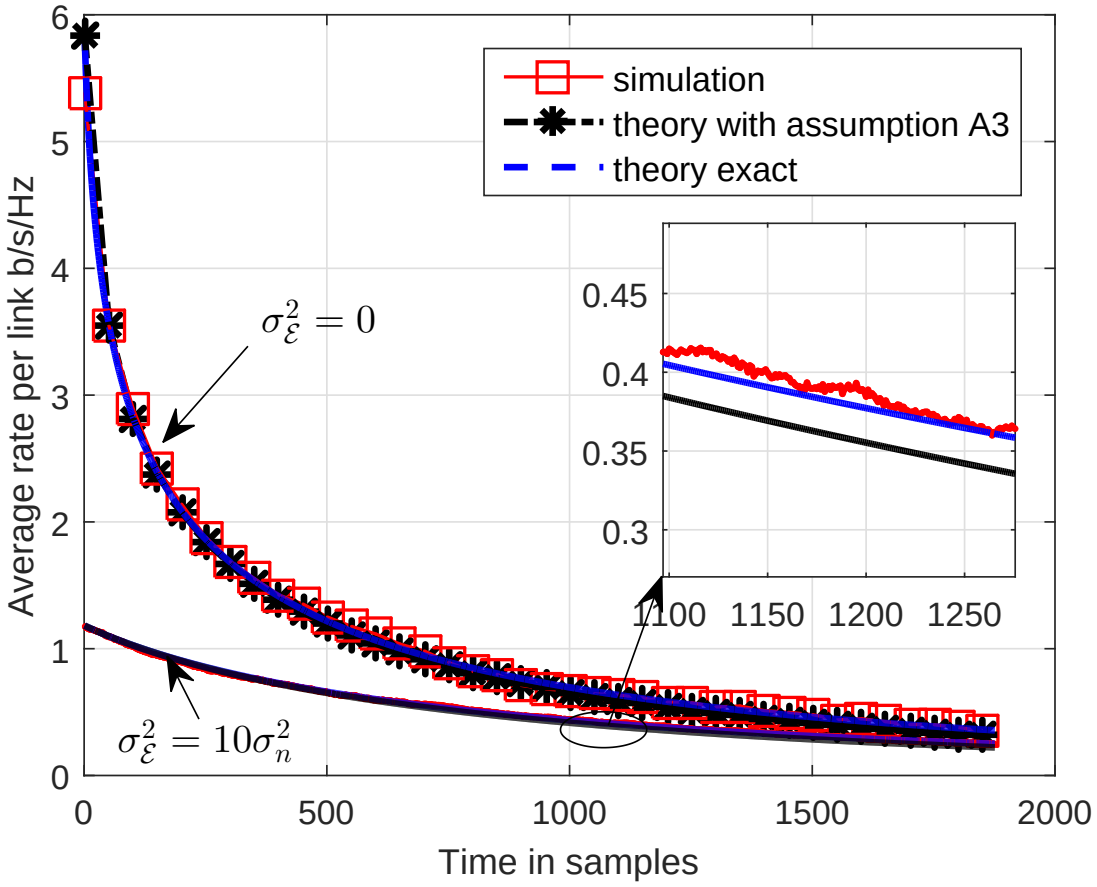

Figure 3.8: Expected rate of a link with time with no CSI error and with CSI error. Theory curves follow the true rate closely.

The proof is given in Appendix B.

3.5.6 Simulations and Results

We present simulation results for a $K = 7$ user system with $M = 4$ antennas for different values of channel estimation error $\sigma_\mathcal{E}^2$ and Doppler β. First we consider perfect channel estimation i.e. $\sigma_\mathcal{E}^2 = 0$. The transmit and receive beams p_i and w_i are formed by running the IA algorithm given in [7] for 50 iterations. SNR for all links is set to 30 dB. The received powers are distributed in an orderly fashion such that each receiver sees $K - 1$ interferers with interference $\gamma_d, 2\gamma_d, \ldots, (K-1)\gamma_d$ dB down respectively from the power in its direct link. We choose $\gamma_d = 3$ dB for our first simulation. We choose carrier frequency $f_c = 2$ GHz

and velocity $v = 36$ km/hr giving a doppler frequency $f_d = vf_c/c = 200/3$ Hz. We use a bandwidth of $1/T_s = 1.25$ MHz. Using Jake's model for 90% correlation the coherence time is $T_{\text{coh}} = 0.1/f_d T_s = 1875$ symbols. Thus we choose $\beta^{1875} = 0.90$ giving us $\beta = 0.9999438$ (see section II. A). Since all links are equivalent according to our topology, the CDF of SINR for one of the links at time $t = 10, 100$, and 1000 is shown in fig. 3.7 from simulation and theory, using (3.22) and the simplified CDF from (3.28). We also see that gamma approximation in (3.28) is quite accurate.

Now, we consider a system with $\sigma_{\mathcal{E}}^2 = 10\sigma_n^2$ i.e. ten times the noise variance where $\sigma_n^2 = -30$ dB. Our system supports one of 8 M-QAM modulation schemes with rates of $1, 2, 3, \ldots, 8$ bits/symbol with corresponding SINR requirements of 9.5860, 12.5963, 17.2812, 19.4506, 23.5397, 25.5715, 29.5310, and 31.5309 dB respectively (based on an uncoded BER of 10^{-5}). Based on these MCS, the expected bit rate achieved per link is shown in fig. 3.8 for both the perfect and imperfect CSI cases. The theoretical curves come by combining (3.24) and (3.22) and optionally approximation A3. Approximation A2 is not needed here. The overlapping curves show that A3 is appropriate. We also see that presence of CSI error significantly degrades the bit rate.

Next we show how the optimal data phase duration can be selected using the derived expressions. The throughput $\text{TH}(T_d)$ for different choices of data phase length is plotted in fig. 3.9 for a training phase of length 100 symbols. For both perfect and imperfect CSI, simulation matches with the expression obtained in (3.27) and also with the numerical integration of the simplified SINR CDF in (3.28). The maximum sum throughput is smaller with imperfect CSI but T_d^{opt} is larger. The reason is that with a small initial channel estimation error there is an incentive to retrain more frequently and revert to higher SINR which is absent when a system always starts off with bad channel estimates.

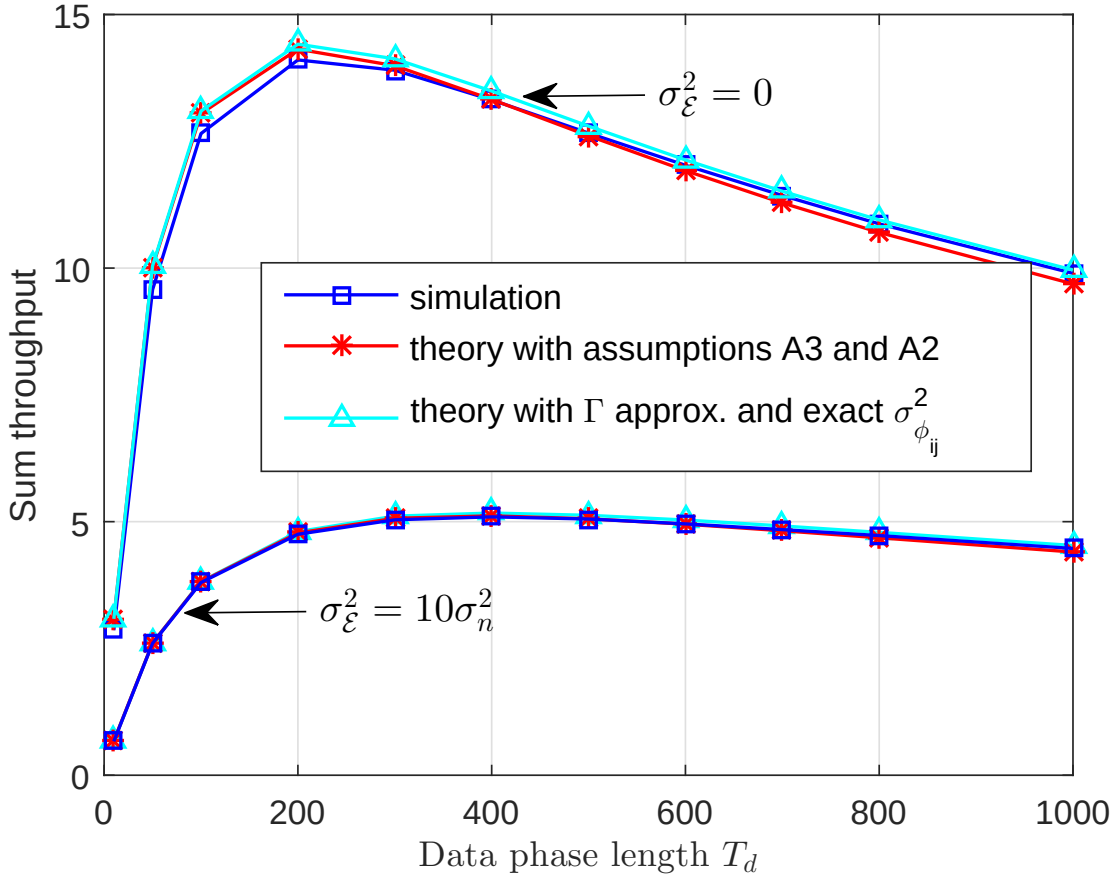

Figure 3.9: TH(T_d) versus T_d for $T_r = 100$, $\sigma_{\mathcal{E}}^2 = 0$ and $\sigma_{\mathcal{E}}^2 = 10\sigma_n^2$. Simulation parameters are $K = 7$, $M = 4$, $\beta^{1875} = 0.9$.

3.5.7 Effect of Interference environment, Doppler and Channel Estimation Error on T_d^{opt} and Maximum Throughput

In this subsection we study how the topology of the interference environment, and other factors, affect the maximum throughput and the choice of data phase length. We consider three kinds of topologies for a 7 user network: 1) each receiver sees 6 interferers at 10 dB, 20 dB, ..., 60 dB signal to interference ratio (SIR) respectively, 2) each receiver sees 6 interferers at 3 dB, 6 dB, ..., 18 dB SIR respectively, and 3) each receiver sees all 6 interferers at 0 dB SIR. Doppler is fixed at 200/3 Hz and channel estimation error variance is increased from 0 to $10\sigma_n^2$. T_d^{opt} and TH(T_d^{opt}) are found using the exact expression in lemma 4, except in

Table 3.1: T_d^{opt} and $\text{TH}(T_d^{\text{opt}})$ versus K. $\gamma_d = 3$ dB, $f_d = \frac{200}{3}$ Hz and $\sigma_{\mathcal{E}}^2 = \sigma_n^2$.

	Number of users (K)					
	2	3	4	5	6	7
T_d^{opt}	334	272	252	256	256	264
$\text{TH}(T_d^{\text{opt}})$ b/s/Hz	5.262	6.376	7.622	8.891	10.14	11.37

$\gamma_d = 10$ case where we use lemma 5 and numerical integration. The results in the left half of fig. 3.10 tell us that as expected, as the CSI error increases, sum throughput drops and the optimum data phase duration increases. The latter is because retraining must be done when the channel changes enough to match the initial CSI error. On the right half of fig. 3.10 effect of Doppler is shown and $f_d = 50/3$ Hz, $200/3$ Hz, and $800/3$ Hz are simulated corresponding to a velocity of 9 km/hr, 36 km/hr and 144 km/hr. We see that while all systems become worse at high Doppler, weaker interference environments are still operable by increasing the duty cycle because the channel misalignment is small. Under strong interference however, IA achieves much smaller throughputs and requires more frequent training, especially in high Doppler. This means that IA may not be the right candidate for such conditions. An interesting fact shown in table (3.1) is that as more users are added to an IA system the sum throughput increases but the optimum data phase duration decreases. This is unlike a block-fading channel where the data phase length is independent of the number of users and is dictated by the channel coherence time.

3.6 IA Under a Jakes Model Channel

Similar to the analysis of Gauss-Markov Channel, we can analyze the optimal data phase duration for the more complex Jakes model which denotes a more realistic channel model. The analysis closely follows the previous section, hence many details are omitted as they can be simply carried over.

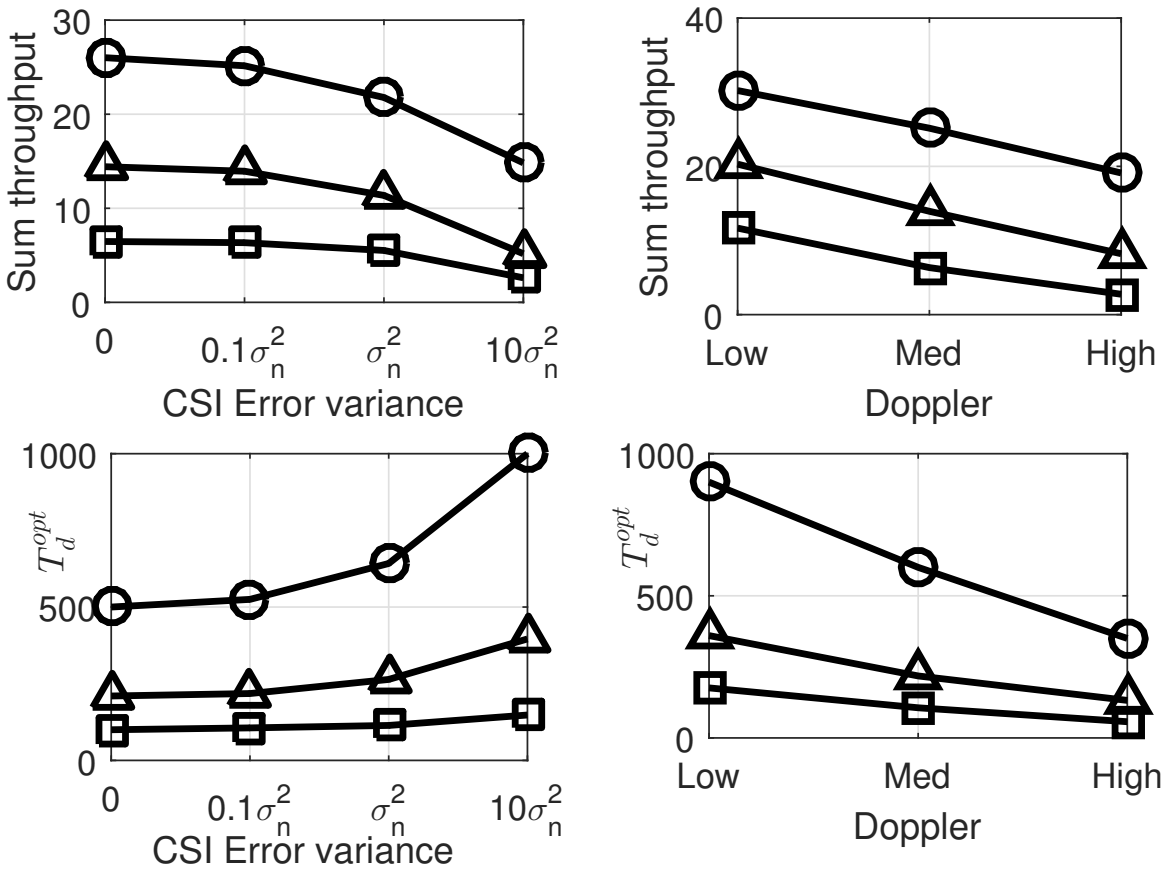

Figure 3.10: A plot of $\mathrm{TH}(T_d^{\mathrm{opt}})$ and T_d^{opt} versus CSI error variance $\sigma_{\mathcal{E}}^2$ and Doppler f_d. Circles denotes a topology with $\gamma_d = 10$ dB, triangles a $\gamma_d = 3$ dB, and squares a $\gamma_d = 0$ dB. Smaller the γ_d, harsher the interference environment.

3.6.1 SINR and Throughput CDF across time

Following along from 3.29, we write

$$\mathrm{SINR}_i(t) = \frac{|w_i^{\mathrm{H}} H_{ii}(t) p_i|^2 P_{ii}}{\sum_{\substack{j=1 \\ j \neq i}}^{j=K} |w_i^{\mathrm{H}} H_{ij}(t) p_j|^2 P_{ij} + \sigma_n^2}. \tag{3.29}$$

The Jake's model of the channel states that the channel now varies as

$$H_{ij}(t) = \beta_{ij}(t) H_{ij}(0) + \sqrt{1 - \beta_{ij}(t)^2} E_{ij}(t). \tag{3.30}$$

Here $\beta_{ij}(t)$ is the Jake's correlation equal to $J_0(2\pi f_{d_i} t)$ with f_{d_i} being the Doppler shift

of the i-th link. Let $\mathcal{H}_{ij} = H_{ij}\sqrt{P_{ij}}$. Channel estimates are obtained during the training phase using MMSE and contain error with known variance $\sigma^2_{\mathcal{E}_{ij}}$. Hence $\hat{\mathcal{H}}_{ij} = \mathcal{H}_{ij} + \mathcal{E}_{ij}$ where $\mathcal{E}_{ij} \sim \mathcal{CN}(0, \sigma^2_{\mathcal{E}_{ij}})$. IA designs the beams so that the observed interference $w_i^{\mathrm{H}}\hat{\mathcal{H}}_{ij}(0)p_j = 0$ (or a negligible value) for $j \neq i$ [7]. Hence for the true channel we have, $w_i^{\mathrm{H}}\mathcal{H}_{ij}(0)p_j = -w_i^{\mathrm{H}}\mathcal{E}_{ij}p_j = \phi_{ij}$ where $\phi_{ij} \sim \mathcal{CN}(0, \sigma^2_{\phi_{ij}})$. It is easy to see that $\sigma^2_{\phi_{ij}} = \sigma^2_{\mathcal{E}_{ij}}$. Using (3.30), the residual interference term in the $j \to i$ link at time t is

$$w_i^{\mathrm{H}}\mathcal{H}_{ij}(t)p_j = \beta_{ij}(t)\phi_{ij} + \sqrt{(1-\beta^2_{ij}(t))P_{ij}}\,\underbrace{w_i^{\mathrm{H}}\bar{E}_{ij}(t)p_j}_{\bar{e}_{ij}}. \tag{3.31}$$

The $\mathrm{SINR}_i(t)$ can be written as

$$\mathrm{SINR}_i(t) = \frac{|s_i|^2 P_{ii}}{\sum_{\substack{j=1 \\ j\neq i}}^{K} |\theta_{ij}|^2 + \sigma_n^2} \tag{3.32}$$

where $s_i \sim \mathcal{CN}(0, P_{ii})$ and $\theta_{ij} \sim \mathcal{CN}(0, 1/\lambda_{ij})$ where $1/\lambda_{ij}(t) = P_{ij}(1-\beta^2_{ij}(t)) + \sigma^2_{\phi}\beta^2_{ij}(t)$.

Using Lemma 5, we can write an approximate but quite accurate formula for complimentary cumulative density function (CCDF = 1- CDF) of $\mathrm{SINR}_m(t)$ as

$$\Pr(\mathrm{SINR}_m(t) > s) = \frac{e^{-\lambda_0\sigma_n^2 s}}{(1+\lambda_0\theta_m(t)s)^{k_m(t)}} \tag{3.33}$$

$1/\lambda_{mj}(t)$ is the sum of two effects, initial un-cancelled interference whose effect decreases with time, and time varying mis-aligned interference which grows with time. Hence we can construct a piecewise approximation as the following with T_0 a suitably chosen time:

$$1/\lambda_{mj}(t) = \begin{cases} \sigma^2_{\phi}\beta^2_{mj}(t) & \text{if } t \leq T_0 \\ P_{mj}(1-\beta^2_{mj}(t)) & \text{if } t > T_0 \end{cases} \tag{3.34}$$

By using this approximation $k_m(t)$ becomes independent of t.

Using eq. 3.24 and eq. 3.25, the throughput of the system can be written as

$$TH(T_d) = \frac{1}{T_d + T_r} \sum_{i=1}^{K} \sum_{t=1}^{T_d} \bar{R}_i(t) \tag{3.35}$$

The shape of the throughput curve versus T_d is concave; it increases sharply as T_d increases due to increasing duty cycle, then decays slowly beyond a point as SINR degradation over the data packet leads to throughput loss. The maximum point can be obtained by solving the equation

$$T_d^{\text{opt}} = \arg\min_{T_d} TH(T_d + 1) < TH(T_d) \tag{3.36}$$

Denoting the partial sum of rates up to time T_d as $P(T_d) = \sum_{t=1}^{T_d} \sum_{m=1}^{K} R_m(t)$, expanding eq. 3.36 T_d^{opt} is the smallest positive integer T_d that satisfies the following condition

$$P(T_d) > (T_d + T_r) \sum_{m=1}^{K} R_m(T_d + 1) \tag{3.37}$$

Eq. (3.37) can be checked for each positive integer T_d until we satisfy the equation.

3.7 Summary

In the first part of this chapter we have in a preliminary fashion considered the problem of capacity maximization in peer to peer networks where each user has multiple antennas that can be used to suppress interference from other users. We have derived an estimate of the capacity loss that results as a function of time from when transmitters cease adaptation to the channel, so that the duty cycle between training and data transmission can be optimized. We find that at low Doppler, it is possible to predict the time varying average capacity fairly well so as to optimize the data duration accordingly. The capacity gain over a scheme that retrains every coherence time is a decreasing function of the Doppler frequency. A practical scheme to achieve the promised capacity was proposed. However, at high Doppler, there

appears to be an inescapable capacity cost in that it can take too long to train compared to the channel coherence time in order to achieve the optimal combination of transmit and receiver antenna weights. In future work, we would like to characterize this gap and find practical algorithms to approach the highest throughput. We will also examine more complicated network topologies where the users experience a variety of Doppler conditions.

In the second part of this chapter we analyze Interference Alignment in a Gauss-Markov time varying channel and provide an exact expression of the CCDF of SINR at time t and a method to calculate the expected rate of a link at time t. We also provide a simpler expression for the CCDF that is almost as accurate. By using some assumptions, we give a formula for the sum throughput of the network for any choice of T_d and T_r which can be used to select the optimal data phase duration that maximizes the sum throughput of the network.

Finally we extend the analysis to the Jakes model of the channel where we provide a numerical method for computing the optimal data phase duration unlike the Gauss-Markov channel where we are able to go further and also provide a simple expression for the throughput of the system for any T_d. Designers can use this analysis to on-the-fly determine the appropriate length of data packets given the channel variation model and pathloss conditions in the real world.

Chapter 4

Practical Techniques for Enabling Distributed & Centralized Interference Alignment

There are more techniques to make Interference Alignment practically possible in a time varying channel beyond simply full beam re-training and optimizing the data phase length to maximize the throughput. One of the first important interference mitigation techniques is receiver tracking.

Receiver tracking works by continuously adapting the receive beam based on a stochastic estimate of the current intended channel and the interference co-variance matrix. The adaptation algorithm's input is the *received* symbol, which is the sum of desired signal and interference and its desired output is the *decoded* symbol. The weights of the adaptation filter correspond to the beam. The adaptation can be accomplished using a periodic update scheme like a Wiener filter or a stochastic update scheme like the LMS and RLS algorithms. Below we show the the additional benefit of using stochastic receiver tracking algorithms in IA in a time varying channel.

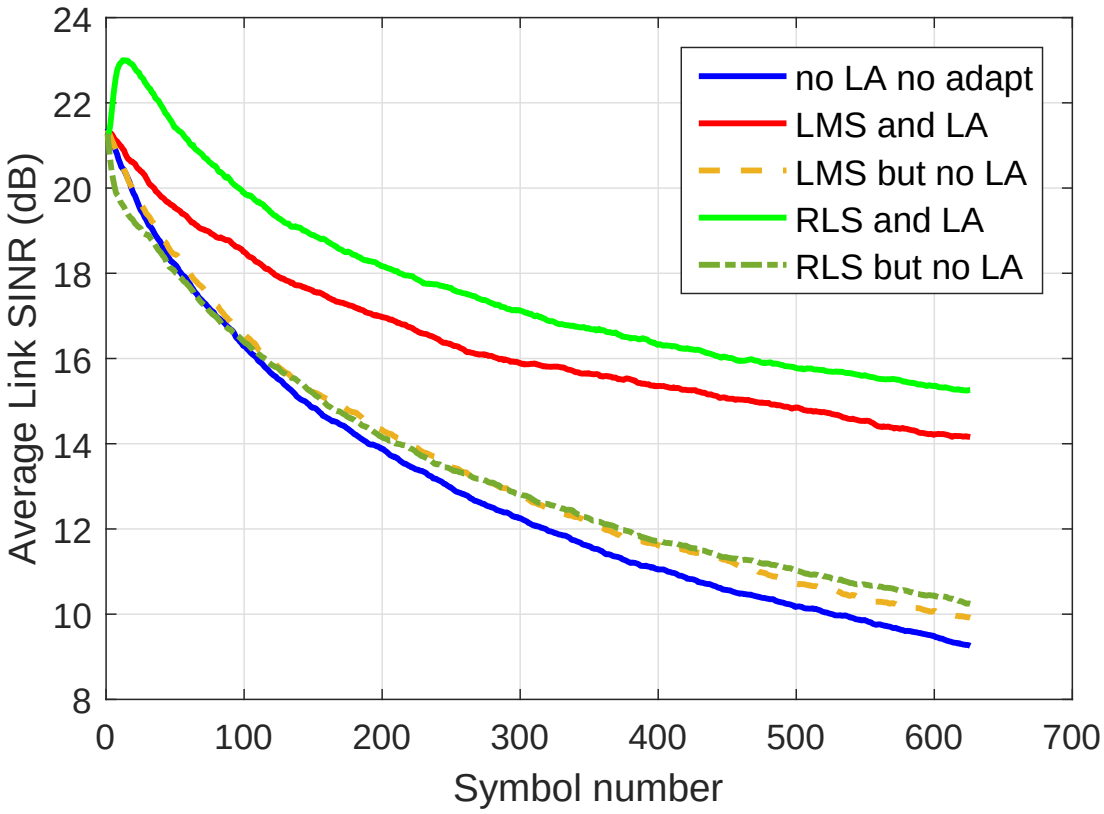

Figure 4.1: Benefit of beam-tracking at the receiver using adaptive algorithms such as LMS and RLS. Since decoded symbols are used for adaptation, having link adaptation is important to reap full benefits of receiver tracking.

4.1 Data Aided Receiver Tracking

Rate and SINR over a data packet can be improved by using receiver tracking algorithms such as LMS and RLS that run in a data aided manner. In the absence of pilots, decoded symbols are used to guide the adaptation. In this case, link adaptation or adaptive modulation and coding is necessary so that successively smaller constellations are sent from the TX to ensure that BER remains low and error free decoding helps LMS/RLS do their job well. The improvement in SINR by using receiver tracking techniques along with and without link adaptation is shown in fig. 4.1. Receiver tracking combined with link adaptation can give additional $5-6$dB gain in SINR at the end of the coherence time.

4.2 Over-the-air versus Feedback Based IA: Overhead comparison

Feedback based IA or centralized IA is the procedure where global channel estimates are made available at a central node (or every TX node) by using channel state feedback. It has its benefits that it uses actual channel estimates, and is a straightforward fast procedure that can execute the beamformer computation on a radio's own hardware once all the estimates are available locally. It is fast converging, robust to errors, and comparatively low overhead in small setups. Its con is that it may involve too much feedback of information to each node or to a central node in order to do the beam computation, which increases overhead as the setup grows larger. It relies on accurate feedback of CSI, which in practice may be inaccurate, corrupted, delayed, or even lost. The centralized method cannot handle lost or delayed CSI.

Over-the-air or distributed IA on the other hand is the procedure of computing IA beams by iteratively optimizing beams at both sides without ever needing global channel state information at any node. Distributed IA does its job by starting from an arbitrary beam estimate and having the TX and RX alternately send pilot symbols and update their beams iteratively. Since only aggregate interference is estimated at each step, a major benefit is that it is more robust to uncoordinated interference and does not suffer from problems like loss or corruption of CSI feedback. Unfortunately, it takes many iterations over the air to reach a good alignment solution (anywhere from 5 to 50) and the overhead may be too much as compared to centralized CSI feedback solution for a small setup.

4.2.1 Feedback Based IA

Steps of feedback based IA are:

1. Sequential antenna by antenna pilot symbol transmission from each TX to RX to enable full channel estimation for all connected links at each RX.

2. Sequential antenna by antenna pilot symbol transmission in the reverse link from each RX to TX to enable full channel estimation for all connected links at each TX.

3. Sending previously computed TX-to-RX channel estimates for each connected forward link by an RX as feedback (data) on the reverse channel, sequentially.

4. Computation of TX & RX beams at each TX using the available knowledge of global channel matrices, presumably starting from common arbitrary initial beams.

5. Beamformed transmission of pilot symbols from all TXs simultaneously or sequentially to the RXs to allow the receivers to estimate the signal and interference co-variance matrix and compute the receive beams appropriately.

4.2.2 Over-the-air Iterative IA

In the same way distributed IA takes the following steps:

1. Starting from arbitrary initial estimates, beamformed transmission of pilot symbols from all TXs simultaneously to the RXs to allow the receivers to estimate the signal and interference co-variance matrix and compute the receive beams appropriately.

2. Beamformed transmission of pilot symbols in the reverse channel from all RXs simultaneously to the RXs to allow the transmitters to estimate the signal and interference co-variance matrix and compute the transmit beams appropriately.

3. Repeat (1) and (2) until convergence of beams or residual interference seen at the receivers is minimal.

4.2.3 Calculation of Beam Training Overhead

Using the above sequence of events, we can compare the overhead imposed during *initial* beam training by both feedback based and over-the-air IA. Consider a system with the following parameters.

- K: Number of User-pairs
- M: Number of antennas per node
- N_1: Length of pilot sequence used for MIMO channel estimation
- N_2: Length of pilot sequence used for concurrent beamformed channel estimation in centralized IA
- N_3: Length of pilot sequence used for concurrent beamformed channel estimation in over-the-air IA
- L: Number of ping pong transmissions done for over-the-air IA

Beam training overhead:

- **Feedback:** (a)N_1K+(b)N_1K+(c)K^2M^2+(d)N_2
- **Over-the-air:** (e)$2LN_3$

Here are the corresponding explanations for the calculations:

(a) Sequential pilot transmission for MIMO channel estimation at receivers.

(b) Sequential pilot transmission in reverse channel for MIMO channel estimation at transmitters.

(c) Feedback of $M \times M$ MIMO channel by K receivers sequentially.

(d) Concurrent pilot transmission for beam computation at receivers.

(e) L ping pongs of N_3 pilot symbols each for updating the beams.

For example, for $K = 3$, $M = 2$, $N_1 = 2$, $N_2 = 3$, $N_3 = 3$, and $L = 10$

- **Feedback:** 51 symbols
- **Over-the-air:** 60 symbols

For example, for $K = 7$, $M = 4$, $N_1 = 4$, $N_2 = 7$, $N_3 = 7$, and $L = 10$

- **Feedback:** 847 symbols
- **Over-the-air:** 140 symbols

For example, for $K = 3$, $M = 2$, $N_1 = 107$, $N_2 = 107$, $N_3 = 107$, and $L = 10$

- **Feedback:** 785 symbols
- **Over-the-air:** 2140 symbols

From the above examples, we see that feedback based IA is better when there are few users or longer pilots must be used (due to low SNR, hardware impairments or other reasons) but distributed IA is better when the number of users is more than 2 and short pilots are used. We expect the feedback based technique to be a good choice in most situations where IA is used to augment the capacity of an existing TDMA/FDMA system such as to combat inter-cell interference in cellular systems. In ad-hoc networks where a large number of users must be managed within a fixed bandwidth, distributed IA may be more promising.

Next we will take a look at how another strategy can be used to improve the IA system's robustness to channel variation by updating the RX and TX beams during data transmission through short pilots.

4.3 RX-TX Beam Updating in the Middle

By transmitting short pilot symbols as feedback in the middle of data transmission, we can allow the TX to update their beams and hence prolong a high SINR regime by driving down misalignment as shown in fig. 4.2. We want to avoid full CSI estimation as that takes a large overhead. The mechanism of doing these updates is essentially doing a few ping-pongs of distributed IA strategy to let the beams update themselves. There can be multiple such updates within a data phase. In this update strategy, we have many variables to tune

to optimize the system performance. We have the option of choosing how many pilots to transmit each time, how long into the data packet to transmit these pilots, and how many ping-pongs (iterations) to do.

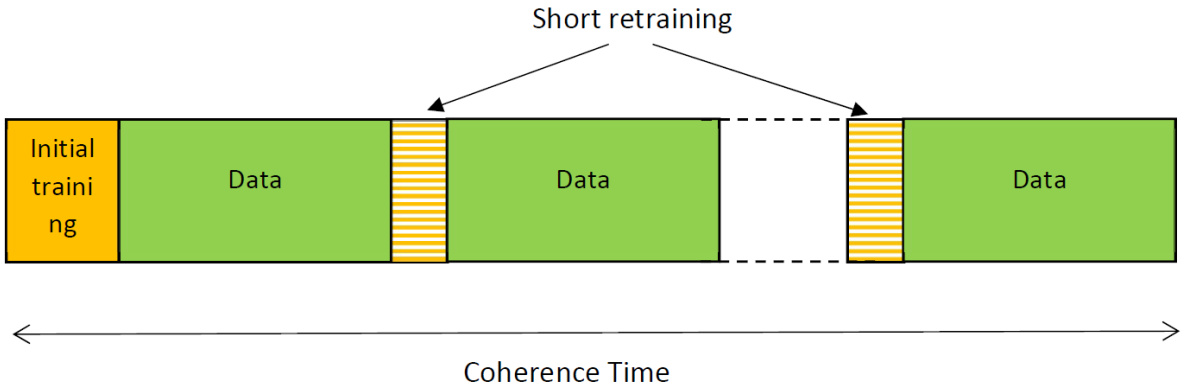

Figure 4.2: Distributed IA protocol to send short retraining pilots to update TX beams in the middle of the data phase.

Here we show the results of simulations showing what are the optimal values of length of short pilots and retraining intervals under different SNR, and Doppler conditions described in table 4.1, leading us to some simple conclusions. The following simulations do not implement receiver tracking and solely show the benefit of beam updating in the middle. Hence, this strategy can be combined with receiver tracking to get additional benefits.

4.3.1 Simulations and Results

At a moderate SNR of 10dB, with very short retraining length, estimation error restricts the capacity. With large retraining lengths (4% of coherence period), overhead becomes the dominant factor as the estimation accuracy reaches a plateau due to the varying channel. 11 symbol long retraining (1% of T_{coh}) gives the maximum throughput.

By assuming a small coherence time of $0.1/(f_d T_s)$, average capacity gains are not seen. But short retrainings help give a smoother throughput curve thus providing less packet errors. Without retraining, sum capacity degrades quickly. Many applications instead assume a channel coherence time of $0.4/(f_d T_s)$ which is too large for an IA system. Compared to

Simulation Scenario	Figures	Parameters
Common Values	-	$K = 3$ users, $M = 2$ ant/user, BW=1MHz, all pathgains= 0dB
Medium SNR, High Doppler	fig. 4.3 , fig. 4.4, fig. 4.5,	SNR = 10dB, $f_d = 100$Hz, $T_{\text{coh}} = 1000$symbols
Low SNR, High Doppler	, fig. 4.6, fig. 4.7	SNR = 5dB, $f_d = 100$Hz, $T_{\text{coh}} = 1000$symbols
High SNR, High Doppler	fig. 4.8, fig. 4.9	SNR = 15dB, $f_d = 100$Hz, $T_{\text{coh}} = 1000$symbols
High SNR, Low Doppler	fig. 4.10	SNR = 15dB, $f_d = 10$Hz, $T_{\text{coh}} = 10,000$symbols

Table 4.1: Different simulation parameters and corresponding figures for those simulations for updating beams in the middle technique.

training at such long intervals, short retrainings provide not just throughput stabilization but also 24% higher average capacity.

At SNR = 5dB, we get improved stability with a 0.2bits/s/Hz loss in average capacity as compared to training once every 1000 symbols and a 0.5bits/s/Hz gain compared to training once every 2500 symbols. At SNR = 15dB, we get a throughput gain of 0.75bits/s/Hz and improved stability as compared to a training schedule every 1000 symbols and 2.4bits/s/Hz compared to a training schedule every 2500 symbols.

As the channel coherence times scales by a factor of 10 to 10^4, surprisingly the required training length to maximize throughput scales only by a factor of 3. Hence, we can achieve higher throughputs than in the high Doppler case.

We conclude that only short retraining lengths are required to maximize the average throughput. We find that $N_{tr} = 11$ at the $T_{\text{coh}} = 1000$ symbols and $N_{tr} = 31$ at $T_{\text{coh}} = 10^4$ symbols are close to optimal between 5 to 15 dB SNR in the high interference scenarios simulated. Periodic retraining stabilizes the throughput curve and also provides higher average capacity as compared to training occurring once every coherence period.

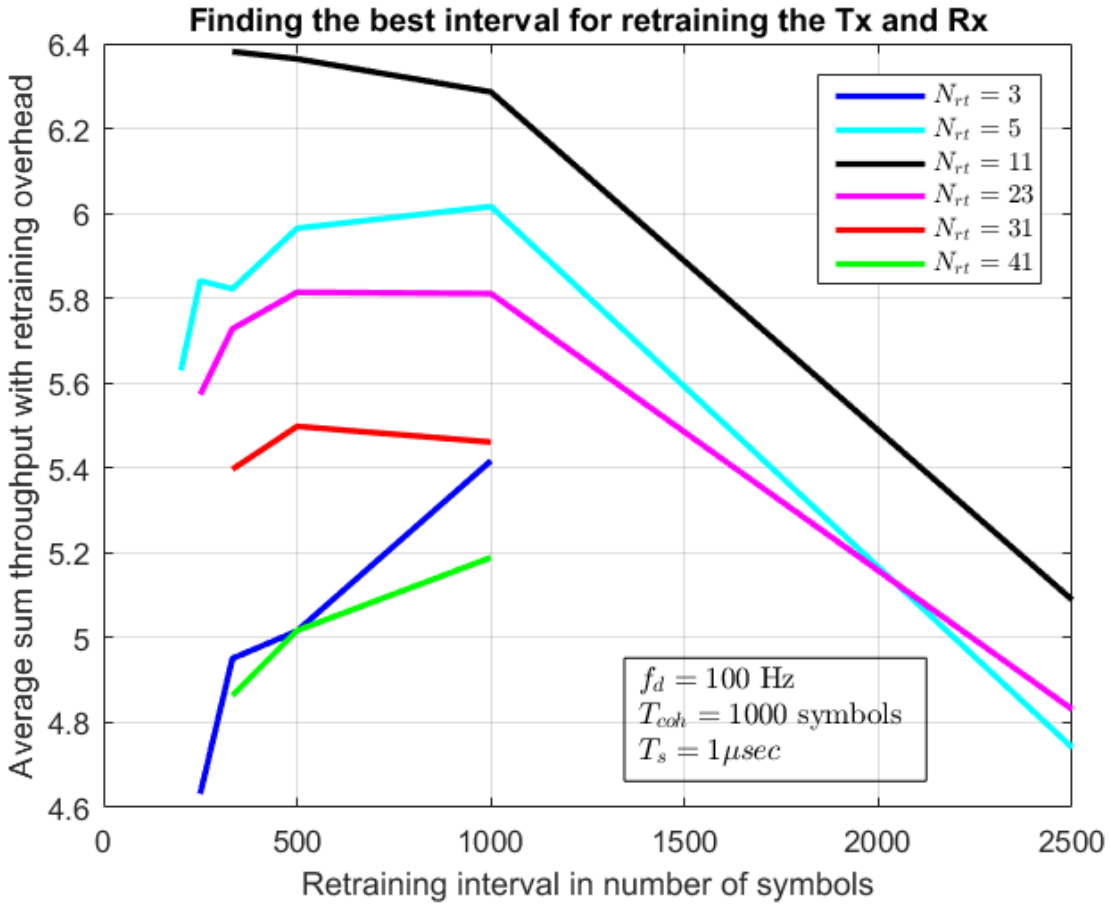

Figure 4.3: Average sum throughput vs TX retraining interval for the system in Table 4.1 at medium SNR, and high Doppler for different lengths of pilot sequence.

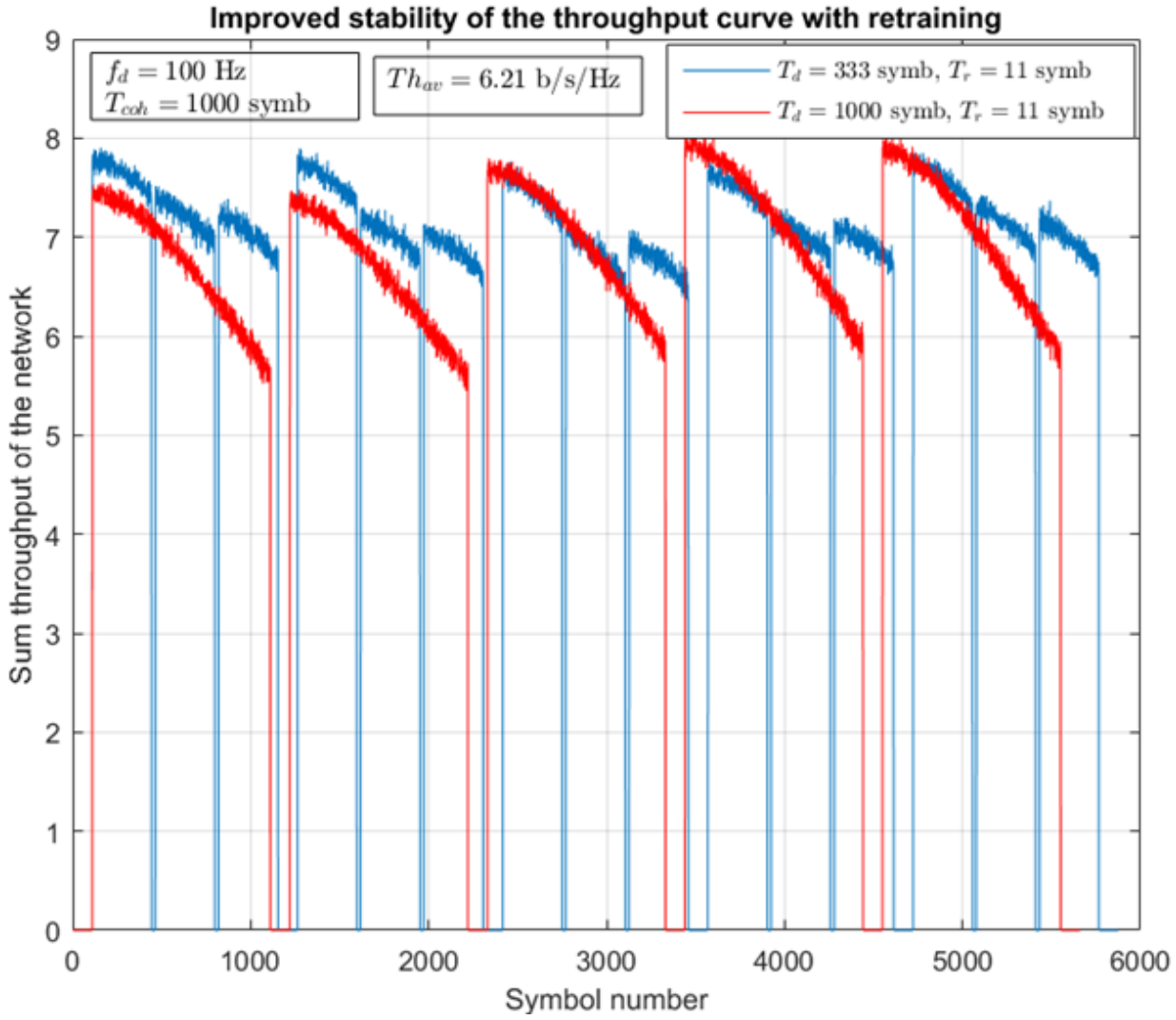

Figure 4.4: Achieved sum rate vs time for the system in 4.1 at medium SNR, and high Doppler, for optimal pilot length = 11 symbols, optimal retraining length= 333 symbols, and suboptimal retraining length = 1000 symbols.

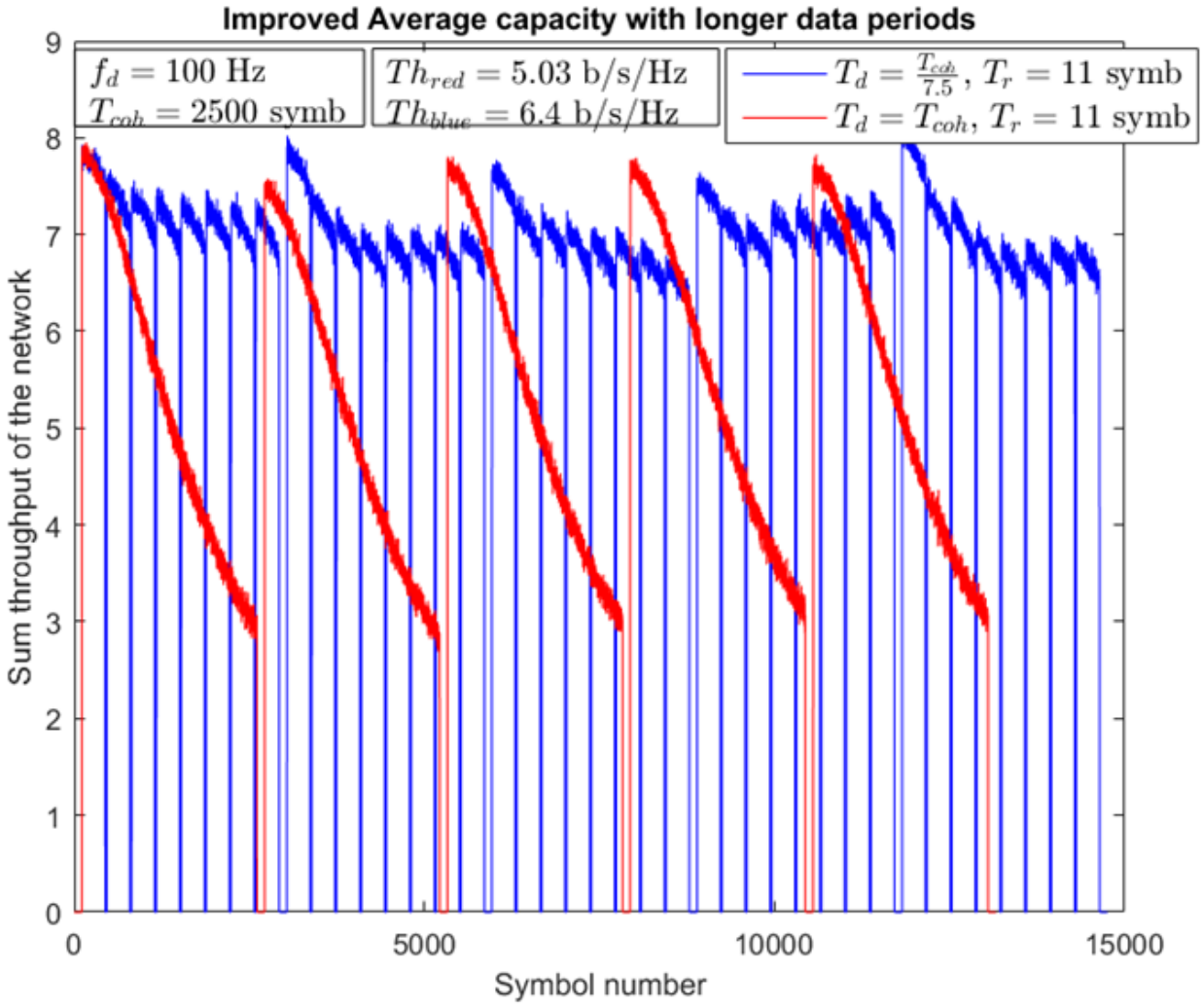

Figure 4.5: Achieved sum rate vs time for the system in 4.1 at medium SNR, and high Doppler, for optimal pilot length = 11 symbols, optimal retraining length= 333 symbols, and highly suboptimal retraining length = 2500 symbols.

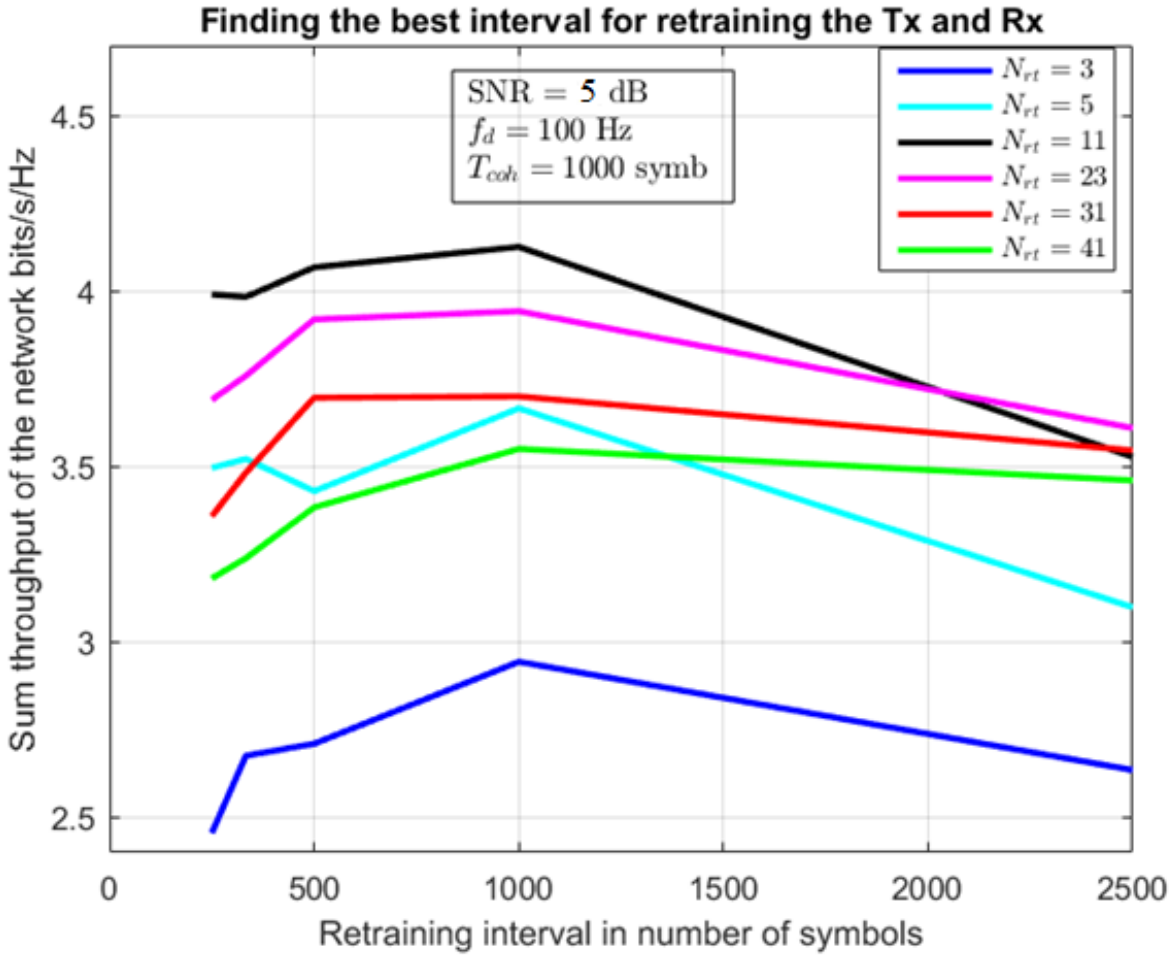

Figure 4.6: Average sum throughput vs TX retraining interval for the system in Table 4.1, at low SNR, and high Doppler, for different lengths of pilot sequence.

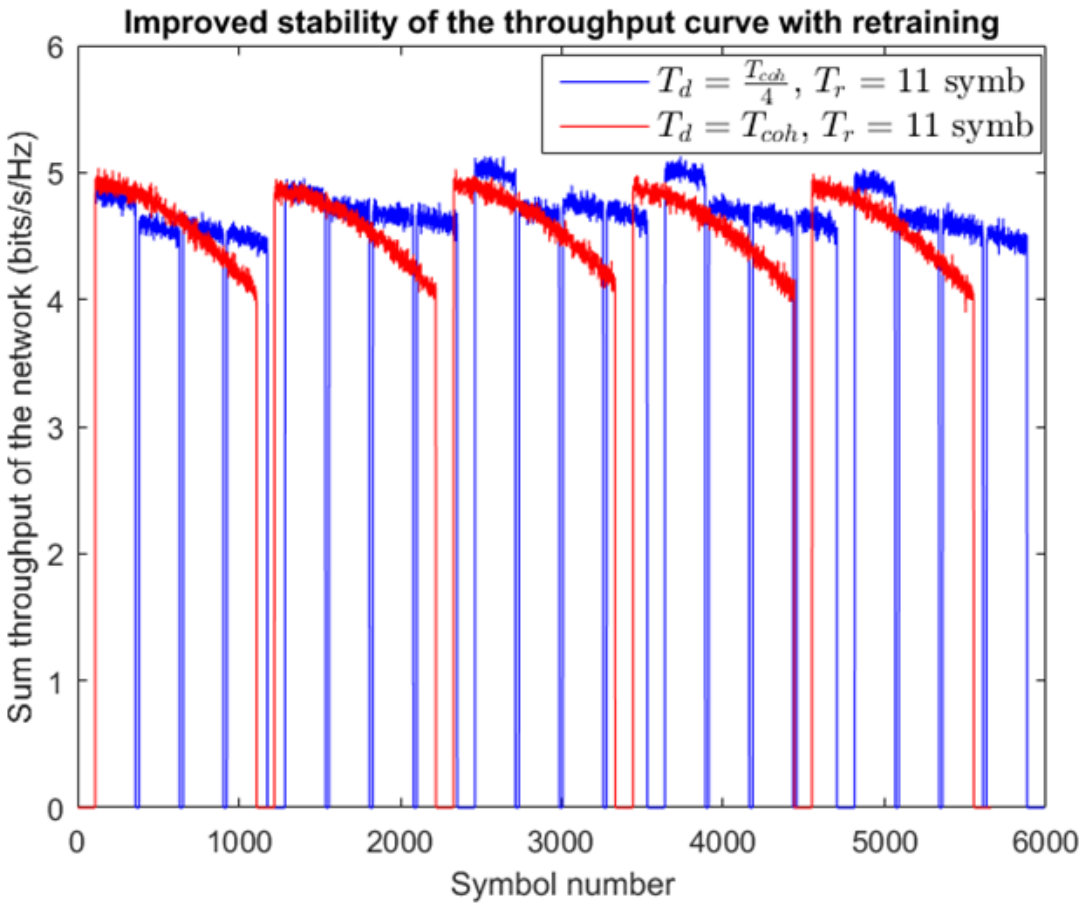

Figure 4.7: Achieved sum throughput vs time for the system in Table 4.1, at low SNR, and high Doppler, for optimal pilot length = 11 symbols, optimal retraining length= 1000 symbols, and a suboptimal retraining length = 250 symbols.

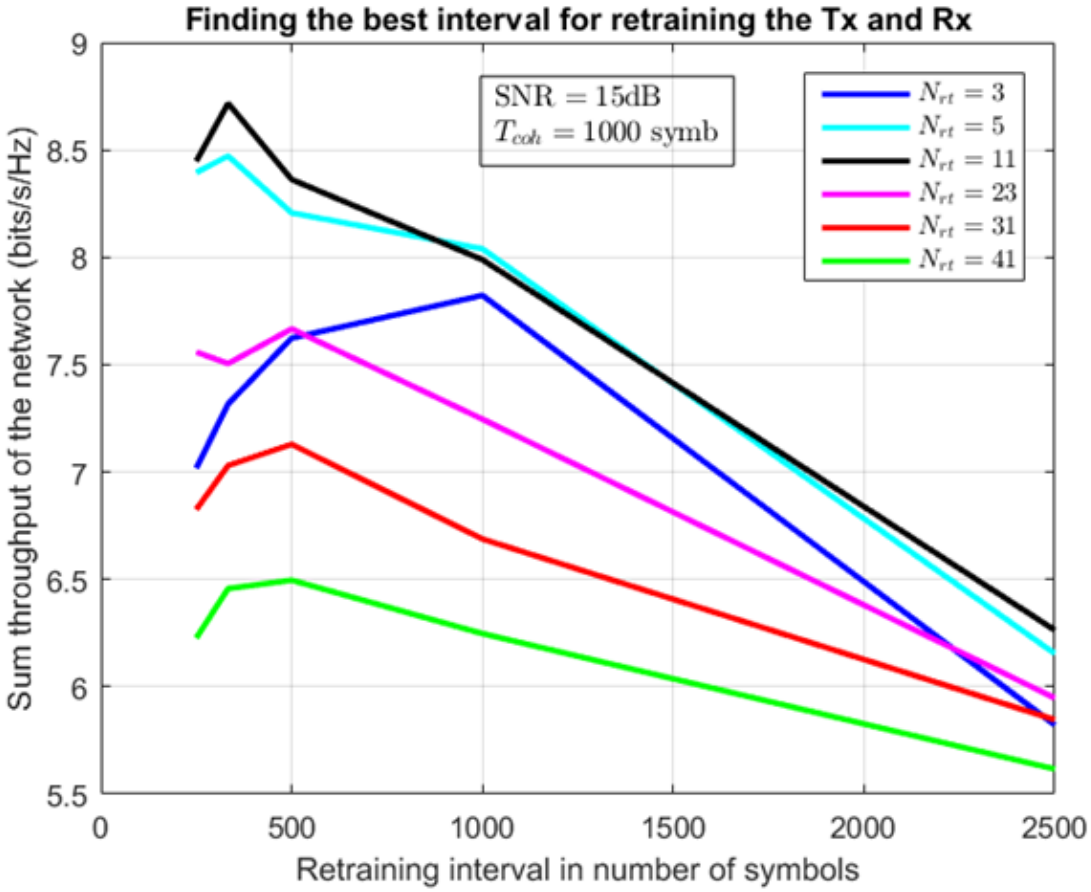

Figure 4.8: Average sum throughput vs TX retraining interval for the system in Table 4.1, at high SNR, and high Doppler, for different lengths of pilot sequence.

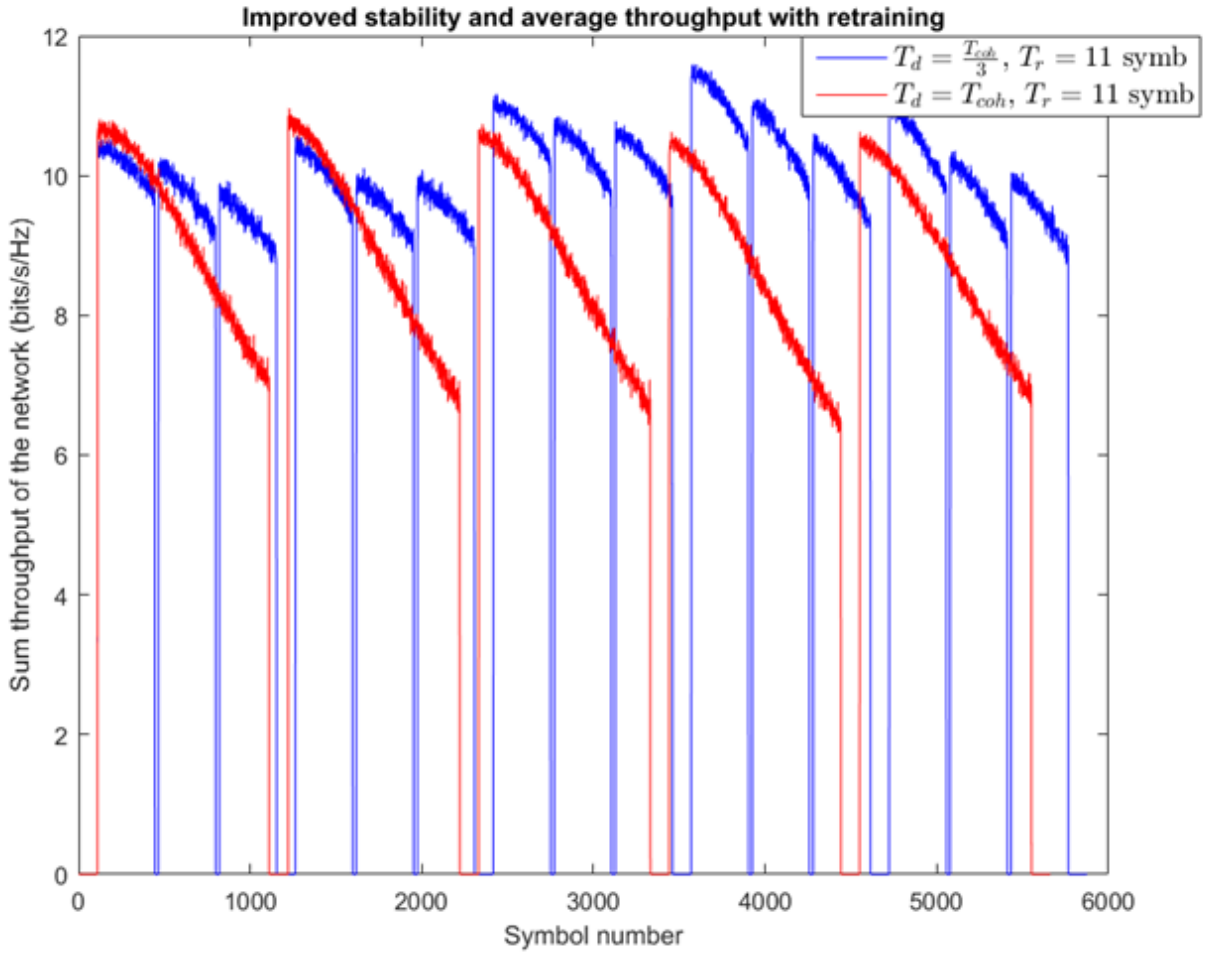

Figure 4.9: Achieved sum rate vs time for the system in Table 4.1, at high SNR, and high Doppler, for optimal pilot length = 11 symbols, optimal retraining length= 333 symbols, and suboptimal retraining length = 1000 symbols.

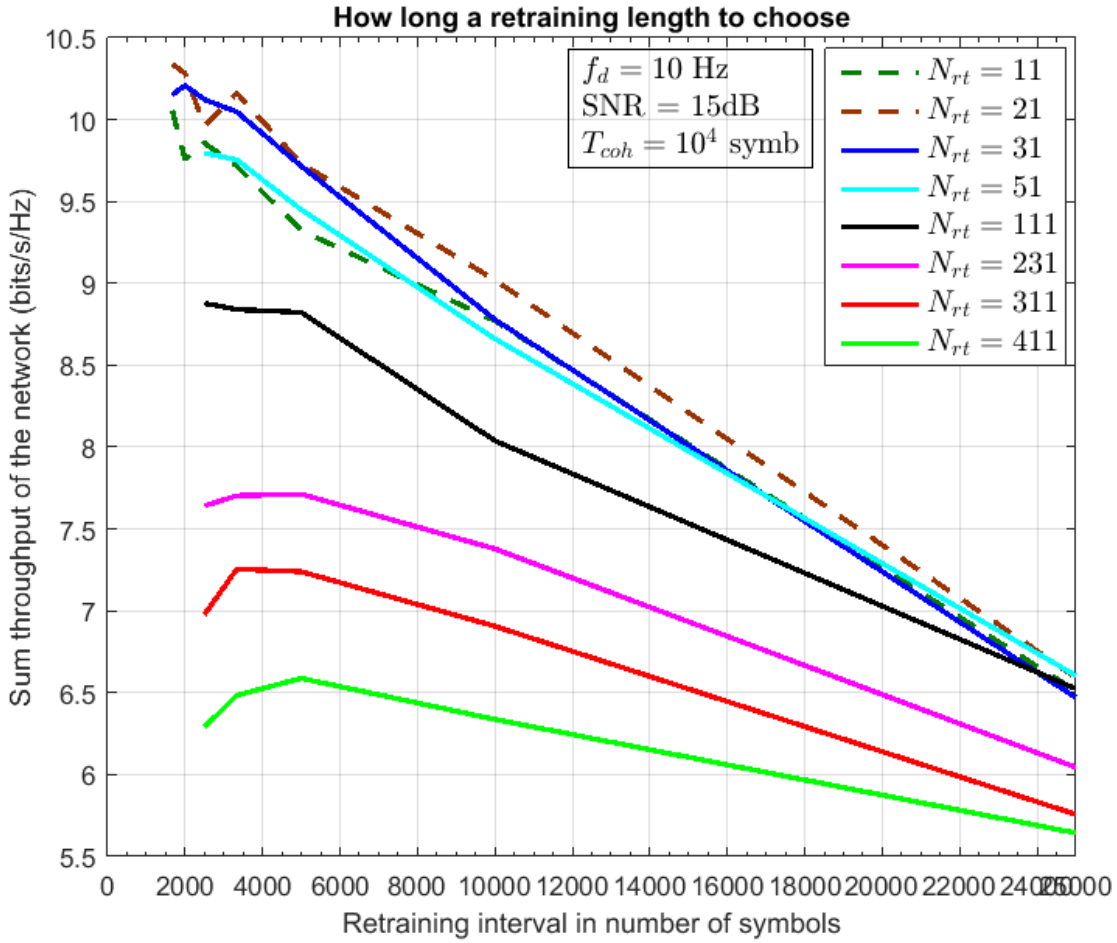

Figure 4.10: Average sum throughput vs time for the system in Table 4.1, at low SNR, and high Doppler for different lengths of pilot sequence.

4.4 Summary

For initial training, distributed IA is more efficient than centralized IA when the number of users and antennas are large (7 users, 4 antennas or larger for instance). For most smaller system settings, centralized IA will be more efficient with lesser overhead. Receiver tracking can be very helpful in improving the SINR at the receiver without using additional pilots. LMS or RLS algorithms can be used to adaptively track the optimal receive beam in the changing channel, but to see a substantial improvement, link adaptation must be used simultaneously, so that the transmitter chooses a small enough constellation that can be decoded almost error free at the receiver. The feedback needed to accomplish link adaptation can be done as part of acknowledgement (ACK) packets or one bit feedback or a side channel during the transmission. Since the feedback is very small, it would not drag down the network spectral efficiency significantly.

Receiver tracking can be combined with retraining in the middle to update the TX beams using short bi-directional pilots. As shown, very short pilots (from 1% to 1/3% of T_{coh}) are optimal for achieving the maximum sum throughput with sufficient interference suppression. Further, optimal lengths of data phases for distributed IA are found to be a fraction of the coherence period, reinforcing the results obtained for centralized IA in section 3.5 that more frequent training than the coherence time is required to maximize throughput. The choice of pilot sizes can be ad-hoc based on the SNR of the links, but the optimal pilot length increases as the SNR decreases in order to get higher quality estimates and decreases as the coherence time decreases because of increasing percentage of overhead.

Chapter 5

MAC Layer for Multiuser Networks: CSMA, TDMA, or Interference Alignment

In this chapter we compare Interference Alignment or IA inspired beamforming based approaches for multiuser concurrent communication to other medium access control (MAC) approaches that allow multiple users to share a channel. Specifically we study CSMA and TDMA and show how IA based approaches can provide better throughput while also maintaining backward compatibility in legacy networks. We present a beamnulling based concurrent CSMA MAC protocol that allows higher throughput than CSMA while being backward signaling compatible. Next, we present a simulation comparing a 7 user TDMA and a 7 users IA system in a time varying channel. Results show that IA is a promising multiuser access control approach, even under a harsh time varying channel.

5.1 A Concurrent CSMA MAC protocol for Mobile Ad Hoc Networks using beamnulling [1]

Traditional algorithms for MAC in mobile ad-hoc networks such as CSMA-CA allow only a single user to transmit at a given time. This means that the sum throughput in a MANET cannot increase to service additional users. Such MAC protocols disregard the possibility that by utilizing multiple antenna processing to handle interference intelligently at the physical layer (PHY), many concurrent user transmissions can co-exist. Previous works have proposed altered versions of CSMA-CA that allow multi user operation but may not necessarily be able to coexist with an existing IEEE 802.11 based network. This chapter proposes a concurrent CSMA MAC protocol that is completely compatible with a traditional CSMA based MAC and follows the same timing structure allowing co-existence of both protocols. Specifically, in concurrent CSMA after a primary user has captured the channel, secondary users listen to the request-to-send (RTS)/ clear-to-send (CTS) handshake and form a beamnull towards the primary receiver. Hence secondary users can communicate concurrently with minimal increase in interference to the primary receiver. Simulations show that the proposed PHY and MAC scheme is able to achieve 2 to 3 times the network spectral efficiency of CSMA with a single antenna and this improvement factor is sustained as the network scales in size. Further the proposed scheme allows the network spectral efficiency (sum throughput per unit bandwidth) to scale with users and improves upon a previous promising approach which uses Interference Alignment.

5.1.1 Introduction

A MANET is a network formed without any central administration which consists of mobile nodes that send packet data over the wireless medium [35]. Examples of a MANET can range from a network of laptops, smartphones to drones and UAVs. MANET's are also a valuable

[1] This section is reproduced from [34] ©2015 IEEE.

resource for military communication as it does not require any infrastructure such as base stations. Ideally, a MANET must be able to support an arbitrary number of users in the network, but due to interference constraints and limitations imposed by the MAC protocol, the network throughput does not scale with users. One way of mitigating this drawback is to allocate additional spectrum to the MANET and allocate orthogonal channels to users. But spectrum is a scarce and costly resource and also limited in availability. A better way of accomodating multiple users in a MANET is to use an improved MAC protocol that can support multiple users concurrently. CSMA-CA is a MAC protocol widely used by Wi-Fi devices that has been adopted by IEEE 802.11 WLAN, but it only supports single user transmission at a time. Our intention is to devise a MAC protocol that is fully compatible with CSMA i.e. nodes following the new MAC protocol can coexist with other nodes following CSMA. Such a constraint allows nodes to be added on the fly to a traditional CSMA network and increase its throughput.

Many kinds of multiuser MAC protocols have been proposed in the past. In [36], authors propose a MAC scheme where a multiuser RTS is transmitted by the access point (AP) and based on a distributed signal to leakage ratio (SLR) thresholding scheme, users reply back with time staggered CTS's. This scheme can provide modest gains in network sum throughput but it is not compatible with CSMA as it changes the protocol structure. Additionally, concurrent transmissions in a MANET impose different interference constraints at receiving users because unlike in AP, joint multi user beamforming is not possible as CSMA limits information exchange among users after channel capture. Authors in [37] propose a similar MAC scheme but allow the AP to decide which subset of users are assigned spatial streams, based on their CTS feedback. This protocol again requires global CSI at the AP and works only in a downlink scenario, not in a MANET. A recent successful technique of interference cancellation is Interference Alignment which can allow the network throughput to scale with its size [45] but it requires extensive CSI knowledge or iterative algorithms to converge to a solution. It is not yet clear how the iterative IA algorithms will fit within a MAC pro-

tocol. One notable effort in this regard has been done in [38] where the authors propose a MAC/PHY scheme where multiple users can communicate concurrently by a combination of interference nulling and alignment. Users follow a MAC scheme called 802.11n^+, similar to 802.11n where the RTS/CTS process is continued by the left over secondary users after the initial channel capture phase, by communicating in a subspace which is orthogonal to the primary user's transmission vectors. Naturally, this works only for those secondary users who have at least one more antenna than the number of spatial streams being transmitted. In order to ensure backward compatibility with CSMA, secondary users must shorten their data packets through fragmentation. While packet fragmentation is optionally allowed in 802.11n, it necessitates the use of buffers and non-sequential decoding at the receiving user which may be prohibitive for delay sensitive applications. Further, wrong selection of fragmentation length can actually reduce throughput [39]. Hence, a PHY/MAC protocol for delay sensitive applications that can seamlessly coexist with CSMA while enabling concurrent transmissions is desired.

In this section, we consider a MANET where each user is allowed to communicate to another user using only a single hop. We assume delay sensitive data such as voice or media is being transmitted over the network which prohibits the use of multiple hops due to latency requirements. Here, it is important to note that restricting communication to a single hop does not mean that all users can always hear each other's transmissions. Rather, in a system with a large hop radius, some users would be hidden from other users. While this prevents some users from communicating, it also enables multiple transmissions to coexist without interference. Since our intention is to describe a MAC protocol which, by definition, applies to nodes within hearing distance of each other, we limit ourselves to a single hop system, as it is sufficient for our analysis. Nonetheless, our protocol is equally applicable to multihop MANETs where the path selection algorithm would define the set of nodes which compete for the channel at every hop. The results can only be better if the proposed protocol is applied to a multihop system (see Section 5.1.4). It has been shown that multiple antenna

techniques such as diversity combining and spatial beamforming allow a system to achieve a higher SNR [40]. Finding the optimal beamforming weights requires channel knowledge at the transmitter. Then, in a multiuser scenario, if the channel knowledge towards another user can be acquired, it can be used to beamnull towards this user to reduce the interference caused. Utilizing the beamnulling capability of users, we develop a concurrent CSMA MAC protocol that allows multiple point-to-point links to coexist and as a result, the MANET can support more users with an acceptable throughput. This MAC protocol is designed in a way that the primary transmission goes through the usual channel capture and RTS-CTS-DATA-ACK phases of CSMA but additional users can communicate by listening to the primary transmission and transmitting their data while beamnulling towards the primary receiver. These secondary transmissions follow an ALOHA like best effort service. We show through simulation that even a simple scheme like this that requires no additional information to be exchanged allows multiple user streams to co-exist. This shows that the throughput of CSMA can be increased using intelligent beamnulling which sets the stage for further work on concurrent MAC protocols.

The section is organised as follows. Section 5.1.2 describes the network topology and the physical layer processing at the user nodes. Section 5.1.3 describes the CSMA MAC protocol how it is modified to support concurrent transmissions. Section 5.1.4 provides the simulation parameters and results and draws conclusions based on them. We use boldface upper case symbols such as $\mathbf{H}$ to denote a matrix, boldface lower case symbols such as $\mathbf{p}$ denote vectors and normal symbols such as s_i or N_r denote scalar values.

5.1.2 System Model and Beamnulling

There are N users in a system. The users are distributed in a circle of radius d with a uniform density and random placement in the circle. Each user node is equipped with N_r antennas. The channel between the i-th and j-th user is denoted by $\mathbf{H}_{ij}$ and is supposed to be reciprocal i.e. $\mathbf{H}_{ji} = \mathbf{H}_{ij}$. Each user transmits at its maximum power $\mathcal{P}$.

System Model

Suppose the j-th user is listening to the i-th user in the presence of other interfering users whose indices are denoted by the set $\mathbb{I}_j$. Then the received signal at user j is given by

$$\mathbf{y}_j = \mathbf{H}_{ij}\mathbf{p}_i s_i + \sum_{k \in \mathbb{I}_j} \mathbf{H}_{kj}\mathbf{p}_k s_k + \mathbf{n}_j \tag{5.1}$$

where $\mathbf{p}_i$ is the beamforming vector chosen by the ith user and s_i is the symbol transmitted by the i-th user with $\mathbb{E}|s_i|^2 = 1$ and $\mathbb{E}s_i s_k^* = 0$. Noise $\mathbf{n}_j$ is assumed to be complex Gaussian $CN(0, \sigma_n^2\mathbf{I})$. It is assumed that each user is transmitting a single spatial stream, hence $\mathbf{p}_i \in \mathbb{R}^{N_r \times 1}$. The beamforming vector $\mathbf{p}_i$ can be chosen to maximise the receive SNR as shown in next subsection on Beamnulling. When the user j only has information about the desired beamformed channel and not the interferers, then it does matched filtering to receive the signal.

$$s_i = \frac{(\mathbf{H}_{ij}\mathbf{p}_i)^* \mathbf{y}_j}{|\mathbf{H}_{ij}\mathbf{p}_i|^2} \tag{5.2}$$

Here $(.)^*$ denotes the hermitian operation. But in some cases the user may also know the covariance matrix $\mathbf{Q_j}$ of the interference it is seeing which may remain constant over some duration. In this case, the user can do better by using a MMSE receiver to detect the signal [41].

$$\begin{aligned} \mathbf{Q_j} &= \mathbb{E}\big[\sum_{k \in \mathbb{I}_j} (\mathbf{H}_{kj}\mathbf{p}_k s_k + \mathbf{n}_j)(\mathbf{H}_{kj}\mathbf{p}_k s_k + \mathbf{n}_j)^*\big] \\ &= \sum_{k \in \mathbb{I}_j} \mathbf{H}_{kj}\mathbf{p}_k\mathbf{p}_k^*\mathbf{H}_{kj}^* + \sigma_n^2\mathbf{I} \end{aligned} \tag{5.3}$$

Then the desired symbol s_i can be decoded using the following transformation, where $(.)^\dagger$ denotes the Moore-Penrose pseudoinverse of the matrix.

$$s_i = \mathbf{p}_i^* \mathbf{H}_{ij}^* (\mathbf{H}_{ij} \mathbf{p}_i \mathbf{p}_i^* \mathbf{H}_{ij}^* + \mathbf{Q}_j)^\dagger \mathbf{y}_j \tag{5.4}$$

Beamnulling

The choice of the beam weight $\mathbf{p}_i$ depends on what objective the transmitter is trying to achieve. In the absence of interference, the beam weight that maximises the receive SNR has a closed form solution. Assuming constant transmitted power $\mathcal{P}$, the solution for $\mathbf{p}_i$ is given by

$$\mathbf{p}_i = \arg\max ||\mathbf{H}_{ij}\mathbf{p}_i||^2 \text{ s.t. } ||\mathbf{p}_i||^2 = \mathcal{P}. \tag{5.5}$$

Say the SVD of the matrix $\mathbf{H}_{ij}$ can be written as $\mathbf{H}_{ij} = \mathbf{U}\mathbf{\Sigma}\mathbf{V}^*$. Then the solution to (5.5) is $\mathbf{p}_i = \sqrt{\mathcal{P}}\mathbf{v}_1$, where $\mathbf{v}_1$ is the 1-st column of the right unitary matrix $\mathbf{V}$ and also the largest eigen mode of the channel $\mathbf{H}_{ij}$ [42]. Alternatively, a user could also choose to transmit omni-directionally by choosing $\mathbf{p}_i = \sqrt{\frac{\mathcal{P}}{N_r}}\mathbf{q}$ where $\mathbf{q} = [1, 1 \cdots 1]^T$.

But to truly enable a multi-user MAC protocol, the choice of beam weights must be such that it minimizes the interference generated when additional user streams are allowed to co-exist. This is where beamnulling comes into play. Say, user i is sending data to user j and user k wishes to talk to user l at the same time. Then a logical strategy for k is to choose its beam weight $\mathbf{p}_k$ so as to send minimum energy towards j. This can be formulated as follows

$$\mathbf{p}_k = \arg\min ||\mathbf{H}_{kj}\mathbf{p}_k||^2 \text{ s.t. } ||\mathbf{p}_k||^2 = \mathcal{P}. \tag{5.6}$$

Again, writing the SVD of the interference channel matrix as $\mathbf{H}_{kj} = \mathbf{U}\mathbf{\Sigma}\mathbf{V}^*$, the solution to (5.6) is $\mathbf{p}_k = \sqrt{\mathcal{P}}\mathbf{v}_{N_r}$, where $\mathbf{v}_{N_r}$ is the last column of matrix $\mathbf{V}$ and also the smallest eigen mode of the channel [42].

An implicit assumption in the derivation of both beamforming and beamnulling solutions is that the knowledge of the point to point channel matrix $\mathbf{H}_{ij}$ and the interference channel

matrix $\mathbf{H}_{kj}$ is available at transmitters i and k respectively. As we will see in the coming section, this assumption is valid as the channel information can be obtained during the CTS phase using the training fields in the MAC header. In cases where the path loss from primary RX to secondary TX is severe enough to wipe out the CTS, the secondary TX goes ahead by simply beamforming towards the secondary RX. In the proposed concurrent CSMA protocol, each user transmitting concurrently is only required to beamnull towards a primary receiver and hence the need for distributed optimisation of the beam weights does not arise.

5.1.3 Concurrent CSMA MAC Protocol

In this section we discuss how we modify the CSMA protocol to achieve concurrent transmission from multiple users. We also discuss the method of obtaining channel state information necessary for beamforming and beamnulling. The protocol timeline is drawn in figure 5.1.

We follow a θ-persistent CSMA model meaning that at each available opportunity, a station transmits with probability θ and remains silent with probability $1-\theta$. As in CSMA, when a previous transmission has ended, all users who have data to send, wait for a duration of distributed inter frame spacing (DIFS) before proceeding into backoff. The transmitter whose backoff counter expires first is assumed to have captured the channel and is called the primary transmitter (TX). This node sends an RTS to its primary receiver (RX) and if the path loss and fading are not severe, receives a CTS from the receiver. The primary TX then selects a beam weight and proceeds to send the data to the primary RX. It is important to note that the primary TX assumes it is the sole user of the spectrum and thus does not do any beamnulling. Rather it selects to either beamform towards the primary receiver or transmit omni-directionally. If the data is properly decoded, the RX broadcasts an acknowledgement (ACK) which concludes the data transmission phase. After a duration of short inter frame spacing (SIFS), the medium is open for contention again.

How concurrent CSMA departs from traditional CSMA is that after the contention phase, it allows users which have data to send to go into a *concurrent listen* mode where they

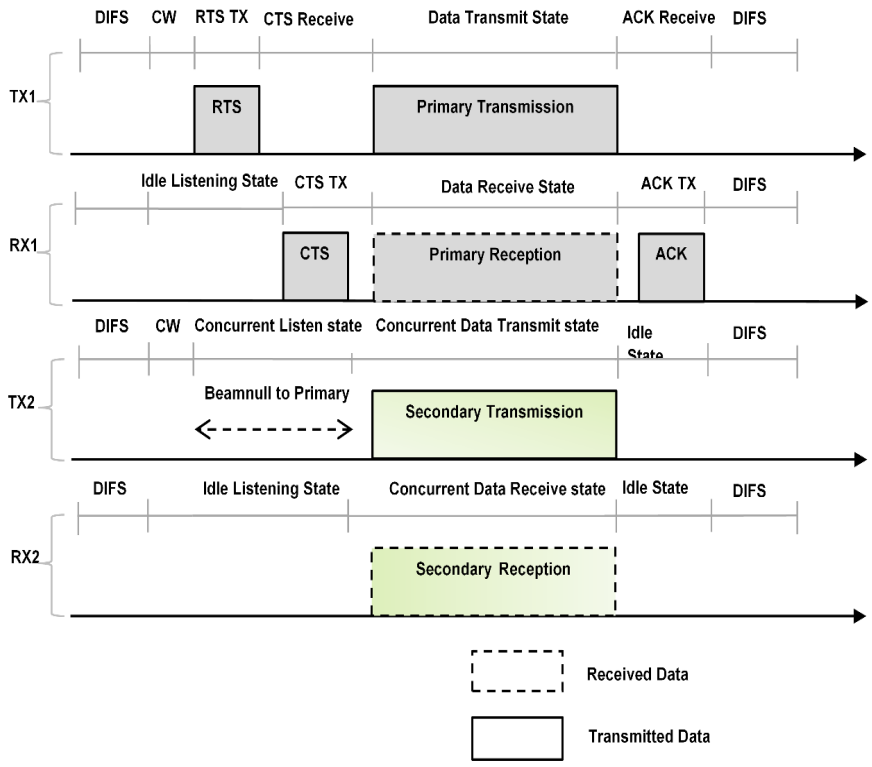

Figure 5.1: Timeline of proposed concurrent CSMA protocol with one secondary user

actively listen to the RTS and CTS from the primary TX-RX pair. RTS and CTS contain information of the network allocation vector (NAV) i.e. the length of impending primary data transmission. Additionally, each packet header contains pilot symbols in the short training field (STF) and long training field (LTF) that are used to estimate the cross coupled channel to the primary receiver [43]. Using the channel coefficients, a secondary transmitter (user) selects a proper beam weight so as to form a null at the primary RX, as explained in the previous section.

All secondary users whose intended receivers are not sensed busy, are allowed to transmit. The secondary transmissions start synchronously with the primary data transmission and end synchronously. This ensures that the primary ACK packet is not corrupted. It is noteworthy that the secondary TX-RX skip the RTS, CTS and ACK phases, rather they only go through CONC_LISTEN and DATA_TX phases. This mandates a subtle change in the MAC software

Table 5.1: Physical and MAC layer parameters for simulation

PHY and MAC Parameters	Value
f_c (MHz)	425
BW (MHz)	1.25
Pathloss exponent	3
Noise Floor (dBm)	-100
Antenna Gain (dBm)	2
Transmit Power $\mathcal{P}$ (mW)	1000
Modulation	16-QAM
RTS (μs)	36
CTS (μs)	40
ACK (μs)	36
SIFS (μs)	55
DIFS (μs)	34
Packet duration (μs)	1000

that all nodes in idle state will sense the channel for any secondary transmission directed towards them, when the primary data transmission window starts. This scheme enables the primary TX-RX pair to talk as per traditional CSMA model but in addition secondary users are able to communicate by beamnulling towards the primary receiver, using a best effort service with no ACK. Hence, the above MAC scheme allows concurrent transmissions from multiple users which results in improved network throughput. Although the modified MAC scheme does not guarantee that the additional interference to the primary or secondary transmissions will be low enough for successfull reception, simulation shows that secondary beamnulling is able to mitigate interference so that the proposed MAC protocol gives a higher sum throughput.

For symbol detection the primary RX uses the matched filtering approach (5.2) since it cannot anticipate the secondary transmissions. The secondary receiver on the other hand can measure the interference channel between itself and the primary TX and can implement an MMSE receiver (5.4), even though it is agnostic of other secondary transmitters.

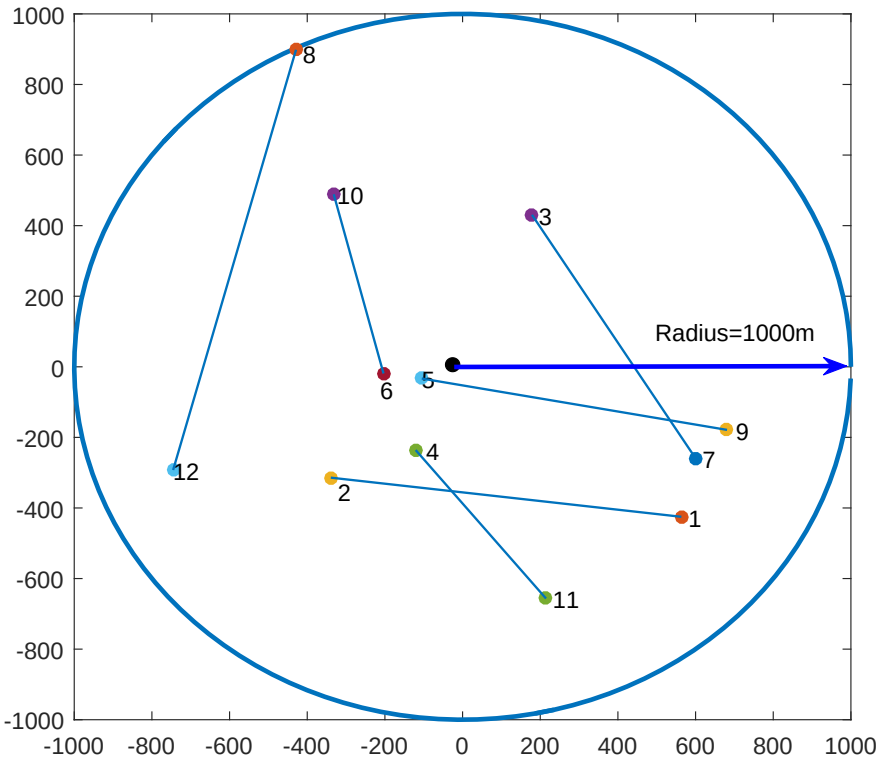

Figure 5.2: Simulated user topology with N=12 users in a circle of 1000m radius.

5.1.4 Simulations and Results

We construct a simulation of a N user system spread out in a circular area of radius d with each user having N_r antennas. N can take values from 2 to 20, d from 100 m to 10000 m and N_r is either 2 or 4. An example simulated user topology is shown in fig. 5.2. Only point to point communication is allowed between users and each user transmits with a constant power $\mathcal{P}$ and fixed modulation scheme. Both the physical layer beamnulling and MAC layer CSMA have been implemented in MATLAB. The program simulated between 100 msec and 1 sec of CSMA operation with each packet lasting 1 msec. The channel was changed every 1 msec. We compare the network spectral efficiency (throughput per unit bandwidth) of the proposed scheme with traditional CSMA. Results were derived from atleast 100 averages to simulate different topographical positioning of users. The detailed simulation parameters

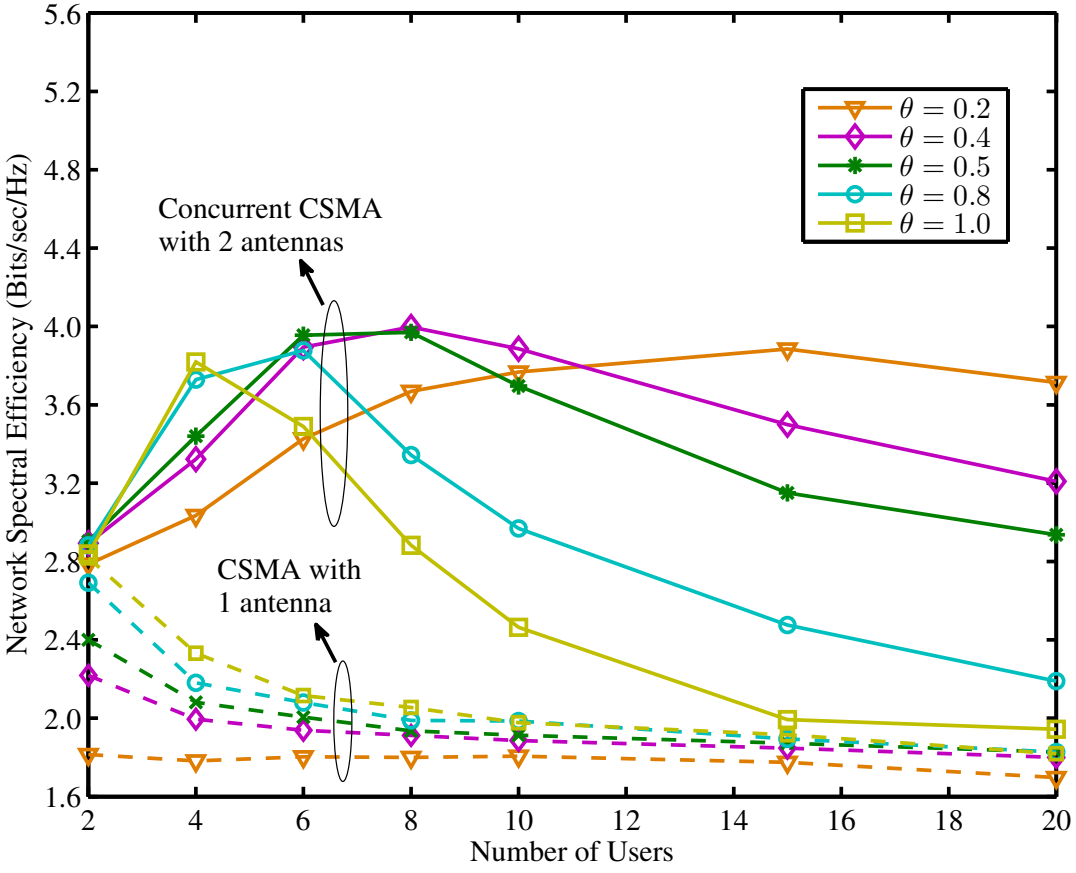

Figure 5.3: Network spectral efficiency scaling of the concurrent CSMA for $N_r = 2$ for various values of θ at a radius of $d = 1000m$

used are given in Table 5.1.

Fig. 5.3 shows a comparison between the network spectral efficiency achieved by the proposed concurrent CSMA protocol using two antennas versus traditional single antenna CSMA for different values of persistence probability θ. As expected, the spectral efficiency of single antenna CSMA scheme decreases as users increase due to more collisions, eventually saturating at about 1.8 bits/s/Hz. Concurrent CSMA however is able to increase the peak spectral efficiency to nearly twice that of CSMA on average over all values of θ by enabling multiple concurrent transmissions. Additionally, the number of users for which the peak throughput is attained depends on the persistence probability θ. Hence, a system designer can choose the optimum θ if the number of users can be learnt. Low θ values are suitable

for a high user scenario (≥ 15) while high θ values are better to support fewer users. Concurrent CSMA also improves the saturation network spectral efficiency, but only for low to moderate values of θ, since for high θ values, the collision probability becomes very high. The throughput improvement is more pronounced when using $N_r = 4$ antennas in Fig. 5.4. We achieve from 2 to 3 times gain in peak network spectral efficiency, depending on the persistence probability. In this case, the saturation spectral efficiency is also increased 2 to 3 times for all values of θ. Using 4 antennas provides additional array gain and better beamnulling capability to users, which manifests itself in the increased peak and saturation throughput. The simulated system uses only a single spatial stream and the gains can be further improved using multiple spatial streams at each user.

We also show that the incremental spectral efficiency gain is sustained as the network scales in size. Fig. 5.5 shows the network spectral efficiency with 4 users and θ=1 for a network size increasing from 100m to 10000m. It can be seen that the gain factor is maintained at all values of network radius d, for the two as well as four antenna scenario. The same plot is shown in Fig. 5.6 for $\theta = 0.6$ exhibiting that the gain in performance is maintained over a range of θ values. The network achieves slightly higher spectral efficiency when users have 4 antennas than when they only have 2 antennas due to higher array gain. Here, we note that if multihop is allowed, then the performance in Fig. 5.5 and 5.6 would improve as distant users can be reached through multiple good quality links instead of the direct link which has a large path loss. The percentage of successful connection attempts for primary and secondary links in the proposed protocol is shown in Fig. (5.7) showing that atleast 60 percent of the primary connections are successful, 90 percent of the time whereas the additional performance improvement comes from the fact that on average 46 percent of the secondary connections are also successful.

We compare our results with the Interference Alignment based approach proposed in [38]. Fig. 5.8 shows a comparison of the network spectral efficiency achieved at the PHY layer (with no MAC layer overhead), with a one to one TX-RX mapping. The figure depicts two

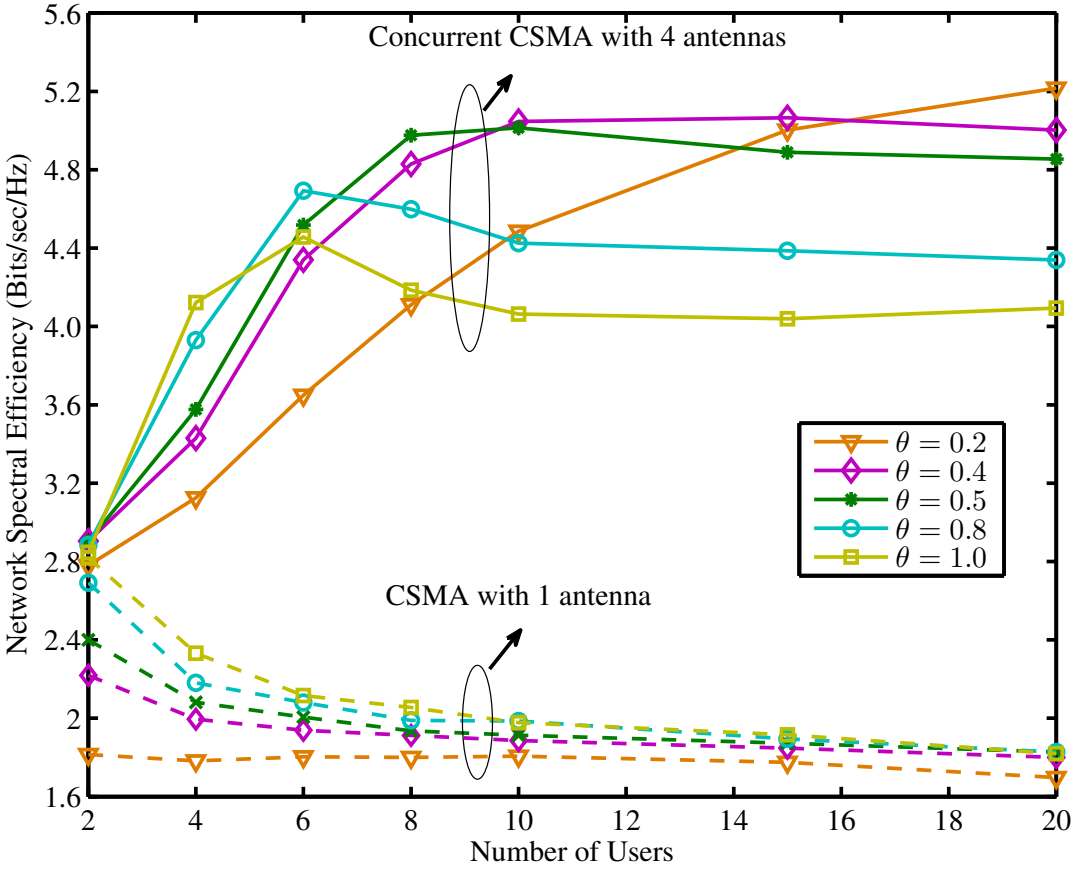

Figure 5.4: Network spectral efficiency scaling of concurrent CSMA with for $N_r = 4$ for various values of θ at a radius of $d = 1000m$

kinds of modulation schemes binary phase-shift keying (BPSK) and 16-QAM or quadrature amplitude modulation for 4 antenna users at a coverage radius of 1000 m. For both the modulation schemes, the IA based approach starts as a better approach for fewer users because it is able to align the interference from the few transmitting users leading to minimal interference and hence higher throughput. But as the number of users increases, the network throughput cannot scale, due to the requirement of perfect alignment which limits the number of user streams to 4. Hence, a perfect alignment strategy is not the best when more users are present in the system because their spatial segmentation can be utilized to achieve a higher network spectral efficiency by allowing more secondary user streams. This figure also raises the question of modulation and coding scheme selection based on the number of users. We

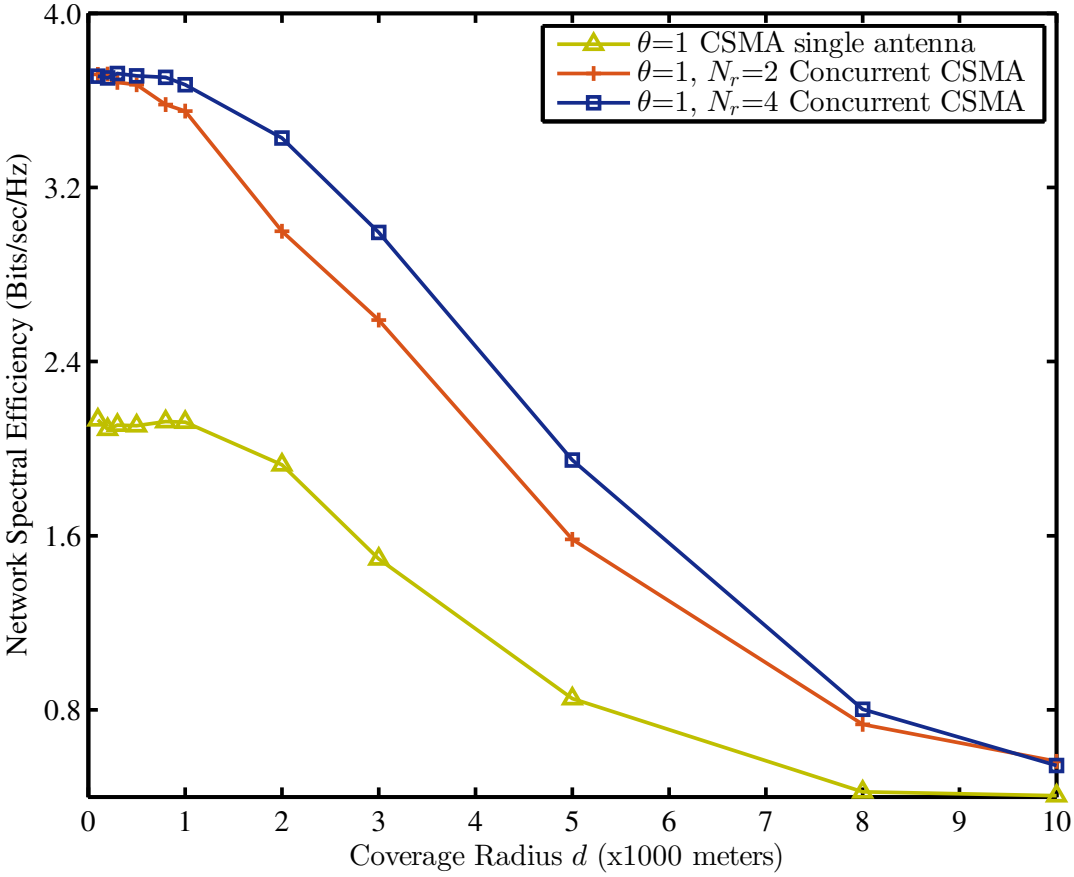

Figure 5.5: Variation of network spectral efficiency with coverage radius d for a network with 4 users and $\theta = 1$

wish to enable this feature in our concurrent CSMA in the future by allowing light weight RTS-CTS exchange between the secondary users like in [38]. The key takeaway is that even though allowing simultaneous channel access to multiple users increases interference, their spatial separation offsets some of the SINR loss to allow the network throughput to scale, atleast weakly, with the number of users. We believe that the scaling is much more evident in Fig. 5.8 than figures 5.3 and 5.4 because in the latter simulation, not all desired secondary TX-RX pairs can talk concurrently because a user may desire to talk to another user who is busy.

In summary, the traditional single user channel access paradigm for wireless medium access is highly suboptimal and a research effort is needed to explore concurrent user MAC

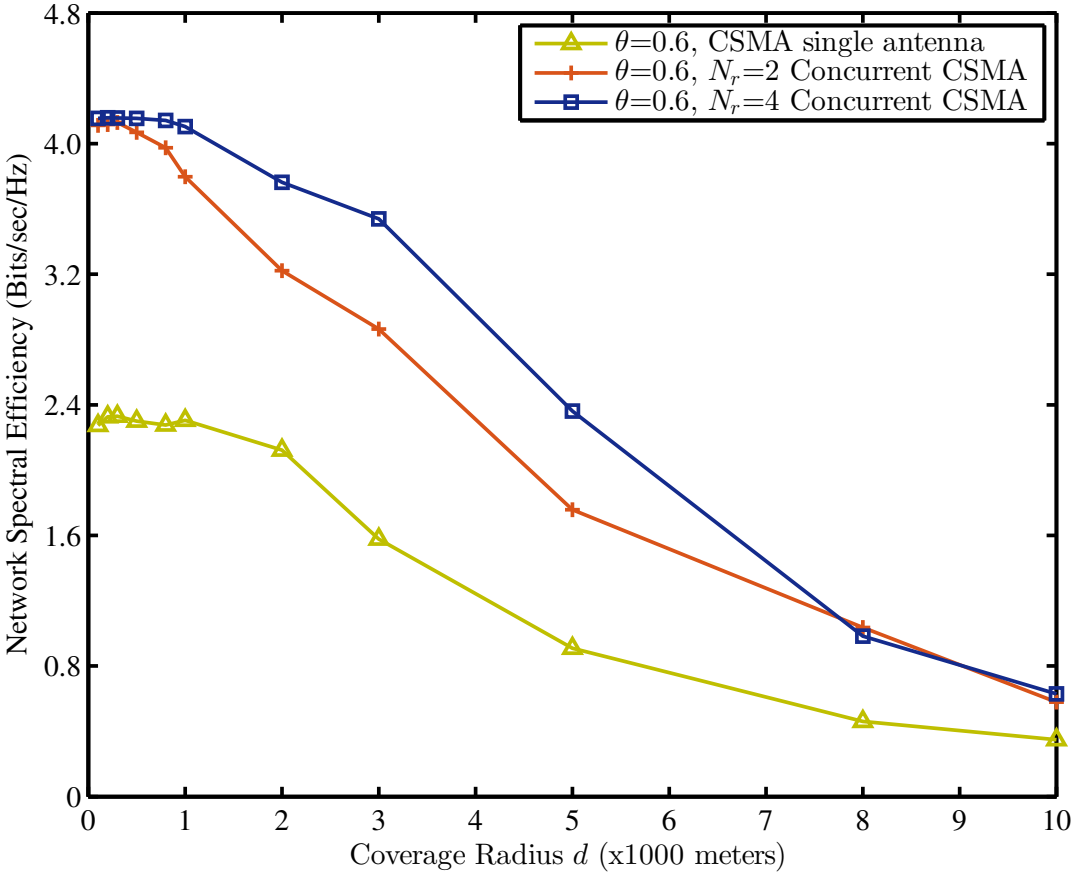

Figure 5.6: Variation of network spectral efficiency with coverage radius d for a network with 4 users and $\theta = 0.6$

protocols. Concurrent CSMA is a step in that direction and it is shown to at least double the throughput of traditional CSMA. It is also shown that while interference alignment may be good for small networks, concurrent transmissions allow the throughput to scale with the number of users. Hence, a combination of the two techniques is a good choice [38].

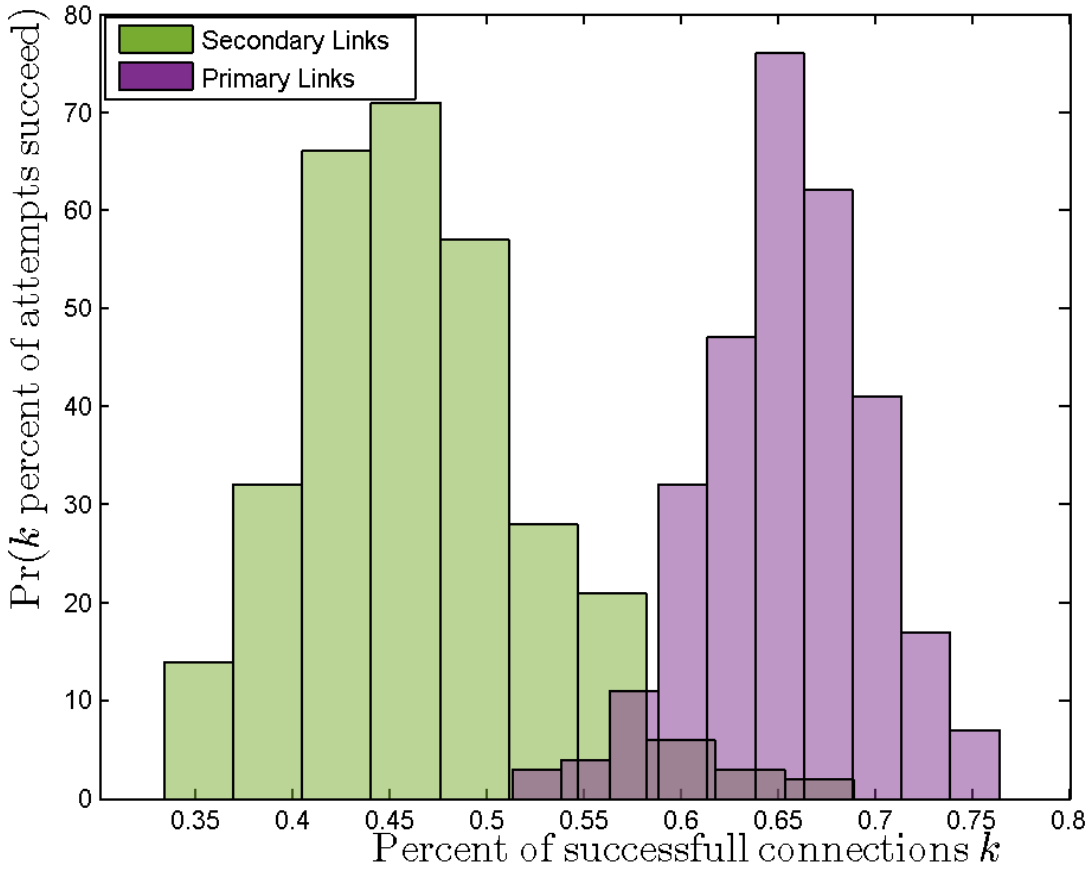

Figure 5.7: Distribution of the percentage of links able to succesfully decode their information in the proposed protocol for primary and secondary links

5.2 TDMA and Interference Alignment in a Time Varying Channel

In this section we want to study how a time division multiple access system would compare to a Interference Alignment system in a time varying channel. This study will also point towards the benefit of IA over TDMA in non- (or very slow) time varying channels. Since in TDMA the transmissions are given pre-decided slots, there is no multi-user interference at the receiver. A point to point MIMO link operating in a TDMA system intends to maximize its own capacity using the knowledge of the MIMO channel. This capacity can be maximized

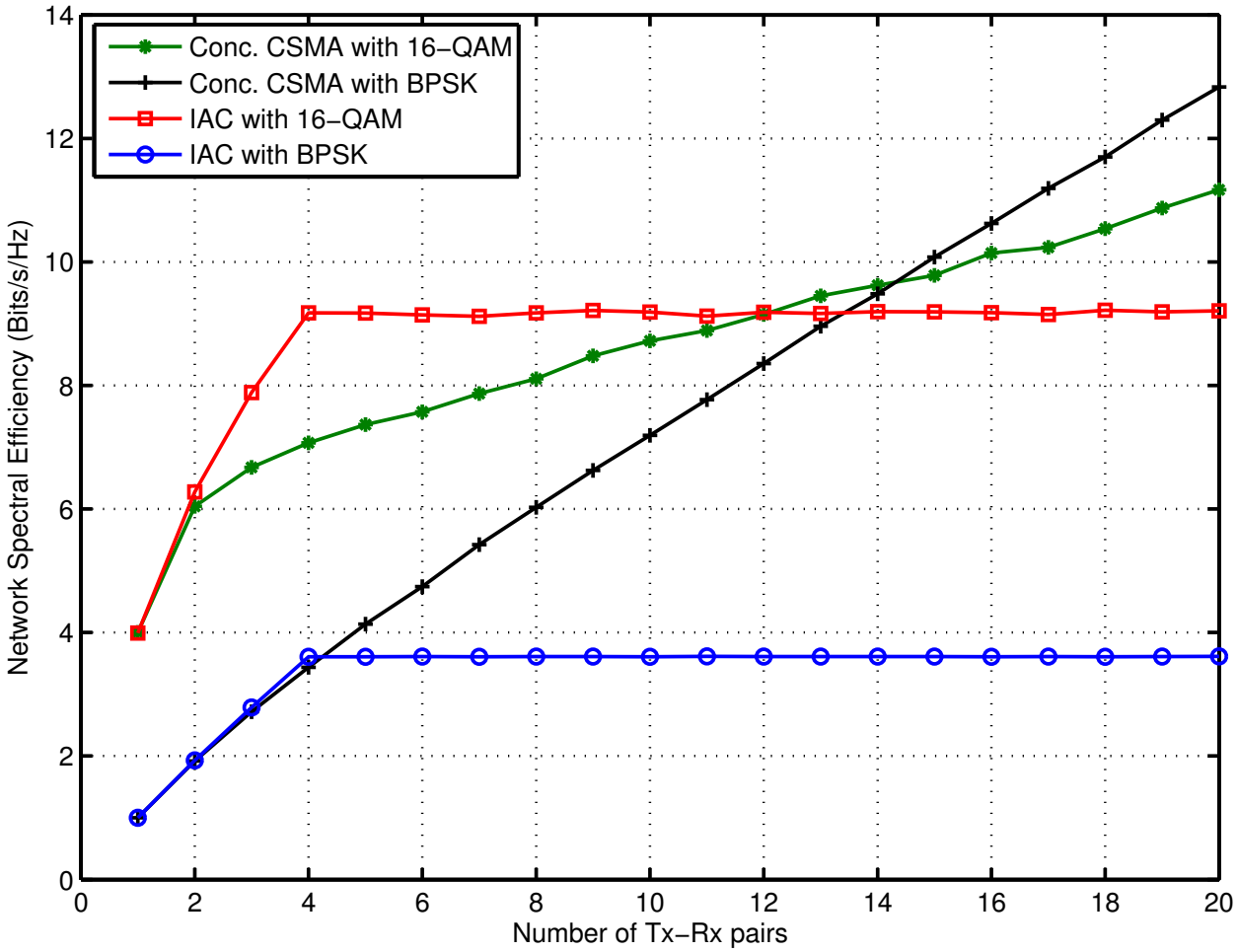

Figure 5.8: Comparison of the the proposed concurrent approach with the Interference Alignment and Cancelltion (IAC) presented in [38]

by choosing the right and left singular vectors of the channel as the transmit and receive beams respectively i.e. if H is the MIMO channel and $H = U\Sigma V$ is the singular value decomposition (SVD) of H, then V must be the transmit beam and U must be the receive beam. Further for a fixed transmit power P, power can be allocated to the spatial streams according to waterfilling solution[44].

5.2.1 Simulation Results

We simulate a $K = 7$ user-pairs system with $M = 4$ antennas per node. We fix the Doppler rate $f_d = 200/3$Hz and bandwidth $1/T_s = 1.25$MHz. The coherence time is then $T_{\text{coh}} =$

$\frac{0.1}{f_d T_s} = 1875$ symbols. The topology of users is such that SNR=30dB and the interferers are successively 3dB, 6dB, ..., and 18dB down from the signal level. We assume that both the TDMA and IA systems use Shannon capacity achieving codes and are able to operate at the instantaneous Shannon rate of $\log_2(1 + \text{SINR})$bits/s/Hz. Initial MIMO channel estimation is done at both TX and RX using 11 symbols long concurrent Zadoff-Chu pilot symbols. The TDMA system uses SVD beamforming and waterfilling to choose the beams. The IA system uses iterative Max-SINR beamforming along with RLS adaptive algorithm at the receiver along with link adaptation (meaning the decisions are error free). The average rate achieved per link during the coherence time is shown in fig. 5.9. It should be noted that there are 7 links in the system and each link achieves this rate on average. Hence the total rate achieved is 7 times this rate. This shows that IA is able to achieve much more throughput than TDMA even under a time varying channel, hence is very promising as a MAC protocol compared to TDMA.

5.3 Summary

In the first part of this chapter, we address the challenge of designing a multi user MAC protocol for single hop mobile ad-Hoc networks with the aim of allowing multiple users to transmit concurrently to increase the network spectral efficiency or equivalently the sum throughput per unit bandwidth. We wish the protocol to be compatible with the existing 802.11 standard MAC protocol, CSMA-CA. We propose a concurrent CSMA protocol that allows secondary users to access the channel concurrently with a primary user by making the secondary users minimize their interference towards the primary receiver through beamnulling. The chapter discusses how the RTS/CTS messages between the primary TX and RX are utilised to obtain channel state information necessary for beamnulling. The secondary transmissions operate synchronously with the primary but do not receive any acknowledgements. Hence, the secondary transmissions follow a best effort service. We present

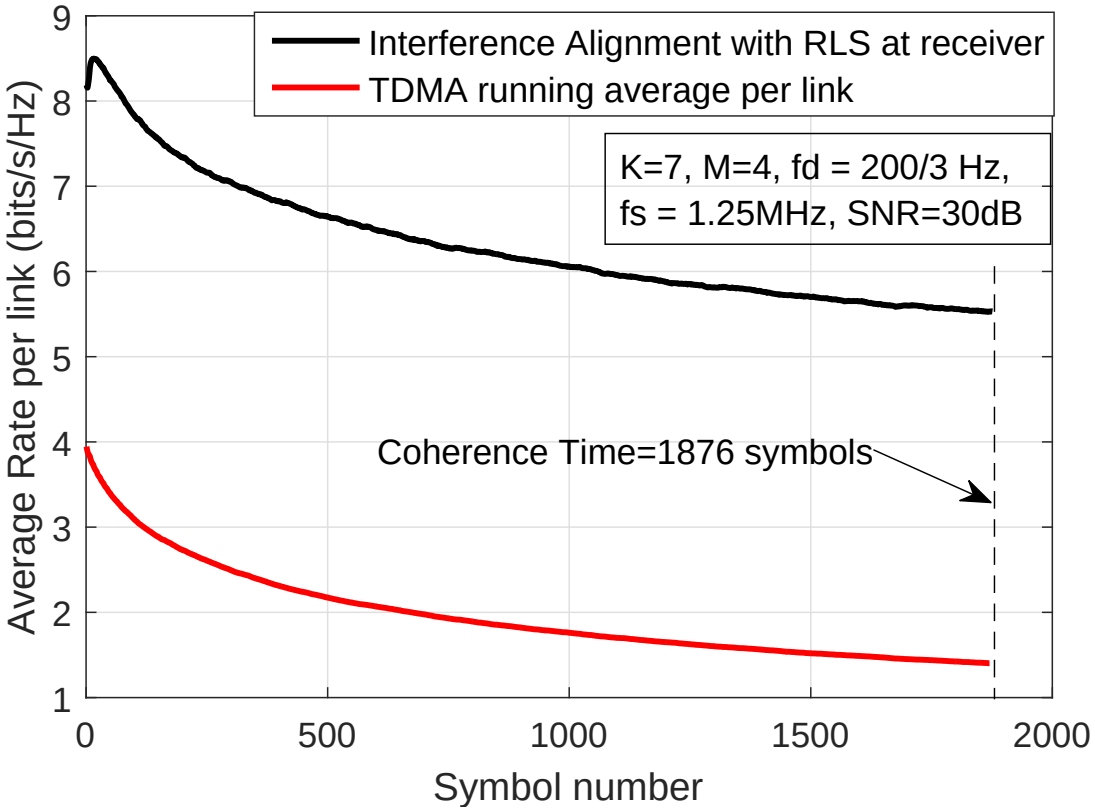

Figure 5.9: Average rate achieved per link in a 7 user 4 antenna IA and TDMA system.

simulation results to show that using this enhanced MAC protocol on nodes having two or four antennas, the peak network throughput increases by a factor between 2 to 3 compared to CSMA. Concurrent CSMA also achieves a consistently higher saturation throughput across a range of persistence probability θ.

We show that this throughput gain is maintained as the network scales in size and that in comparison to a previous Interference Alignment based strategy [38], the proposed scheme allows the throughput to scale with the number of users. Concurrent CSMA is a guiding step towards a MAC protocol that truly utilizes all the degrees of freedom available in a wireless network to allow seamless addition of users and throughput scaling. Moreover, it is so designed so that it does not cause an interference to a co-existing CSMA network.

The reader may be curious about the fact that we only simulated a single stream for CSMA transmissions where multiple streams are optimal. This was done to simplify the system. To our knowledge, there is no known mechanism to optimally decide whether one user should do MIMO transmission or two interfering users should do single stream transmissions. Having each user send one stream allows extra dimensions to be filled by other users' streams. This seems to be a win-win situation as everyone can use their largest eigenvector to get a good gain. But deciding how to distribute beams between MIMO and more active users in a concurrent network is left as a topic for future work.

In the second part, we show that an IA system performs better than a TDMA system in a time varying channel and hence is a better choice for a MAC protocol promising better throughput and concurrent communications ability.

Chapter 6

Conclusions

In conclusion, in this thesis we have looked at ways to enable concurrent communications in wireless networks by analyzing and tackling some of the challenges that occur in practical networks. First, we identified Interference Alignment as a promising strategy for concurrent communications and listed the challenges it still faces in implementation. We focused mainly on mitigating the effects of a time varying channel on an aligned system and deriving the optimal set of parameters to use in this case. In the last part of this thesis, we presented a new MAC protocol based on beamnulling that can add concurrent communication capability to an existing network while maintaining compatibility with the current protocol. We summarize this work's contributions as follows:

6.1 Summary of Contributions

We present analysis and closed form expressions of the cumulative density function of the signal to interference and noise ratio over time for a general Interference Alignment system. These expressions also provide us an easy way to calculate the average throughput of the system for any chosen length of data phase T_d. Thus, under the time varying channel, we are able to optimize the data phase length to maximize average throughput. This capability will be very helpful for system designers trying to set the network parameters in wireless

networks with mobile nodes. We also present results using which nodes can jointly choose how long to transmit data in the current fading, to maximize throughput.

In order to optimize distributed IA, which is difficult to analyze, we present results showing that data-aided receiver tracking along with link adaptation improves the received SINR significantly. Further, updating the TX beam in the middle of the data phase also provides increased throughput stability or increased capacity or both. We have provided many simulations showing how the optimal length of pilots and retraining frequency varies with SNR and Doppler. This can give an indication of the optimal value to the system designer, which can be refined while in operation.

Lastly, we present a new concurrent CSMA MAC protocol that is compatible with CSMA and allows concurrent or *secondary* transmissions along with the *primary* transmission by beamnulling towards the *primary* receiver. The network throughput can be increased 2 to 3 times compared to that of CSMA with a single antenna transmission. Our protocol also allows the network throughput to scale slowly as more users are added unlike CSMA and another competing protocol which do not scale. This provides a building block for more complicated MAC protocols to be built on.

6.2 Future work

Interference Alignment has some limitations to its promise of concurrent communication. First, it is sensitive to staleness of the channel state information and second, the number of antennas imposes a limit on how many users can align (see eq. 2.1). A scalable solution to multiuser communication must include a mix of alignment, time sharing and/or frequency sharing. The problem of which group of users should align and which should remain orthogonal is a hard yet interesting resource allocation problem. It can be envisaged that users moving slowly relative to each other can align and share the channel better whereas fast moving users would be better served on orthogonal channels. Even more interesting would

be to include power allocation and a variable number of spatial streams into the decision matrix. Ensuring fairness among users in Interference Alignment systems is another open problem since fairness and sum rate maximization usually go in opposite ways.

One important future responsibility we believe is to find novel use-cases of IA in everyday life. Whether it be indoor device to device data transfer, inter-cell interference coordination in cellular communications, creating mesh networks on the go, or serving as a connective fiber in remote or disaster stricken areas, it is the application that will drive the adoption of this advanced concurrent communications technology. But there are some applications that look especially promising.

With the advent of higher frequencies like millimeter wave and terahertz, signals are either completely or nearly line-of-sight (LoS) which means the effect of time varying fading of the channel on an alignment system will be greatly reduced since LoS channels change much slower. Hence alignment can become a particularly exciting opportunity if properly investigated.

Second, coordination between indoor neighboring WiFi access points by using alignment can greatly mitigate the co-channel interference in WiFi that significantly reduces its capacity at present. Any indoor, device to device communication of the future can benefit from interference alignment because the mobility of users will be low and signals will remain aligned for a long time. I hope that the field of multi-user communication remains vibrant in the future by continuing fundamental research and making new discoveries to revolutionize what is possible in communications.

Appendices

Appendix A

Proof for Section 3.4

We want to prove that the pdf of $x_{kl}(t)$ conditioned on $x_{kl}(0)$ is given by

$$f_{x_{kl}(t)|x_{kl}(0)} = \mathcal{CN}(\rho_t x_{kl}(0), ||p_l||^2(1-\rho_t^2)I_M). \tag{A.1}$$

Let $X = x_{kl}(0)$, $Y = x_{kl}(t)$ and $Z = [x_{kl}(0), x_{kl}(t)]^T$. Then

$$f_Z(z) = \frac{1}{\pi^{2M}|K_z|}\exp(-z^H K_z^{-1} z) \tag{A.2}$$

and

$$f_X(x) = \frac{1}{\pi^{M}|K_X|}\exp(-x^H K_X^{-1} x), \tag{A.3}$$

where

$$K_Z = ||p_k||^2 \begin{bmatrix} I & \rho_t I \\ \rho_t I & I \end{bmatrix}, \tag{A.4}$$

$|K_Z| = ||p_k||^{4M}(1-\rho_t^2)^M$, $K_X = ||p_k||^2 I$ and $|K_X| = ||p_k||^{2M}$.

Hence we can write the pdf of Y conditioned on X as

$$\begin{aligned} f_{Y|X}(y|x) &= \frac{f_Z(z)}{f_X(x)} \\ &= \frac{1}{\pi^M ||p_k||^{2M}(1-\rho_t^2)^M} \exp\left(-\frac{(y-\rho_t x)^H (y-\rho_t x)}{||p_k||^2(1-\rho_t^2)}\right) \\ &= \mathcal{CN}(\rho_t x, ||p_k||^2(1-\rho_t^2)I). \end{aligned} \tag{A.5}$$

.

Appendix B

Proofs for Section 3.5

B.1 Proof of Lemma 3

Since S is always non-negative, the complementary CDF of S is 1 for $s < 0$. For $s \geq 0$,

$$\begin{aligned}
&\Pr\left(\frac{X}{Y+\sigma_n^2} > s\right) = \Pr\left(X > (Y+\sigma_n^2)s\right) \\
&= \int_{y=0}^{\infty} \int_{x=(y+\sigma_n^2)s}^{\infty} \lambda_0 e^{-\lambda_0 x} f_Y(y) \qquad \text{(B.1)} \\
&= e^{-\lambda_0 \sigma_n^2 s} \left[\prod_{i=1}^{L} \lambda_i\right] \sum_{j=1}^{L} \int_{y=0}^{\infty} \frac{e^{-\lambda_j y} e^{-\lambda_0 y s}}{\prod_{\substack{k=1 \\ k\neq j}}^{L} (\lambda_k - \lambda_j)}. \qquad \text{(B.2)} \\
&= \left[\prod_{i=1}^{L} \lambda_i\right] \sum_{j=1}^{L} \frac{e^{-\lambda_0 s \sigma_n^2}}{\prod_{\substack{k=1 \\ k\neq j}}^{L} (\lambda_k - \lambda_j)(\lambda_j + \lambda_0 s)}. \qquad \text{(B.3)}
\end{aligned}$$

B.2 Proof of Corollary 1

$$\mathrm{E}[S] = \int_0^{\infty} 1 - F_S(s)\, ds \qquad \text{(B.4)}$$

After some simple manipulations, the integral reduces to

$$\mathrm{E}\left[S\right] = \left[\prod_{i=1}^{L} \lambda_i\right] \sum_{j=1}^{L} \frac{e^{\lambda_j \sigma_n^2}}{\prod_{\substack{k=1 \\ k\neq j}}^{L} (\lambda_k - \lambda_j)\lambda_0} \int_{\lambda_j \sigma_n^2}^{\infty} \frac{e^{-z}}{z}\, dz \tag{B.5}$$

Recognizing the integral as exponential integral $E_1(\lambda_j \sigma_n^2)$ completes the proof.

B.3 Proof of Lemma 4

Substituting $y = (x + \theta_0)/x$ we get $I_1(a, b) = \int_{(b+\theta_0)/b}^{(a+\theta_0)/a} \left[\frac{y^{K-2}}{y-1} - \frac{y^{K-2}}{y-1+\theta_0/\theta_1}\right] dy$. Use long division for e.g. $y^{K-2}/(y - 1 + \theta_0/\theta_1) = \sum_{p=0}^{K-3} \left(1 - \frac{\theta_0}{\theta_1}\right)^p y^{K-3-p} + \frac{\left(1-\frac{\theta_0}{\theta_1}\right)^{K-2}}{y-1+\theta_0/\theta_1}$, integrate and take the limits.

B.4 Proof of Lemma 5

Using [33] the pdf of total interference in Lemma 2 can be approximated as $Y \sim \Gamma(k, \theta)$. Then simply following the proof of Lemma 3 we reach the result.

Bibliography

[1] Viveck R. Cadambe and Syed Ali Jafar, "Interference Alignment and Degrees of Freedom of the K-User Interference Channel," *IEEE Trans. Inf. Theory*, vol. 54, no. 8, Aug. 2008.

[2] Syed A. Jafar, "Interference Alignment A New Look at Signal Dimensions in a Communication Network", Foundations and Trends® in Communications and Information Theory, vol. 7, no. 1, pp 1-134. http://dx.doi.org/10.1561/0100000047

[3] Tiangao Gou, and Syed A. Jafar, "Degrees of Freedom of the K User $M \times N$ MIMO Interference Channel," in *IEEE Trans. Inf. Theory*, vol. 56, no. 12, pp. 6040-6057, Dec 2010.

[4] Guy Bresler, Dustin Cartwright, and David Tse, "Feasibility of Interference Alignment for the MIMO Interference Channel," *IEEE Trans. Inf. Theory*, vol. 60, no. 9, Sep. 2014.

[5] Jatin Thukral and Helmut Bolcskei, "Interference alignment with limited feedback," in *Proc. 2009 IEEE International Symp. Inf. Theory*, pp. 1759-1763, Seoul 2009.

[6] Omar El Ayach and Robert W. Heath, Jr., "Interference alignment with analog channel state feedback," *IEEE Trans. Wireless Commun.*, vol. 11, no. 2, pp. 626-636, 2012.

[7] Krishna Gomadam, Viveck R. Cadambe, and Syed Ali Jafar, "A Distributed Numerical Approach to Interference Alignment and Applications to Wireless Interference Networks," *IEEE Trans. Inf. Theory*, vol. 57, no. 6, pp. 3309-3322, Jun. 2011.

[8] Dimitris S. Papailiopoulos, and Alexandros G. Dimakis, "Interference Alignment as a Rank Constrained Rank Minimization," in *IEEE Trans. Sig. Proc.*, vol. 60, no. 8, Aug 2012.

[9] Steven W. Peters and Robert W. Heath Jr., "Interference alignment via alternating minimization," *2009 IEEE International Conference on Acoustics, Speech and Signal Processing*, Taipei, pp. 2445-2448, 2009.

[10] I. Santamaria, O. Gonzalez, Robert W. Heath Jr. and Steven W. Peters, "Maximum Sum-Rate Interference Alignment Algorithms for MIMO Channels," *2010 IEEE Global Telecommunications Conference GLOBECOM*, Miami, FL, pp. 1-6, 2010.

[11] G. Sridharan and W. Yu, "Linear Beamformer Design for Interference Alignment via Rank Minimization," in *IEEE Trans. Sig. Proc.*, vol. 63, no. 22, pp. 5910-5923, Nov.15, 2015.

[12] A. Gholami Davoodi and S. A. Jafar, "Aligned Image Sets Under Channel Uncertainty: Settling Conjectures on the Collapse of Degrees of Freedom Under Finite Precision CSIT," in *IEEE Trans. Inf. Theory*, vol. 62, no. 10, pp. 5603-5618, Oct. 2016.

[13] S. Morteza Razavi and Tharmalingam Ratnarajah, "Performance Analysis of Interference Alignment Under CSI Mismatch," *IEEE Trans. Veh. Technol.*, vol. 63, no. 9, Nov. 2014.

[14] Yi Jiang, Babak Daneshrad, and Gregory J Pottie, "A Practical Approach to Joint Timing, Frequency Synchronization and Channel Estimation for Concurrent Transmissions in a MANET." *IEEE Trans. Wireless Commun.*, vol. 16, no. 6, pp. 3461-3475, June 2017.

[15] Seogoo Lee, Andreas Gerstlauer, and Robert W. Heath, Jr., "Distributed Real-Time Implementation of Interference Alignment with Analog Feedback," in *IEEE Trans. Veh. Technol.*, vol. 64, no. 8, pp. 3513-3525, Aug 2015.

[16] Martin Mayer, Gerald Artner, Gabor Hannak, Martin Lerch and Maxime Guillaud, "Measurement Based Evaluation of Interference Alignment on the Vienna MIMO Testbed," *The Tenth International Symposium on Wireless Communication Systems (ISWCS)*, Ilmenau, Germany, pp. 1-5, 2011.

[17] H. Zhao, "Addressing Practical Challenges in High-Capacity Multi-Antenna Communication Systems," Order No. 22620702, University of California, Los Angeles, Ann Arbor, 2019. ProQuest, https://search.proquest.com/docview/2316417338?accountid=14512.

[18] Gerald Matz, Franz Hlawatsch, Chapter 1 - Fundamentals of Time-Varying Communication Channels, Editor(s): Franz Hlawatsch, Gerald Matz, "Wireless Communications Over Rapidly Time-Varying Channels", Academic Press, 2011, page 1-63.

[19] Thomas Zemen, Member, IEEE, and Christoph F. Mecklenbruker, "Time-Variant Channel Estimation Using Discrete Prolate Spheroidal Sequences," in *IEEE Trans. Sig. Proc.*, vol. 53, no. 9, Sept. 2005.

[20] Hemant Saggar, Greg Pottie, and Babak Daneshrad, "On Maximizing the Average Capacity with Interference Alignment in a Time Varying Channel, in *Information Theory and Applications Workshop*, San Diego, Feb 2016.

[21] John G. Proakis, *Digital Communications*, 5th Edition, McGraw Hill, 2007.

[22] Steven E. Pav, "Moments of the log non-central chi-square distribution," [Online]. Available: http://arxiv.org/abs/1503.06266v1, Mar 2015.

[23] Hemant Saggar, Babak Daneshrad, and Gregory J. Pottie, "The Distribution of SINR and the achieved Throughput in Interference Alignment under a Gauss Markov Channel, in *88th IEEE VTC*, Chicago, Aug 2018.

[24] Omar El Ayach, Angel Lozano, and Robert W. Heath, Jr., "On the Overhead of Interference Alignment: Training, Feedback, and Cooperation," *IEEE Trans. Wireless Commun.*, vol. 11, no. 11, Nov. 2012.

[25] P. G. Sudheesh, M. Magarini and P. Muthuchidambaranathan, "Optimal overhead selection for interference alignment in time-varying two-user MIMO X channel," *2016 IEEE Distributed Computing VLSI, Electrical Circuits and Robotics (DISCOVER)*, Mangalore, pp. 128-132, 2016.

[26] M. Ozawa, T. Ohtsuki, W. Jiang and Y. Takatori, "Interference Alignment for Time-Varying Channel with Channel and Weight Predictions Based on Auto Regressive Model," *2015 IEEE Global Communications Conference (GLOBECOM)*, San Diego, CA, pp. 1-6, 2015.

[27] R. K. Mungara, G. George and A. Lozano, "Overhead and Spectral Efficiency of Pilot-Assisted Interference Alignment in Time-Selective Fading Channels," *IEEE Trans. Wireless Commun.*, vol. 13, no. 9, pp. 4884-4895, Sept. 2014.

[28] Christos Komninakis, Christina Fragouli, Ali H. Sayed, and Richard D. Wesel, "Multi-Input Multi-Output Fading Channel Tracking and Equalization using Kalman Estimation," *IEEE Trans. Sig. Proc.*, vol. 50, no. 5, pp. 1065-1076, May 2002.

[29] Heejung Yu, Youngchul Sung, Haksoo Kim, and Yong H. Lee, "Beam Tracking for Interference Alignment in Slowly Fading MIMO Interference Channels: A Perturbations Approach Under a Linear Framework," *IEEE Trans. Sig. Proc.*, vol. 60, no. 4, Apr. 2012.

[30] Min Dong, Lang Tong and B. M. Sadler, "Optimal insertion of pilot symbols for transmissions over time-varying flat fading channels," *IEEE Trans. Sig. Proc.*, vol. 52, no. 5, pp. 1403-1418, May 2004.

[31] Franz Hlawatsch and Gerald Matz, *Wireless Communication Over Rapidly Time-Varying Channels.* Burlington, MA: Elsevier, 2011, pp. 1-63.

[32] Marcus Bibinger, "Notes on the sum and maximum of independent exponentially distributed random variables with different scale parameters," arXiv:1307.3945 [math.PR].

[33] Robert W. Heath, Jr., Tao Wu, Young Hoon Kwon, and Anthony C. K. Soong, "Multiuser MIMO in Distributed Antenna Systems With Out-of-Cell Interference," *IEEE Trans. Sig. Proc.*, vol. 59, no. 10, Oct. 2011.

[34] Hemant Saggar, Yi Jiang, Babak Daneshrad, and Greg Pottie, "A Concurrent CSMA MAC protocol for Mobile Ad Hoc Networks using beamnulling, in *IEEE MILCOM*, Tampa, Oct 2015.

[35] M. Frodigh, P. Johansson and P. Larsson, "Wireless Networking-The art of networking without a network," *Ericsson Review*, no. 4, 2000.

[36] Lin X. Cai et al., "A Distributed Multi User MIMO MAC Protocol for Wireless Local Area Networks," *IEEE Globecom*, pp. 1-5, Nov. 30-Dec. 4 2008.

[37] E. Kartsakli et al., "Multiuser MAC Protocols for 802.11n Wireless Networks," *IEEE Int. Conf. Commun.*, pp. 1-5, 14-18 June 2009.

[38] K. C.J. Lin, S. Gollakota and D. Katabi, "Random access heterogeneous MIMO networks," *Proc. ACM SIGCOMM*, New York, pp. 146-157, 2011.

[39] B.P. Crow et al., "Investigation of the IEEE 802.11 medium access control (MAC) sublayer functions," *IEEE INFOCOM, Sixteenth Annu. Joint Conf. IEEE Comput. and Commun. Soc.* vol.1, pp. 126-133, 7-12 Apr 1997.

[40] A.J. Paulraj et al., "An overview of MIMO communications - a key to gigabit wireless," *Proc. of the IEEE*, vol.92, no.2, pp. 198-218, Feb 2004.

[41] D. P. Palomar, J.M. Cioffi and A. M. Lagunas, Joint Tx-Rx Beamforming Design for Multicarrier MIMO Channels: A Unified Framework for Convex Optimization, IEEE Trans. Signal Process., vol. 51, no.9, pp. 2381-2401, Sept. 2003.

[42] E. G. Larsson and P. Stoica, "Optimal Beamforming with Channel known at Transmitter," in *Spectral Analysis of Signals*, New York, Cambridge University Press, 2008, ch. 6, pp. 80-81.

[43] M. S. Gast, "802.11n: A Survival Guide," OReilly Media, Apr. 2012.

[44] Thomas M. Cover and Joy A. Thomas, "Elements of Information Theory" in Wiley Series in Telecommunications and Signal Processing, Wiley-Interscience, USA, 2006.

[45] O. El Ayach, S.W. Peters and R.W. Heath Jr., "The practical challenges of interference alignment," *IEEE Wireless Commun. Mag.*, vol.20, no.1, pp. 35-42, February 2013.